

AD-A056 308

ILLINOIS UNIV AT URBANA-CHAMPAIGN DEPT OF MECHANICAL --ETC F/G 20/4
THEORY, COMPUTER PROGRAM, AND ILLUSTRATIVE EXAMPLES FOR THE TWO--ETC(U)
MAR 78 J C DUTTON, A L ADDY

DAAK40-76-C-0942

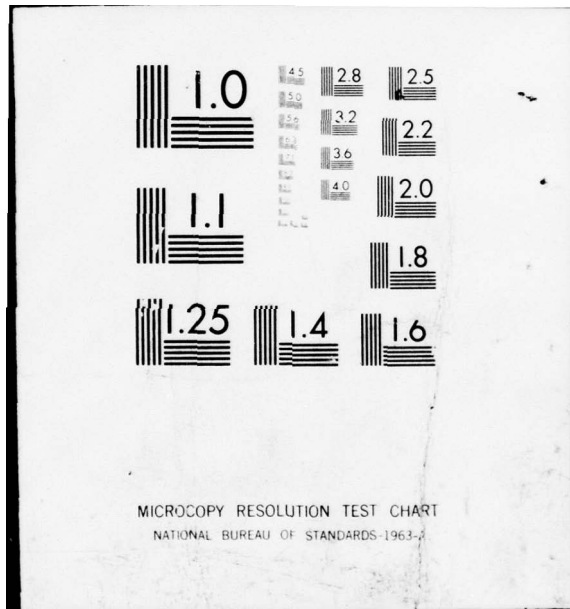
UNCLASSIFIED

DRDMI-T-CR-78-10

NL

OF 2
AD A056 308





MICROCOPY RESOLUTION TEST CHART
NATIONAL BUREAU OF STANDARDS-1963-A

LEVEL II

AD A 056308



TECHNICAL REPORT T-CR-78-10

THEORY, COMPUTER PROGRAM, AND ILLUSTRATIVE
EXAMPLES FOR THE TWO-DIMENSIONAL
BOUNDARY LAYER FLOW OF IDEAL GAS

J. C. Dutton and A. L. Addy
Department of Mechanical and Industrial Engineering
University of Illinois at Urbana-Champaign
Urbana, Illinois 61801

AD NU. _____
BDC FILE COPY

**U. S. ARMY
MISSILE
RESEARCH
AND
DEVELOPMENT
COMMAND**

29 March 1978

**DD
PREPARED FOR**
[Handwritten signature]



APPROVED FOR PUBLIC RELEASE; DISTRIBUTION UNLIMITED

Redstone Arsenal, Alabama 35809

Prepared for:
Aeroballistics Directorate
Technology Laboratory
US Army Missile Research and Development Command
Redstone Arsenal, Alabama 35809

78 07 11

DISPOSITION INSTRUCTIONS

**DESTROY THIS REPORT WHEN IT IS NO LONGER NEEDED. DO NOT
RETURN IT TO THE ORIGINATOR.**

DISCLAIMER

**THE FINDINGS IN THIS REPORT ARE NOT TO BE CONSTRUED AS AN
OFFICIAL DEPARTMENT OF THE ARMY POSITION UNLESS SO DESIGNATED
BY OTHER AUTHORIZED DOCUMENTS.**

TRADE NAMES

**USE OF TRADE NAMES OR MANUFACTURERS IN THIS REPORT DOES
NOT CONSTITUTE AN OFFICIAL INDORSEMENT OR APPROVAL OF
THE USE OF SUCH COMMERCIAL HARDWARE OR SOFTWARE.**

18/DRDMI-T

19/CR-78-14

UNCLASSIFIED

SECURITY CLASSIFICATION OF THIS PAGE (When Data Entered)

REPORT DOCUMENTATION PAGE		READ INSTRUCTIONS BEFORE COMPLETING FORM
1. REPORT NUMBER 9 Technical Report T-CR-78-10	2. GOVT ACCESSION NO.	3. RECIPIENT'S CATALOG NUMBER
4. TITLE (and Subtitle) 6 THEORY, COMPUTER PROGRAM, AND ILLUSTRATIVE EXAMPLES FOR THE TWO-DIMENSIONAL BOUNDARY LAYER FLOW OF IDEAL GASES	5. TYPE OF REPORT & PERIOD COVERED	
7. AUTHOR(s) 10 J. C. Dutton (Graduate Rsch Asst & NSF Engy Trainee) A. L. Addy (Professor of Mechanical Engineering)		6. PERFORMING ORG. REPORT NUMBER
9. PERFORMING ORGANIZATION NAME AND ADDRESS Department of Mechanical & Industrial Engng University of Illinois at Urbana-Champaign Urbana, IL 61801		8. CONTRACT OR GRANT NUMBER(s) 15 DAAK 40-76-C-0942
11. CONTROLLING OFFICE NAME AND ADDRESS Commander, US Army Missile R&D Command Attn: DRDMI-TI Redstone Arsenal, AL 35809		10. PROGRAM ELEMENT, PROJECT, TASK AREA & WORK UNIT NUMBERS 12/11P
14. MONITORING AGENCY NAME & ADDRESS (if different from Controlling Office) Commander, US Army Missile R&D Command Attn: DRDMI-TD Redstone Arsenal, AL 35809		12. REPORT DATE 11 29 March 1978
16. DISTRIBUTION STATEMENT (of this Report) Approved for public release; distribution unlimited.		13. NUMBER OF PAGES 88
17. DISTRIBUTION STATEMENT (of the abstract entered in Block 20, if different from Report)		15. SECURITY CLASS. (of this report) UNCLASSIFIED
18. SUPPLEMENTARY NOTES		15a. DECLASSIFICATION/DOWNGRADING SCHEDULE
19. KEY WORDS (Continue on reverse side if necessary and identify by block number) 2-D boundary layer flow Axisymmetric or plane geometries FORTRAN IV computer program Input/output instructions and samples		
20. ABSTRACT (Continue on reverse side if necessary and identify by block number) A computer program has been developed to calculate the two-dimensional boundary layer flow of ideal gases. The program is written in FORTRAN IV, and is based on the solution technique of Walz et al. Axisymmetric or plane geometries can be analyzed with the boundary layer laminar or turbulent, compressible or incompressible and either with or without heat transfer. A brief outline of the theory upon which the program is based is presented (Continued)		

UNCLASSIFIED

SECURITY CLASSIFICATION OF THIS PAGE (When Data Entered)

78 07 11 006
444 733
Lee

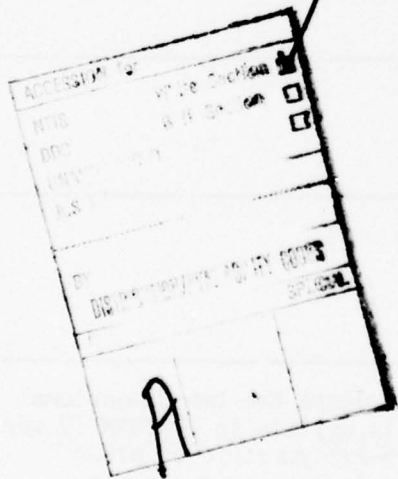
UNCLASSIFIED

SECURITY CLASSIFICATION OF THIS PAGE(When Data Entered)

20. Abstract (Cont'd)

together with complete input instructions and sample input and output. In addition, results computed with this program are compared to available data and analytical solutions for a number of flow situations of interest.

*The computer program was developed and example calculations were carried out using the CDC CYBER 175 computer system operated by the Computing Services Office, University of Illinois at Urbana-Champaign, Urbana, IL 61801.



UNCLASSIFIED

SECURITY CLASSIFICATION OF THIS PAGE(When Data Entered)

TABLE OF CONTENTS

	Page
LIST OF TABLES	iv
LIST OF FIGURES	v
NOMENCLATURE	vii
I. INTRODUCTION	1
II. THEORETICAL DEVELOPMENT	1
A. General	3
B. Laminar Boundary Layers	6
C. Turbulent Boundary Layers	8
D. Transition	8
E. Heat Transfer Correction	10
III. COMPUTER PROGRAM	13
A. General Description	13
B. Input/Output Variable List and Discussion	14
C. Starting of the Computations	19
D. Input Instructions and Example	22
IV. COMPARISONS TO EXPERIMENT AND ANALYTICAL SOLUTIONS	25
A. Turbulent Incompressible Boundary Layers	25
B. Turbulent Compressible Boundary Layers	26
C. Laminar Boundary Layers	27
D. Boundary Layers with Heat Transfer	28
E. Boundary Layer with Transition	29
F. Miscellaneous Examples	29
V. CONCLUSIONS	31
REFERENCES	60
APPENDIX A. COMPRESSIBLE BOUNDARY LAYER (COMPBL) PROGRAM LISTING	63
APPENDIX B. ERROR MESSAGES AND DISCUSSION	83

LIST OF TABLES

	Page
Table I β vs H from Hartree solutions	32
Table II Summary of procedure for determining starting values ZSTART, HSTART, BSTART	33

LIST OF FIGURES

	Page
Figure 1	Location of coordinates X, Y, R; approach flow variables M_∞ (MINF), Re_∞/L (REINFL), T_∞ ; and angle β (BSTART)...
	(a) Axisymmetric case 34
	(b) Plane two-dimensional case 34
Figure 2	H vs M_∞ used in determining HSTART value for compressible flows 35
Figure 3	Example input file for NACA 0012 airfoil flow . 36
Figure 4	(a) Example printout from file OUTPUT for case given in Fig. 3 37
	(b) Comparison of computed results and data for case given in Fig. 3 39
Figure 5	Example printout from file TAPE4 40
Figure 6	Comparison of computed results and data for Ludwig-Tillmann accelerating flow (1300) [†] . . 41
Figure 7	Comparison of computed results and data for Ludwig-Tillmann strong adverse pressure gradient flow (1200) 42
Figure 8	Comparison of computed results and data for Clauser, flow number 1 (2200) 43
Figure 9	Comparison of computed results and data for Moses, case 3 (3800) 44
Figure 10	Comparison of computed results and data for Bradshaw and Ferriss relaxing flow (2400) . . . 45
Figure 11	Comparison of computed results and data for McLafferty-Barber supersonic flow 46
Figure 12	Comparison of computed results and data for Winter, Smith, and Rotta subsonic waisted body flow, $M_\infty = 0.6$ 47
Figure 13	Comparison of computed results and data for Winter, Smith, and Rotta supersonic waisted body flow, $M_\infty = 1.4$ 48

[†] Numbers in parentheses are flow identification numbers used at the Stanford conference on turbulent boundary layers.

	Page
Figure 14 Comparison of computed results and data for Winter, Smith, and Rotta supersonic waisted body flow, $M_\infty = 2.8$	49
Figure 15 Comparison of computed results and data for Alstatt-AEDC transonic flow	50
Figure 16 Comparison of present computations and finite difference calculations of Smith and Clutter for Hiemenz cylinder flow	51
Figure 17 Comparison of present computations with Hartree calculations and Smith and Clutter finite difference calculations for Schubauer elliptic cylinder flow	52
Figure 18 Comparison of present computations and Flügge-Lotz-Eichelbrenner finite difference calculations for compressible laminar flow	53
Figure 19 Comparison of present computations and analytical solution of Chapman and Rubesin	54
Figure 20 Comparison of present computations and data of Boldman, Schmidt, and Ehlers	55
Figure 21 Comparison of present computations and data taken from McNally [16] ^{††} for flow over a NACA 0012 airfoil (This is a repeat of Fig. 4b)	56
Figure 22 Predicted boundary layer characteristics for flow over a conical afterbody with turbulent boundary layer assumed to begin at the expansion	57
Figure 23 Predicted boundary layer characteristics for flow over a cylindrical missile/conical afterbody combination with turbulent boundary layer assumed to begin on missile body	58
Figure 24 Predicted boundary layer characteristics for flow in a Mach 2 plane two-dimensional nozzle with hyperbolic entrance and expansion section .	59

^{††}Numbers in brackets refer to entries in REFERENCES.

NOMENCLATURE

I. SYMBOLS

<u>Text</u>	<u>Computer Program</u>	<u>Definition</u>
a		Coefficient in the trial temperature profile, defined by Eq. (19)
A _H	FAH	Coefficient in solution to mechanical energy equation, defined by Eq. (16)
A _Z	FAZ	Coefficient in solution to momentum equation, defined by Eq. (15)
b	B---*	Coefficient in the trial temperature profile, defined by Eq. (20)
B _H	FBH	Coefficient in solution to mechanical energy equation, defined by Eq. (16)
B _Z	FBZ	Coefficient in solution to momentum equation, defined by Eq. (15)
c		Coefficient in the trial temperature profile, defined by Eq. (21)
c _f	CF	Local skin friction coefficient, $c_f = \frac{\tau_w}{\frac{1}{2}\rho_\delta u_\delta^2}$
c*		Sonic speed at M = 1
f _w "		Second derivative of dimensionless stream function used by Smith and Clutter [26], $f_w'' = \frac{c_f}{2} \sqrt{Re_x}$
F ₁ , F ₂ , F ₃ , F ₄ , F ₅ , F ₆	FF1, FF2, FF3, FF4, FF5, FF6	Universal functions in Eqs. (5), (7), and (31)

*Blanks indicate that additional alphanumeric symbols may be added for further identification, e.g., corresponding to subscript notation.

<u>Text</u>	<u>Computer Program</u>	<u>Definition</u>
H	H---	Incompressible, adiabatic shape factor, $H = \frac{(\delta_3)_u}{(\delta_2)_u}$
H*	H---S	Shape factor, $H^* = \frac{\delta_3}{\delta_2}$
IDENT		Computer variable used at Stanford conference [18] for flow identification purposes
k		Thermal conductivity
K	CHT---	Heat transfer correction parameter introduced in Eqs. (30) and (31)
L		Length measured along body surface, Eqs. (37) and (38)
[L]	[L]	Denotes dimensions of length
M	M----	Mach number
M*	M----S	Dimensionless speed ratio, $M^* = \frac{u}{c^*}$
MW		Molecular weight
n	N	Exponent of $R\delta_2$ in definition of Z , equal to 1 for laminar boundary layers, 0.268 for turbulent boundary layers
p		Pressure
Pr		Prandtl number
q		local heat flux
Q		Total heat transferred from wall to boundary layer, defined in Eqs. (37) and (38)
R	R	Body radius

<u>Text</u>	<u>Computer Program</u>	<u>Definition</u>
r	RL,RT	Recovery factor, either laminar or turbulent
R_{δ_2}	RD2	Reynolds number based on momentum thickness, $R_{\delta_2} = \frac{\rho_{\delta} u_{\delta} \delta_2}{\mu_w}$
$\frac{Re_{\infty}}{L}$	REINFL	Unit Reynolds number of approach flow, $\frac{Re_{\infty}}{L} = \frac{\rho_{\infty} u_{\infty}}{\mu_{\infty}}$
R		Universal gas constant
s	SL,ST	Reynolds analogy factor, either laminar or turbulent
St		Stanton number
T	T---	Temperature
TI	FSTINT	Freestream turbulence intensity, in percent
u		Streamwise velocity component
w	W	Exponent in viscosity power law relation
x,X	X---	Streamwise coordinate defined in Fig. 1; in Section II only, x refers to coordinate along boundary
y,Y	Y---	Normal coordinate defined in Fig. 1; in Section II only, y refers to coordinate normal to boundary
Z	Z---	Momentum parameter defined by $Z = \delta_2 R_{\delta_2}^n$
α		Angle measured from stagnation point on circular cylinder, Fig. 16

<u>Text</u>	<u>Computer Program</u>	<u>Definition</u>
β	BSTART	$\beta\pi \equiv \text{BSTART} * \text{PI}$ is included angle at leading edge for plane or axisymmetric external flows, Fig. 1
β_E		Transformed angle for axisymmetric flows, $\beta_E = \frac{\beta}{3 - \beta}$
γ	G	Specific heat ratio of ideal gases
δ	---D	Boundary layer thickness
δ_1	D1	Displacement thickness, $\delta_1 = \int_0^{\delta} \left(1 - \frac{\rho}{\rho_{\delta}} \frac{u}{u_{\delta}}\right) dy$
δ_2	D2	Momentum thickness, $\delta_2 = \int_0^{\delta} \frac{\rho}{\rho_{\delta}} \frac{u}{u_{\delta}} \left(1 - \frac{u}{u_{\delta}}\right) dy$
δ_3	--D3	Mechanical energy loss thickness, $\delta_3 = \int_0^{\delta} \frac{\rho}{\rho_{\delta}} \frac{u}{u_{\delta}} \left[1 - \left(\frac{u}{u_{\delta}}\right)^2\right] dy$
δ_4	D4--	Density loss thickness, $\delta_4 = \int_0^{\delta} \frac{\rho}{\rho_{\delta}} \frac{u}{u_{\delta}} \left(\frac{\rho_{\delta}}{\rho} - 1\right) dy$
θ	THET---	Temperature ratio, $\theta = \frac{T_e - T_w}{T_e - T_{\delta}}$
π	PI	Constant, 3.14159----
λ	PPAR---	Pohlhausen parameter, $\lambda = \frac{\rho_w (\delta_2)^2}{\mu_w} \frac{du_{\delta}}{dx}$
μ	MU---	Absolute viscosity

<u>Text</u>	<u>Computer Program</u>	<u>Definition</u>
ξ		Dummy integration variable in Eqs. (37) and (38); streamwise coordinate along boundary
ρ		Density
τ		Shear stress

II. SUBSCRIPTS AND SUPERSSCRIPTS

<u>Text</u>	<u>Computer Program</u>	<u>Definition</u>
e		Denotes adiabatic wall conditions
i,i+1,i-1	----I, ----IP1, ----IM1	Subscripted quantity evaluated at $X = X_i, X_{i+1}$ or X_{i-1}
inst	---INST	Instability
j,j+1		Superscripted quantity evaluated at (j)th or (j+1)st iteration
lam	-----L	Laminar
m	----M	Mean value
r		Reference
sep		Separation
trans	---TRANS	Transition
turb	-----T	Turbulent
u	--U---	Subscripted quantity depends only on velocity profile
w	--W---	Subscripted quantity evaluated at the wall
x		Subscripted quantity based on distance from stagnation point
δ	-D----	Subscripted quantity evaluated at the edge of the boundary layer
o		Refers to stagnation conditions
∞	---INF	Refers to conditions of approach flow
-	---B--	Refers to average values over integration step

I. INTRODUCTION

In a large number of flow situations of engineering interest, the characteristics of the developing boundary layer are of practical importance. Examples include the design of supersonic nozzles, flow over airfoils, incipience of separation in pressure recovery devices, boundary layer growth on missile bodies and afterbodies and the resulting effect on the base region, etc.

The purpose of this study was to develop an easy-to-use FORTRAN IV computer program which could be employed routinely as a boundary layer predictive tool for a wide variety of two-dimensional ideal gas flows. A number of the available methods were considered, with the rather well-documented [1-3]* integral method of Walz and his co-workers being chosen for use. The motivation for this choice was in part due to the fact that the method described in [3] was one of the four integral methods judged "good" at the Stanford conference on incompressible turbulent boundary layers and in part due to the flexibility of Computational Method II which is detailed in [1]. This method may be applied to incompressible or compressible, laminar or turbulent, plane two-dimensional or axisymmetric boundary layers in arbitrary pressure gradients, either with or without heat transfer. The computations may be started at a stagnation point, a sharp leading edge, or at an arbitrary streamwise location for either laminar or turbulent boundary layers with the proper specification of the starting parameters. Transition is predicted using the laminar instability calculations of Wazzan, et. al. [4], together with the data of Granville [5] for the distance between the instability and transition points. Alternately, the transition point can be specified externally as an input. Separation is also predicted.

Included in this report is an outline of the theory upon which the method is based, a description of the computer program (COMPBL) which has been developed, detailed input instructions and example input and output, and comparisons of computed results to both experiments and analytical solutions for a number of flow fields. A complete program listing and explanation of error messages are included in the appendices.

*Numbers in brackets refer to entries in REFERENCES.

II. THEORETICAL DEVELOPMENT

A. General

Computational Method II of Walz [1], on which program COMPBL is based, utilizes the integral momentum and mechanical energy equations for the boundary layer:

$$\frac{d\delta_2}{dx} + \delta_2 \cdot \frac{1}{u_\delta} \frac{du_\delta}{dx} \left[2 + \frac{\delta_1}{\delta_2} - M_\delta^2 \right] - \frac{\tau_w}{\rho_\delta u_\delta^2} = 0 \quad (1)$$

$$\frac{d\delta_3}{dx} + \delta_3 \cdot \frac{1}{u_\delta} \frac{du_\delta}{dx} \left[3 + 2 \frac{\delta_4}{\delta_3} - M_\delta^2 \right] - \frac{2}{\rho_\delta u_\delta^3} \int_0^\delta \tau \, du = 0. \quad (2)$$

Momentum equation (1) is transformed by introducing the new dependent variable,

$$z = \delta_2 R \delta_2^n, \quad (3)$$

where

$$R \delta_2 = \frac{\rho_\delta u_\delta \delta_2}{\mu_w}, \quad (4)$$

to

$$z' + z \frac{u_\delta'}{u_\delta} F_1 - F_2 = 0 \quad \text{where } (' \equiv \frac{d}{dx}). \quad (5)$$

F_1 and F_2 are universal functions which may be evaluated once the trial solutions for the velocity profiles for laminar and turbulent boundary layers and the coupling law between the temperature and velocity profiles are specified.

* The coordinate x used in this section is the coordinate along the boundary and is not necessarily the same as the coordinate x used in Section III or program COMPBL.

The ratio,

$$H^* \equiv \frac{\delta_3}{\delta_2} = \frac{\int_0^\delta \frac{\rho u}{\rho_\delta u_\delta} [1 - (\frac{u}{u_\delta})^2] dy}{\int_0^\delta \frac{\rho u}{\rho_\delta u_\delta} (1 - \frac{u}{u_\delta}) dy} \quad (6)$$

is introduced into the mechanical energy equation (2) to obtain

$$H^*{}' + H^* \frac{u_\delta'}{u_\delta} F_3 - \frac{F_4}{Z} = 0 \quad (7)$$

where F_3 and F_4 are also universal functions dependent on the trial velocity profiles, the temperature-velocity coupling law, and for the turbulent case, empirical shear stress and dissipation integral relations.

Except for the small influence of R_{δ_2} on F_4 , the universal functions may be reduced to depend only on H , M_δ , and θ where $M_\delta(x)$ and the heat transfer parameter,

$$\theta(x) \equiv \frac{T_e - T_w}{T_e - T_\delta} \quad (8)$$

are specified inputs. H is defined by:

$$H = (H^*)_u = \frac{(\delta_3)_u}{(\delta_2)_u} = \frac{\int_0^\delta \frac{u}{u_\delta} [1 - (\frac{u}{u_\delta})^2] dy}{\int_0^\delta \frac{u}{u_\delta} (1 - \frac{u}{u_\delta}) dy} \quad (9)$$

where the u subscript denotes that the enclosed quantity depends only on the velocity distribution in the boundary layer (i.e., incompressible and adiabatic). Noting the integral definitions of H^* and H in Eqs. (6) and (9) and, in particular, the similar manner in which the factor ρ/ρ_δ enters the integrands in the numerator and denominator of H^* , it is reasonable to expect as a first approximation that,

$$H^* \approx H. \quad (10)$$

The final relation used for

$$H^* = H^*(H, M_\delta, \theta) \quad (11)$$

is based on the consideration of limiting cases as established by Jischa [6]. For $M_\delta = 0$ this relation yields $H^*/H = 1$ and for $M_\delta \gg 1$, $H^*/H \approx 1.18$ (depending on the value of θ); thus the approximation (10) is confirmed. The reduction of the universal functions for the general compressible case with heat transfer to H -dependent functions which characterize incompressible, adiabatic (constant property) flows requires the development of additional relationships which will not be detailed here. The interested reader is referred to [1].

Once the universal functions have been specified as functions of H , M_δ , and θ for laminar and turbulent boundary layers, the solution proceeds as a step-by-step simultaneous integration of Eqs. (5) and (7), with Eq. (11) also utilized. This procedure is carried out with a predictor-corrector iterative scheme as follows. Given values of H_i and Z_i at point x_i in the boundary layer, a value of H_{i+1} at x_{i+1} is first predicted (using dH/dx between x_i and x_{i-1}). Average values of the universal functions over the integration step $\Delta x = (x_{i+1} - x_i)$ can then be evaluated, e.g., $\bar{F}_1 = F_1((H_i + H_{i+1})/2, (M_{\delta i} + M_{\delta i+1})/2, (\theta_i + \theta_{i+1})/2)$. Using these average values and approximating the variation of the freestream velocity, u_δ , as a straight line over the interval Δx , i.e.,

$$u_\delta(x) = (u_\delta)_i + \left[\frac{(u_\delta)_{i+1} - (u_\delta)_i}{x_{i+1} - x_i} \right] (x - x_i), \quad (12)$$

Eqs. (5) and (7) become linear, first-order, ordinary differential equations. They are integrated, respectively, to:

$$Z_{i+1} = A_Z Z_i + B_Z \bar{F}_2 \Delta x \quad (13)$$

and

$$H_{i+1}^* = A_H H_i^* + B_H \bar{F}_4 \frac{2}{(Z_{i+1} + Z_i)} \Delta x \quad (14)$$

where

$$A_Z = \left(\frac{u_{\delta_i}}{u_{\delta_{i+1}}} \right)^{\bar{F}_1}, \quad B_Z = \frac{\left[1 - \left(\frac{u_{\delta_i}}{u_{\delta_{i+1}}} \right)^{1+\bar{F}_1} \right]}{(1 + \bar{F}_1) \left(1 - \frac{u_{\delta_i}}{u_{\delta_{i+1}}} \right)} \quad (15)$$

and

$$A_H = \left(\frac{u_{\delta_i}}{u_{\delta_{i+1}}} \right)^{\bar{F}_3}, \quad B_H = \frac{\left[1 - \left(\frac{u_{\delta_i}}{u_{\delta_{i+1}}} \right)^{1+\bar{F}_3} \right]}{(1 + \bar{F}_3) \left(1 - \frac{u_{\delta_i}}{u_{\delta_{i+1}}} \right)} \quad (16)$$

The value of H_{i+1} at x_{i+1} is then found by inverting Eq. (11) using the value of H_{i+1}^* from (14). If this corrected value of H_{i+1} agrees with the predicted value to within an amount specified by a convergence criterion, the boundary layer parameters such as displacement and momentum thicknesses, skin friction coefficient, etc. are determined. If not, iterations proceed until convergence for H_{i+1} is obtained. Note that this scheme obviates numerical differentiation of the given freestream velocity distribution and that the justification for linearizing $u_\delta(x)$ over the interval Δx rests on taking a large number of base points, x_i , since any function can be approximated as piecewise linear if the intervals are sufficiently small.

B. Laminar Boundary Layers

For laminar boundary layers, the universal functions are evaluated using a one-parameter trial solution for the velocity distribution based on the Hartree wedge-flow profiles. The separation profile is given when H falls to a value of 1.515 in which case the skin friction simultaneously vanishes, viz.,

$$(H_{\text{sep}})_{\text{lam}} = 1.515. \quad (17)$$

In accelerated flows values of H up to 1.7 are encountered. The exponent n in the definition of Z , Eq. (3), has a value of 1.0 for laminar flow.

The development of the universal functions for both laminar and turbulent boundary layers is also dependent on the coupling

relation between the velocity and temperature profiles. The equation used is based on the analysis of van Driest [7] and is essentially an extension of the Crocco-Busemann relation for $Pr \neq 1$:

$$\frac{T}{T_\delta} = a + b\left(\frac{u}{u_\delta}\right) + c\left(\frac{u}{u_\delta}\right)^2 \quad (18)$$

where

$$\begin{aligned} a &= \frac{T_w}{T_\delta} = 1 + r \frac{(\gamma - 1)}{2} M_\delta^2 - \frac{T_e - T_w}{T_\delta} \\ &= 1 + r \frac{(\gamma - 1)}{2} M_\delta^2 (1 - \theta) \end{aligned} \quad (19)$$

$$b = \frac{T_e - T_w}{T_\delta} = \theta r \frac{(\gamma - 1)}{2} M_\delta^2 \quad (20)$$

$$c = -r \frac{(\gamma - 1)}{2} M_\delta^2 \quad (21)$$

and r is the recovery factor in Eqs. (19-21).

Equation (18) is derived strictly under the assumptions that $Pr \approx 1$ and that the streamwise wall temperature and pressure gradients vanish (i.e., $dT_w/dx = dp/dx = 0$). However, as pointed out by White [8], this approximation is "surprisingly accurate for gases under general boundary-layer flow conditions at high and low Mach numbers and for laminar and turbulent flow."

Based on the temperature distribution of Eq. (18), the dimensionless local heat flux is given by the Reynolds analog expression

$$\frac{q_w}{\rho_\delta u_\delta^3} = -\frac{r}{2} \frac{c_f}{2s} \theta, \quad (22)$$

where s is the Reynolds analogy factor. Section E will give an alternate method of calculating the heat transfer when strong wall temperature and/or pressure gradients are present.

C. Turbulent Boundary Layers

The trial solution for the velocity profile used in developing the universal functions for the turbulent boundary layer is a combination of the turbulent log law and the law of the wake suggested by Coles [9]. In addition, the empirical shear stress relation of Ludwig and Tillmann [10] and the empirical dissipation laws of both Rotta [11]-Truckenbrodt [12] and Felsch [13,1,2,3] are used. The Rotta-Truckenbrodt relation is employed for flows with favorable pressure gradients, while in regions of adverse pressure gradient, the Felsch law is used. The temperature and velocity profiles are again coupled using Eq. (18).

Near the separation point for turbulent boundary layers, it has been noted that the velocity profiles actually depend on two parameters, rather than the single one used in this analysis. Hence, there is no single value of H which can be assigned to the turbulent separation point, i.e., $1.50 < (H_{sep})_{turb} < 1.57$. However, the following approximation is used:

$$(H_{sep})_{turb} \approx (H_{sep})_{lam} = 1.515. \quad (23)$$

The upper bound on H for turbulent boundary layers is 2.0. The Ludwig-Tillmann exponent, $n = 0.268$, is used in the definition of Z , Eq. (3).

D. Transition

Transition from a laminar to a turbulent boundary layer is accomplished in program COMPBL either by specifying the axial location of transition as an input (variable XTRAN) or by normal calling of the transition subroutine (TRANS). This subroutine utilizes a correlation to the incompressible, adiabatic, laminar stability computations of Wazzan, et. al. [4] as listed in White [8]. The instability point is located when $(R\delta_2)_u$, which is monitored at each axial location in the laminar boundary layer, exceeds $(R\delta_2)_{inst}$ from the Wazzan correlation. The transition location is then found by calculating the mean Pohlhausen parameter, λ_m , from:

$$\lambda_m = \frac{1}{(x_{trans} - x_{inst})} \int_{x_{inst}}^{x_{trans}} \lambda(x) dx \quad (24)$$

where

$$\lambda = \frac{\rho_w (\delta_2)_u^2}{\mu_w} \frac{du_\delta}{dx} \quad (25)$$

at each streamwise location and using the curve fit listed in White [8] to Granville's [5] data for the distance between the instability and transition locations. In addition, a correction factor is employed to account for the effects of free-stream turbulence intensity on the transition location. The expression used is the correlation given by Korst, et. al. [14] to Granville's flat plate data. The combination of these two curve fits gives the following result:

$$(R\delta_2)_{\text{trans}} = (R\delta_2)_{\text{inst}} + (450 + 400e^{60\lambda_m})(900 - 760\text{TI} + 159\text{TI}^2)/900 \quad (26)$$

where TI is the freestream turbulence intensity, in percent. For freestream turbulence intensities exceeding approximately 2.16%, the laminar instability and transition points coincide.

Once the transition point has been located, the calculations are switched from the laminar to the turbulent regime with the aid of the following relations:

$$H_{\text{turb}} = H_{\text{lam}} \quad (27)$$

and $(\delta_2)_{\text{turb}} = (\delta_2)_{\text{lam}}$ (28)

The second relation implies that,

$$z_{\text{turb}} = \delta_2 R\delta_2^{0.268} = z_{\text{lam}} R\delta_2^{-0.732} \quad (29)$$

Thus in this technique, the momentum thickness, δ_2 , is continuous across the transition point, whereas other of the derived boundary layer parameters such as displacement and boundary layer thicknesses, skin friction coefficient, etc., are not, due to their totally different behavior for laminar and turbulent boundary layers.

E. Heat Transfer Correction

The coupling law Eq. (18) was derived under the assumptions that the Prandtl number is approximately unity and that the pressure and streamwise wall temperature gradients vanish. In the situation where only the properties of the velocity boundary layer are of predominant interest, this relation is adequate even if the assumptions are badly violated, since in this case only the average properties of the temperature profile enter the analysis. But this is not the case when the heat transfer is desired; then the actual shape of the temperature distribution is of utmost importance since the local heat flux is proportional to the derivative of this distribution in the direction normal to the wall.

To account for the effects that the pressure and streamwise wall temperature gradients (with $Pr \approx 1$) might have on the calculation of the heat transfer, Walz [1] substituted the following trial solution for the temperature profile,

$$\frac{T}{T_\delta} = a + [b + K(x)] \frac{u}{u_\delta} + [c - K(x)] \left(\frac{u}{u_\delta}\right)^2, \quad (30)$$

into the thermal energy integral equation to obtain:

$$K' + KF_5 - F_6 = 0. \quad (31)$$

Note that Eq. (18) is a special case of Eq. (30) with $K \equiv 0$. Part of the rationale behind this choice is that analytical solutions, such as [15], have shown that for nonisothermal walls the local heat flux need not vanish when the temperature difference ($T_e - T_w$) vanishes (i.e., $b = 0$) as would be the case when using Eq. (18). To account for this fact, Walz included the correction factor $K(x)$ in the coefficient of u/u_δ in the trial temperature profile.

The coefficients F_5 and F_6 in Eq. (31) are again universal functions and are evaluated in the same manner as explained above for the universal functions of the momentum and mechanical energy equations. Equation (31) is solved in parallel with Eqs. (5) and (7), so that the complete scheme involves simultaneous integration of the momentum, mechanical energy, and thermal energy integral equations together with relation (11) for $H^*(H, M\delta, \theta)$. The dimensionless heat flux in this case is given by a "modified Reynolds analogy":

$$\frac{q_w}{\rho_\delta u_\delta} = \frac{-r}{2} \frac{c_f}{2s} \theta \left(1 + \frac{K}{b}\right). \quad (32)$$

As shown later, however, this heat transfer correction procedure has met with only moderate success.

The theory discussed above in Sections A, B, C, and E is a synopsis of that developed by Walz in [1]. For further details, this reference should be consulted.

III. COMPUTER PROGRAM

A. General Description

Program COMPBL has the following characteristics and capabilities:

1. Computational Method II of Walz [1] is utilized to compute the integral parameters for two-dimensional laminar or turbulent boundary layers.
2. Arbitrary pressure gradients are handled with the boundary layer either compressible or incompressible, axisymmetric or plane two-dimensional, and with or without heat transfer.
3. The transition location may either be specified as an input or predicted by the Wazzan [4]-Granville [5] method described in Section II-D.
4. Separation is predicted when the value of the shape parameter $H \equiv (\delta_3)_u / (\delta_2)_u$ falls to 1.515 in which case the skin friction simultaneously vanishes.
5. The computations may be started with the boundary layer either laminar or turbulent at a stagnation point, a sharp leading edge, or an arbitrary axial location.
6. Freestream velocity input data may be specified by the Mach number M or the dimensionless velocity ratio $M^* \equiv u/c^*$, while wall temperature data may be input as either $\theta \equiv (T_e - T_w) / (T_e - T_\delta)$ or T_w/T_∞ .
7. Options are available whereby:
 - a. Calling of the transition subroutine is suppressed for boundary layers thought to remain laminar;
 - b. The heat transfer calculation is corrected using the method described in Section II-E; and
 - c. Intermediate values of H and other variables are printed for debugging purposes.
8. COMPBL is written in FORTRAN IV with typical run times on the CDC CYBER 175 of $\frac{1}{2}$ - 1 CPU seconds.

Following is a list of the limitations of the method and program:

1. The program is limited to ideal gas flows with certain of the input variables defaulted to values for air. However, these defaults are easily overridden on input (see Section III-B).
2. The effects of surface roughness, freestream turbulence level (except for its influence on the transition location), shock-boundary layer interactions, and varying stagnation pressure are not considered.
3. Transition is assumed to occur at a point in an essentially discontinuous manner.
4. The phenomena of relaminarization and laminar separation with reattachment are not treated automatically. These

cases may be calculated, however, by restarting the computations at the proper location.

5. The output consists of only the integral boundary layer parameters. Velocity and temperature profiles are not calculated.

B. Input/Output Variable List and Discussion

A list of the input variables read from file INPUT follows. The first four (4) variables are literal variables:

FLOW.....literal variable describing the initial flow regime of the boundary layer; equal to "LAMINAR" or "TURBULENT"
GEOM.....literal variable describing the two-dimensional geometry; equal to "PLANE 2-D" or "AXISYM"
MTYPE.....literal variable describing whether velocity input data is in terms of Mach number, M, or $M^* = u/c^*$; equal to "MACH" or "MSTAR"
TTYPE.....literal variable describing whether wall temperature input data is in terms of $\theta = (T_e - T_w)/(T_e - T_\delta)$ or T_w/T_∞ , equal to "THETA" or "TWTINF"

The next seventeen (17) variables are entered via NAMELIST BL:

ZSTART...starting value of Z (default = 0.0); see Section III-C
HSTART...starting value of H (default = 1.572); see Section III-C
BSTART...(BSTART * PI) is the included angle at the leading edge for both plane two-dimensional and axisymmetric external flows (default = 0.0); see Fig. 1 and Section III-C
MINF.....Mach number (or M^* for MTYPE = "MSTAR") of approaching flow; see Fig. 1
REINFL...unit Reynolds number of approach flow, $\rho_\infty U_\infty / \mu_\infty$; see Fig. 1
XTRAN....X location of specified transition point (default = 0.0)
FSTINT...freestream turbulence intensity, in percent (default = 0.0); used only in transition subroutine to locate transition point
G.....ratio of specific heats (default = 1.405)
W.....exponent on viscosity power law, i.e.,

$$\frac{\mu}{\mu_0} = \left(\frac{T}{T_0}\right)^W \quad (\text{default} = 0.7)$$

RL.....laminar recovery factor (default = 0.85)
RT.....turbulent recovery factor (default = 0.88)
SL.....laminar Reynolds analogy factor (default = 0.80)

ST.....turbulent Reynolds analogy factor (default = 0.82)
 EPS.....convergence criterion variable, e.g., convergence
 on H if:

$$\left| \frac{H_i^{j+1} - H_i^j}{H_i^{j+1}} \right| < \text{EPS} \quad (\text{default} = 1.0 \text{ E-4})$$

NOTRAN...logical variable which if .TRUE. suppresses calling
 of the transition subroutine for boundary layers
 thought to remain laminar (default = .FALSE.).
 Note that NOTRAN = .TRUE. is equivalent to setting
 XTRAN to a value greater than the largest X input
 location.
 HTCORR...logical variable which if .TRUE. invokes the use
 of the heat transfer correction procedure described
 in Section II-E for calculation of the local dimen-
 sionless heat flux (default = .FALSE.)
 ERROR....logical variable which if .TRUE. causes intermediate
 H values and variables associated with the turbu-
 lent dissipation integral and heat transfer correc-
 tion parameter to be printed for debugging purposes
 (default = .FALSE.)

The next five (5) input variables give the local informa-
 tion for each point at which the boundary layer parameters are
 to be calculated:

X.....axial location of the boundary point; see Fig. 1
 Y.....normal location of the boundary point; see Fig. 1
 M OR M*..local freestream Mach number or M* (depending on
 the value of MTYPE)
 R.....cross-sectional radius for axisymmetric bodies or
 normal distance from centerline to boundary for
 plane two-dimensional bodies; see Fig. 1
 THETA OR
 TWTINF...local wall temperature data (depending on the value
 of TTYPE); for adiabatic flows THETA \equiv 0

The output variables written to file OUTPUT are:

X.....axial location of the boundary point
 Z.....local value of $Z = \delta_2 R \delta_2^n$
 H.....local value of

$$H \equiv \frac{(\delta_3) u}{(\delta_2) u} = \frac{\int_0^\delta \frac{u}{u_\delta} [1 - (\frac{u}{u_\delta})^2] dy}{\int_0^\delta \frac{u}{u_\delta} (1 - \frac{u}{u_\delta}) dy}$$

D1D2.....shape factor,

$$\frac{\delta_1}{\delta_2} = \frac{\int_0^{\delta} (1 - \frac{\rho u}{\rho_{\delta} u_{\delta}}) dy}{\int_0^{\delta} \frac{\rho u}{\rho_{\delta} u_{\delta}} (1 - \frac{u}{u_{\delta}}) dy}$$

D1.....displacement thickness, $\delta_1 = \int_0^{\delta} (1 - \frac{\rho u}{\rho_{\delta} u_{\delta}}) dy$

D2.....momentum thickness,

$$\delta_2 = \int_0^{\delta} \frac{\rho u}{\rho_{\delta} u_{\delta}} (1 - \frac{u}{u_{\delta}}) dy$$

D999.....99.9% boundary layer thickness, i.e.,

$$\frac{u(y = D999)}{u_{\delta}} = 0.999$$

RD2.....momentum thickness Reynolds number, $R_{\delta_2} = \frac{\rho_{\delta} u_{\delta} \delta_2}{\mu_w}$

CF.....local skin friction coefficient, $c_f = \frac{\tau_w}{\frac{1}{2} \rho_{\delta} u_{\delta}^2}$

QDIM.....dimensionless local wall heat flux, $\frac{q_w}{\rho_{\delta} u_{\delta}^3}$

The variables written to file TAPE4 are:

X.....axial location of the boundary point

RCORR.....corrected radius or normal location, $RCORR = R + D1$

File TAPE4 contains corrected boundary coordinate information consisting of the axial coordinate, X, and the corrected axisymmetric radius or plane two-dimensional centerline distance obtained by adding the displacement thickness to R. This information can be used, for example, in the design of supersonic nozzles where the wall coordinates obtained from the inviscid solution are relieved by an amount equal to the displacement thickness or for external flows where the corrected body shape is obtained by adding the displacement thickness to the original body shape.

A sketch of the coordinate system setup is shown in Fig. 1. The orientation of the X-Y axes is completely arbitrary as shown by the possible choices X-Y, X'-Y', and X''-Y'' in each of the two cases sketched. The only exceptions to this statement are in the case where the transition location is specified as an input. In this situation it is assumed that axial coordinate X increases in the downstream direction (which is the case for all choices shown in Fig. 1), and that specified location XTRAN is not equal to 0.0 (which is equivalent to "OFF"). For all choices of the X-Y axes, R remains the body

radius for axisymmetric geometries or the distance between the centerline and the boundary for plane two-dimensional geometries. In the axisymmetric case R must be entered while for plane bodies R is entered only if the corrected boundary coordinates are desired.

The boundary is approximated by a series of straight-line segments; the distance between any two input points is given by:

$$\Delta x = [(x_{i+1} - x_i)^2 + (y_{i+1} - y_i)^2]^{1/2}. \quad (33)$$

For increased accuracy, therefore, use of a large number of base points is recommended since both the boundary location and the freestream velocity distribution are approximated by piecewise linear functions. The program also tends to run faster when using a larger number of input locations because savings in the number of iterations required for convergence usually outweighs the fact that more points are calculated. It should also be noted that the program does a certain amount of interval subdivision automatically so that the number of base points actually calculated is greater than the number entered.

Also shown in Fig. 1 is the location of the upstream variables M_∞ (MINF), Re_∞/L (REINFL), and T_∞ . This location may be either the undisturbed approach flow as shown in the external flow of Fig. 1(a) or the freestream adjacent to the first input point as shown in Fig. 1(b). T_∞ is the approach flow static temperature used in forming the dimensionless wall temperature ratio $T_w/T_\infty \equiv TWTINF$. For flows in which the freestream stagnation conditions are known, the unit approach Reynolds number $Re_\infty/L \equiv REINFL$, may be calculated with the aid of the following equation:

$$\frac{Re_\infty}{L} \equiv REINFL = \frac{p_\infty M_\infty}{\left[\frac{\mu_0}{M W} \frac{T_\infty}{\gamma} \right]^{1/2} \left[1 + \frac{\gamma - 1}{2} M_\infty^2 \right]^{1/2} \frac{\gamma + 1}{2(\gamma - 1)} - W} \quad (34)$$

The meaning of variable $BSTART$ is also shown in Fig. 1(a).

The input variables G , W , RL , RT , SL , and ST have been defaulted to values corresponding to air. For gases other than air the appropriate values for the specific heat ratio, G , and the viscosity power law exponent, W , should be entered with the following expressions for recovery factors and Reynolds analogy factors being recommended:

$$RL \approx Pr^{1/2} \quad RT \approx Pr^{1/3} \quad SL \approx ST \approx Pr^{2/3}. \quad (35)$$

For each base point, the output is written to files OUTPUT and TAPE4 and is identified only by the axial coordinate, X , of the point. In addition, the boundary layer parameters are written only for locations corresponding to the input base points, with two possible exceptions. If ERROR = .TRUE. is specified, the output at all of the calculated points, including the automatic subdivisions, is printed together with some intermediate results. The printout may become quite long in this case. The second exception is that the output data for the base point directly downstream from a transition location may not be printed, with the results at an intermediate subdivided location being substituted. This is a consequence of the automatic interval dividing scheme which is used. When transition is to be predicted, it is recommended that an initial run be made to approximately locate the laminar instability and transition points and then the boundary layer recalculated with a relatively fine gridpoint spacing around these locations so that the instability and transition points may be found more precisely.

The variables Z and H have been included in the output to provide a means for monitoring the calculations and the state of the boundary layer. As mentioned previously, in any region where H is only slightly greater than 1.515 for laminar boundary layers or where $1.515 < H < 1.57$ for turbulent boundary layers, the onset of separation is imminent. The output values of Z and H are also helpful in setting the values of ZSTART and HSTART when the boundary layer calculations are restarted at some downstream location. Downstream restarting of the calculations may be used, for example, if convergence problems (hopefully nonexistent) are encountered in the integration scheme or if the phenomena of relaminarization or laminar separation with reattachment, which are not handled automatically, are to be analyzed. This procedure avoids recalculation of the upstream portion of the flow.

The local dimensionless heat flux which is written to OUTPUT is defined as:

$$QDIM = \frac{q_w}{\rho_\delta u_\delta^3}, \quad (36)$$

where q_w is the local wall heat flux. The total heat per unit depth transferred from the wall to the boundary layer for plane two-dimensional geometries is given by:

$$Q = \int_0^L q_w(\xi) d\xi, \quad (37)$$

while for axisymmetric bodies the heat transfer is given by,

$$Q = 2\pi \int_0^L q_w(\xi) R(\xi) d\xi \quad (38)$$

where ξ is measured along the boundary. Positive signs for q_w and Q indicate heat transfer from the wall to the boundary layer.

The dimensional variables in the input/output lists are: ZSTART, REINFL, XTRAN, X, Y, R, Z, D1, D2, D999, and RCORR. All have dimensions of length, [L], except for REINFL which has dimensions of reciprocal length, [L]⁻¹. The only requirement that need be met concerning units is that input variables ZSTART, REINFL, XTRAN, X, Y, and R be entered with the same length unit. On output Z, D1, D2 and D999 will have this same unit of length.

Specific instructions regarding the input procedure together with an example are given in Section III-D.

C. Starting of the Computations

In order to begin integrating the first order ordinary differential equations given by (5) and (7) initial values of Z and H must be specified. This is accomplished through input variables ZSTART and HSTART as follows.

ZSTART When the computations are started at a sharp leading edge or a stagnation point, the value ZSTART = 0.0 is used. If, however, the calculations are started at an arbitrary streamwise location, where the boundary layer thickness is not zero, the definition of Z is employed:

$$ZSTART = \delta_2 R \delta_2^n \quad (39)$$

n = 1.0 for laminar boundary layers
= 0.268 for turbulent boundary layers

Hence, the momentum thickness, δ_2 , must be known at the starting location. The momentum thickness Reynolds number, $R\delta_2$,

may be calculated from the unit Reynolds number of the approach flow, Re/L , as:

$$R_{\delta_2} = \frac{\rho_{\delta} u_{\delta} \delta_2}{\mu_w} = \delta_2 \frac{Re_{\infty}}{L} \frac{M_{\delta_i}^*}{M_{\infty}^*} \left(\frac{1 + \frac{\gamma-1}{2} M_{\infty}^2}{1 + \frac{\gamma-1}{2} M_{\delta_i}^2} \right)^{\frac{1}{\gamma-1}}$$

$$\left[\frac{1 + \frac{\gamma-1}{2} M_{\delta_i}^2}{(1 + r \frac{\gamma-1}{2} M_{\delta_i}^2 [1 - \theta_i]) (1 + \frac{\gamma-1}{2} M_{\infty}^2)} \right]^w \quad (40)$$

where the subscript "i" denotes the starting location.

HSTART For stagnation points or sharp leading edges the procedure for determining HSTART is the same whether the boundary layer is started in the laminar or turbulent regimes since the first step is always calculated as laminar (although it can be made arbitrarily small). For plane two-dimensional geometries and non-zero included wedge angles, $\beta\pi \equiv \text{BSTART}$: $\text{PI} \neq 0$, the starting value of H in both the incompressible and compressible cases is obtained from Table I, which is a compilation of the Hartree solutions, since in the immediate vicinity of the leading edge the flow may be considered incompressible. For plane flat plate flows, $\beta\pi = 0$, the starting value of H is obtained from Fig. 2, which details the effect of compressibility (M_{∞}) on HSTART.

For axisymmetric geometries with subsonic approach flow, $0 < M_{\infty} \leq 1$, HSTART is obtained from Table I using the transformed angle β_E where:

$$\beta_E = \frac{\beta}{3 - \beta} \quad (41)$$

For supersonic flow, $M_{\infty} > 1$, approaching on axisymmetric body, the flow fields along the cone approximating the bow of the body and along a flat plate are similar so that Fig. 2 is also used in this case.

To determine HSTART for boundary layer calculations initiated at an arbitrary axial location, either the local skin friction coefficient, c_f , or the displacement thickness, δ_1 , must be known at the starting location in addition to the momentum thickness which is required for ZSTART. For laminar

boundary layers HSTART may be determined by solving either of the following transcendental equations for H:

$$c_f \text{ known: } \frac{(H - 1.515)^{0.7158}}{[1 + r \frac{\gamma-1}{2} M_{\delta_i}^2 (H - \theta_i) (2 - H)]} = \frac{c_f R \delta_2}{3.4522} \quad (42)$$

or

$$\frac{\delta_1}{\delta_2} \text{ known:}$$

$$[4.0306 - 4.2845(H - 1.515)^{0.3886}] [1 + r \frac{\gamma-1}{2} M_{\delta_i}^2 (H - \theta_i) (2 - H)] + r \frac{\gamma-1}{2} M_{\delta_i}^2 (H - \theta_i) = \frac{\delta_1}{\delta_2} \quad (43)$$

For turbulent boundary layers, the following equations are used:

$$c_f \text{ known: } \frac{(H - 1.515)^{0.7}}{[1 + r \frac{\gamma-1}{2} M_{\delta_i}^2 (H - \theta_i) (2 - H)]} = \frac{c_f R \delta_2^{0.268}}{0.07788} \quad (44)$$

or

$$\frac{\delta_1}{\delta_2} \text{ known:}$$

$$[1 + 1.48(2-H) + 104(2-H)^{6.7}] [1 + r \frac{\gamma-1}{2} M_{\delta_i}^2 (H - \theta_i) (2 - H)] + r \frac{\gamma-1}{2} M_{\delta_i}^2 (H - \theta_i) = \frac{\delta_1}{\delta_2} \quad (45)$$

The approximation $H^* \approx H$ is used in the above equations and is completely adequate for the purpose of determining HSTART. For incompressible boundary layers, $M_{\delta_i} \ll 1$, the above equations are greatly simplified and all but (45) can be solved explicitly for H. For cases with heat transfer where the Stanton number, St, is known, HSTART may be found from Eqs. (42) or (44) using $c_f = (St)(2s)$, assuming that the Reynolds analogy is accepted.

BSTART Variable BSTART is required only for boundary layer calculations started at sharp leading edges or stagna-

tion points. For either axisymmetric or plane geometries
BSTART * PI = $\beta\pi$ is the total included angle at the nose.

A summary of the procedure used in determining the starting values ZSTART, HSTART, and BSTART is presented in Table II.

D. Input Instructions and Example

The input variables listed in Section III-C are entered in the following way. The first card (record) is used to enter a title which is printed on files OUTPUT and TAPE4 to identify the results. Any message up to 80 columns can be used, but for aesthetic reasons the title should be centered in the 80 columns. It is suggested that the length unit for dimension [L] be entered as part of this title. On the next card the four literal variables FLOW, GEOM, MTYPE, and TTYPE are input in 4A10 format. The value of these literals should be left justified in each 10 column block. NAMELIST "BL" which encompasses input variables ZSTART - ERROR is input via the next card(s). The first column on each NAMELIST card should be blank. All variables in "BL" except MINF and REINFL are defaulted so that at a minimum only these two and the selected variables to be overridden need be entered. The remaining cards (records) contain the local data: X, Y, M (or M*), R, THETA (or TWTINF) for each point at which the boundary layer parameters are to be found. These variables are entered in 5F10 format and as many points as desired can be used. For boundary layers starting at sharp leading edges or stagnation points, the first of these local data cards should contain the information for the tip. In the case where the computations are started at an arbitrary axial location, the first local data card should consist of the information for the point at which ZSTART and HSTART were determined.

As an example, the flow over a NACA 0012 airfoil at zero angle of attack is considered. This example is taken from the report by McNally [16] who cites Becker [17] as the original source of the data. The airfoil profile and freestream M* distribution are shown in Fig. 4(b).

A schematic of the input file for this case is shown in Fig. 3. The first card contains the centered title, while the second contains the input values of literal variables FLOW, GEOM, MTYPE, and TTYPE. For this example, the boundary layer is assumed to begin in the LAMINAR regime; the airfoil has PLANE 2-D geometry; the velocity input data is in terms of MSTAR; and the wall temperature data is in terms of TWTINF. Note that the value of each literal is left justified in its

10 column block. NAMELIST BL requires only a single card for this example and as required it begins with the first column blank and the characters \$BL and ends with \$. Since the boundary layer calculations are started at a stagnation point, ZSTART = 0., but this is the default value so it isn't entered. From the average angle between the first two input points, it is easily determined that BSTART = 0.73951. Entering Table I with this value of $\beta = \text{BSTART}$ yields HSTART = 1.6190. From the test conditions described in [16], the following values for the approach flow M^* and unit Reynolds number are obtained: MINF = 0.30863 and REINFL = 2.04146×10^6 [ft⁻¹]. Since a normal call to the transition subroutine is to be made, the default values of both XTRAN and NOTRAN are used. Also the freestream turbulence intensity is assumed to be zero, the flowing gas is air, and neither the heat transfer correction nor the error options are desired; consequently, all other variables except G (γ) are left at their default values. G is overridden from 1.405 to 1.4. The remaining cards contain the local data X, Y, MSTAR, R, and TWTINF for each base point in 5F10 format. Note that R values are not necessary and therefore not entered for this plane two-dimensional geometry since corrected boundary coordinate data is not desired in this case. The airfoil is assumed to be isothermal at the approach flow stagnation temperature, $T_{O,\infty}$ so that $T_w/T_\infty \equiv \text{TWTINF} = 1.0161$. In this example the unit for input variables (REINFL)⁻¹, X, and Y is feet.

The listing of file OUTPUT for this example flow is shown in Fig. 4(a). The locations of the laminar instability and transition points are clearly indicated, as shown. Fig. 4(b) compares the results computed from COMPBL with the experimental data.

As an example for calculating corrected wall coordinates, turbulent boundary layer computations were carried out from the throat to the exit of a plane two-dimensional Mach 2 nozzle. The listing of file TAPE4 for this example is presented in Fig. 5.

IV. COMPARISONS TO EXPERIMENT AND ANALYTICAL SOLUTIONS

In order to test the accuracy of both the method and the computer program, boundary layer computations were carried out for a number of flow situations for which either data or analytical solutions are available. The resulting comparisons are shown in Figs. 6-21. In addition, the results of calculations for a conical boattail, a cylindrical missile body/conical boattail combination, and a plane two-dimensional Mach 2 nozzle are presented in Figs. 22-24 to demonstrate how the boundary layer computations can be coupled to inviscid solutions. Unless otherwise indicated, adiabatic wall conditions ($\theta = \theta_0$) are used and the ideal gas is air.

A. Turbulent Incompressible Boundary Layers

Since the turbulent regime is probably more common and therefore of more practical importance than the laminar, a large number of calculations were made for this case. The five example flows analyzed for the incompressible turbulent regime were all test cases used at the Stanford conference and were taken from reference [18]. In each case the value of HSTART was determined by taking the average of the H values found from Eqs. (44) and (45). The comparisons of the computations to the data are shown in Figs. 6-10.

The first case is the Ludwig and Tillmann accelerating flow (IDENT = 1300)⁺ which may be considered as relatively "easy" to predict. As shown in Fig. 6, the agreement between the calculations and the data is excellent. The remaining four example flows can be placed in the "difficult" category, being either strong adverse pressure gradient, separating, or relaxing flows. The results for the Ludwig and Tillmann strong adverse pressure gradient case (1200) are shown in Fig. 7. The agreement is good up to about $X = 3m$ at which point the data tends toward separation while the computations do not. In this region, however, Coles and Hirst [18] point out that the data contains large discrepancies in the momentum balance. Figure 8 presents the comparison for Clauser, flow number 1 (2200). The computations and data agree reasonably well except perhaps in the downstream section where δ_2 is overestimated and c_f is underestimated. Large momentum balance discrepancies are again noted for this region. The comparison for Moses, case 3 (3800) which is a case of extremely strong adverse pressure gradient leading to separation, is shown in Fig. 9. The data indicates separation at

⁺ Computer variable IDENT was used at the Stanford conference on turbulent boundary layers for flow identification purposes.

approximately $X = 19.2$ in. while the calculations do not indicate separation at all. Although momentum balance discrepancies again occur for the data in the downstream section, they probably cannot fully explain the lack of agreement between the data and predictions. The final incompressible turbulent boundary layer calculation is the Bradshaw and Ferriss relaxing flow (2400) shown in Fig. 10. The predictions and data are in good agreement except for the underprediction of the skin friction coefficient, c_f , at the downstream stations.

Of all the flow cases used for the Stanford conference, Coles and Hirst [18] list those data sets which they feel are preferable because of experimental reliability, superior instrumentation, etc. The Ludwig-Tillmann accelerating flow and the Bradshaw-Ferriss relaxing flow fall into this category, and for these cases the program results agree well with the data. In any event, since the nominal flow situation is much less difficult than the last four examples considered above, it is valid to conclude that the program developed herein is reasonably accurate for incompressible turbulent boundary layers.

B. Turbulent Compressible Boundary Layers

Five test boundary layers were also computed for the compressible turbulent regime. The first of these, shown in Fig. 11, is a very strong adverse pressure gradient supersonic flow reported by McLafferty and Barber [19]. The agreement between the calculations and the data is relatively good, although the streamwise gradients of the prediction curves are not as large as those indicated by the data. Notice that the boundary layer is very near separation for $X > 2.5$ in. It should be mentioned that rather than determining HSTART from Eq. (45) for the given initial value of δ_1/δ_2 , HSTART was obtained by computing the supersonic flat plate boundary layer at the given entrance conditions in the streamwise direction until the initial entrance value of δ_2 was matched. This method was used since it modelled well the entrance region to the test section and since the data points for the shape factor, δ_1/δ_2 , were taken from a small graph in [19].

The next three cases are taken from the report by Winter, Smith, and Rotta [20] and consist of the flow over a waisted body of revolution at approach Mach numbers of $M_\infty = 0.6, 1.4,$ and 2.8 . The measured freestream Mach number distributions indicate that the pressure gradient is initially adverse (for $x/l > 0.4$) followed by a relaxation region. The average value of H determined from Eqs. (44) and (45) was used for HSTART.

As shown in Figs. 12, 13, and 14 the shape factor, δ_1/δ_2 , is well predicted in all three cases as is the momentum thickness for $M_\infty = 0.6$ and 1.4. However, the skin friction coefficient and the momentum thickness for $M_\infty = 2.8$ are overpredicted, particularly in the region of the body waist ($x/l = 0.7$). Lewis, Kubota, and Webb (21) have noted that the integral momentum balance is not satisfied in this region, although it is doubtful that this can account entirely for the discrepancy between the data and the computations.

The final compressible turbulent flow considered is the transonic shock wave/boundary layer interaction case investigated by Alstatt [22]. The freestream Mach number variation, shown in Fig. 15, contains regions of both strong acceleration and strong deceleration leading to separation. Since only displacement thickness measurements were reported, the values of ZSTART and HSTART were determined by computing the flat plate boundary layer at the entrance conditions in the streamwise direction until the entrance value of δ_1 was matched. As shown in Fig. 15, the measured and computed values of the displacement thickness agree very well, except perhaps near $X = 14$ in. where the calculations show a sharp peak. The separation point was computed as $X \approx 21.4$ in. agreeing well with the measured value of $X = 21.75$ in.. Alstatt [22] reported an instability problem in the boundary layer solution technique of Nash and Hicks [23] for a number of different eddy-viscosity models occurring just downstream of $X = 16$ in.; no such problems were encountered here.

Since all of the cases discussed above for the compressible turbulent regime are considered as "difficult" and since the computations and data agree reasonably well for the most part, it can be concluded that program COMPBL yields accurate approximations to the boundary layer behavior for this regime.

C. Laminar Boundary Layers

For laminar boundary layers, three examples were calculated as shown in Figs. 16, 17, and 18. All three boundary layers begin at a plane stagnation point, HSTART = 1.625, BSTART = 1.0. The first two cases are incompressible non-similar flows over a circular cylinder investigated by Hiemenz [24] and over an elliptic cylinder reported by Schubauer [25]. For each of these cases, Smith and Clutter [26] have computed the corresponding laminar boundary layers using their well known finite difference technique, while for the elliptic cylinder Hartree [27] reported earlier hand-performed calculations. In both cases, the agreement between the results

computed here from the Walz approximation theory and the "exact" finite difference calculations is remarkable. The computed separation point for the circular cylinder is $\alpha \approx 80.3^\circ$ agreeing well with Hiemenz' observed value of $\alpha \approx 80^\circ$. Neither the present results nor Smith and Clutter's calculations indicate separation for the elliptic cylinder, although Schubauer measured it to occur at $X = 1.99 \pm 0.02$. However, using a polynomial fit to Schubauer's measured pressure distribution, rather than the one given by Hartree, yielded separation at $X = 1.96$ with the present method. The results shown in Fig. 17 are for the Hartree fit to the pressure distribution since this is the one upon which the Smith and Clutter calculations were based.

Figure 18 compares the results of the present computation scheme with the finite difference calculations of Flügge-Lotz and Eichelbrenner [28] (taken from [29]) for a laminar, compressible airfoil-type flow. The agreement is good except that the separation point is predicted to be somewhat too far downstream.

Based on these examples, the present method appears to be very accurate for laminar boundary layers.

D. Boundary Layers with Heat Transfer

Two heat transfer cases were considered. The first, shown in Fig. 19, consists of a laminar, Mach 3 flow over a flat plate with the wall temperature distribution shown in the figure. An analytical solution of this problem is given by Chapman and Rubesin [15]. The computation of the heat transfer based on the simple Reynolds analogy, $K = 0$, is greatly in error as may be expected for the strong axial wall temperature gradient present here. Using the heat transfer correction procedure ("modified Reynolds analogy") discussed in Section II-E, $K = K(x)$, puts the computed heat transfer into much better agreement with the analytical solution although it seemingly overcorrects for the effect of variable wall temperature.

The second heat transfer case, taken from the report by Boldman, Schmidt, and Ehlers [30], is a turbulent boundary layer flow on the walls of a cooled, supersonic nozzle. Both the wall temperature and freestream Mach number vary strongly in the axial direction as shown in Fig. 20. The heat transfer computations based on the Reynolds analogy, $K = 0$, do not agree well with the data and err, as expected, on the high side for the strong favorable pressure gradient within the nozzle. However, the "corrected" results, which are not presented, are

in even poorer agreement with the data. As for the case above, the corrections are too strong and in fact predict a change in the direction of the heat transfer for the region near the throat which is clearly incorrect.

It is therefore recommended that the simple Reynolds analogy be used if only a rough estimate of the heat transfer is desired. These results should be adequate as long the wall temperature and pressure streamwise gradients are not too strong. If a more refined computation is necessary, it is felt that the results of the correction procedure (invoked by `HTCORR = .TRUE.`) should be used with caution. Also, it is helpful to remember that since the properties of the velocity boundary layer depend only on the average aspects of the thermal layer, the computations for the velocity quantities may be accurate even though those for the heat transfer are not.

E. Boundary Layer with Transition

A transitional boundary layer case consisting of flow over a NACA 0012 airfoil was computed as shown in Fig. 21. This example was taken from the report by McNally [16] and was used in explaining the input procedure, Section III-D. The data and predictions for the displacement and momentum thicknesses agree very well except for just downstream of the transition point where the computations for the displacement thickness show a sudden drop. As discussed previously, this is a consequence of the pointwise nature with which the transition process is assumed to occur in the calculations. Across the transition location, H is taken as continuous, and Z is chosen to make the momentum thickness, δ_2 , continuous (as can be verified in Fig. 21). Other boundary layer parameters such as displacement thickness and skin friction, which are derived from these two dependent variables, are therefore discontinuous at transition. The comparison of the data and computations in Fig. 21 for the displacement thickness suggests that perhaps a "hand-smoothing" operation is warranted to remove the discontinuity.

Note also that the predicted transition location agrees well with the measured transition range.

F. Miscellaneous Examples

The final three examples illustrate the way in which program COMPBL can be used in conjunction with inviscid solutions to predict boundary layer characteristics in design situations. The first two cases consider the flow over the 10° conical afterbody shown in Fig. 22. The inviscid wall Mach number dis-

tribution was determined from the method of characteristics using program TSABPP-2 developed by Addy [31]. The approach Mach number is assumed to be $M_\infty = 2$ and the ambient static pressure and temperature are taken as sea-level values, $P_\infty = 14.7$ psia and $T_\infty = 520^\circ\text{R}$, which yield a very high unit Reynolds number, $Re_\infty/L \approx 1.4 \times 10^7 \text{ ft}^{-1}$. For the first case, Fig. 22, the turbulent boundary layer is assumed to start at the expansion giving the integral parameters shown in the bottom half of the figure. Figure 23 shows the more realistic situation for which the turbulent boundary layer is assumed to begin growing on the missile body and therefore is of finite thickness just upstream of the expansion. This second case demonstrates the capability of program COMPBL to calculate through a "discontinuity" in the Mach number distribution. The wall Mach number was assumed to be constant at $M = 2$ up to $X = -0.001$ ft. and then for $0 \leq X \leq 4$ ft., the method of characteristics results were used. Note that the expansion fan produces rather large discontinuities in the shape factor, δ_1/δ_2 , and the skin friction coefficient, c_f .

The last example, Fig. 24, is of the flow through a plane two-dimensional Mach 2 nozzle. The wall Mach numbers were computed using the method of characteristics nozzle design program NOZCS written by Addy with typical laboratory operating conditions being chosen as: $P_0 = 600$ kPa, $T_0 = 300$ K, throat radius = 1 cm. The turbulent boundary layer is assumed to start at the throat. Figure 5 shows the corrected boundary coordinate results from file TAPE4. At the nozzle exit the corrected centerline distance is 1.714 cm compared to the method of characteristics inviscid design value of 1.686 cm.

V. CONCLUSIONS

A FORTRAN computer program based on Computational Method II of Walz [1] has been developed to calculate the integral parameters for the two-dimensional boundary layer flow of ideal gases. The flexibility of the program allows plane or axisymmetric geometries with the boundary layer either laminar or turbulent, incompressible or compressible, and either with or without heat transfer. In addition, the location of transition can either be predicted or specified as an input.

In order to test the accuracy and reliability of the method and program, a number of boundary layers were computed for which either data or analytical solutions are available for comparison. Five incompressible turbulent and five compressible turbulent boundary layer examples were analyzed, most of which fall in the "difficult" category. For most of these cases the agreement between the data and the predictions is good. For the laminar and transitional boundary layers calculated, the computed results agree with the data or analytical solutions extremely well. However, the heat transfer predictions have met with less success. For rough estimates of the heat transfer, it is suggested that the default Reynolds analogy be used. The heat transfer correction procedure or "modified Reynolds analogy", discussed in Section II-E, should be used cautiously since it has been only moderately successful.

A major asset of the program is its computational speed. A typical boundary layer can be calculated on the CDC CYBER 175 in $\frac{1}{2}$ - 1 CPU seconds, making parametric design studies practical.

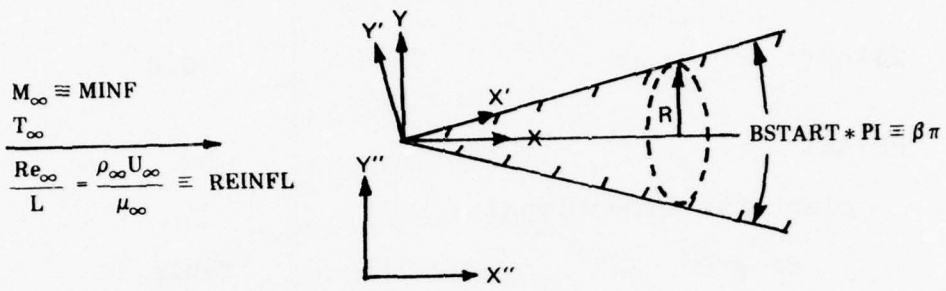
Based on these characteristics, it is felt that program COMPBL is a useful and accurate tool for estimating the integral boundary layer parameters in a wide variety of flow situations.

TABLE I. β vs H from Hartree Solutions

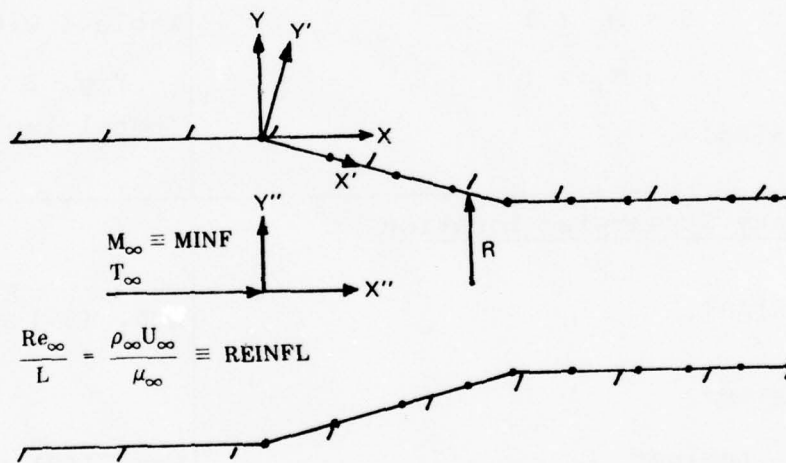
β or β_E	H
-0.1988	1.515
-0.19	1.5200
-0.18	1.5250
-0.16	1.5333
-0.14	1.5400
-0.10	1.5517
0	1.5720
0.1	1.5857
0.2	1.5950
0.3	1.6018
0.4	1.6070
0.5	1.6113
0.6	1.6150
0.8	1.6207
1.0	1.6250
1.2	1.6290
1.6	1.6345
2.0	1.6380

TABLE II. Summary of Procedure for Determining Starting Values ZSTART, HSTART, BSTART

<p><u>Sharp Leading Edge or Stagnation Point</u></p> <p>ZSTART:</p> <p>HSTART:</p> <p>plane two-dimensional</p> <p>$\beta\pi \neq 0$</p> <p>$\beta\pi = 0$</p> <p>axisymmetric</p> <p>$0 < M_\infty \leq 1$</p> <p>$M_\infty > 1$</p> <p>BSTART:</p>	<p>0.0</p> <p>Table I</p> <p>Fig. 2</p> <p>Table I with $\beta_E = \frac{\beta}{3-\beta}$</p> <p>Fig. 2</p> <p><u>(total included angle)</u></p> <p>π</p>
<p><u>Arbitrary Streamwise Location</u></p> <p>ZSTART:</p> <p>HSTART:</p> <p>laminar</p> <p>turbulent</p> <p>BSTART:</p>	<p>Eqs. (39) and (40)</p> <p>Eqs. (42) or (43)</p> <p>Eqs. (44) or (45)</p> <p>not needed</p>



(a) AXISYMMETRIC CASE



(b) PLANE TWO-DIMENSIONAL CASE

Figure 1. Location of coordinates X, Y, R ; approach flow variables M_∞ (MINF), Re_∞/L (REINFL), T_∞ ; and angle β (BSTART).

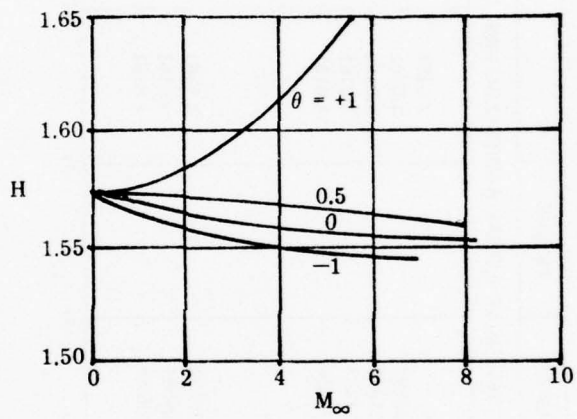


Figure 2. H vs M_∞ used in determining HSTART value for compressible flows (after Walz [1], Fig. 6.5).

COMPRESSIBLE BOUNDARY LAYER RESULTS--COMPUTATIONAL METHOD II OF WALZ

MCNALLY TRANSITION EXAMPLE--NACA 0012 AIRFOIL (L=PT.)
 INPUT PARAMETERS:

FLOW = LAMINAR GEOM = PLANE 2-D MTYPE = MSTAR
 ITYPE = 14TEMP XSTART = 0. HSTART = 1.619
 RSTART = 7.395 MINE = .284 REINPL = .20418E+07
 XTRAN = 0. FSTINT = 0. G = 1.400
 W = .7000 AL = .8500 RT = .8820
 SL = .8000 ST = .8200 EPS = .1000E-03
 ROTRAN = P ATCORR = F ERROR = F

RESULTS:

AXIAL LOCATION [L]	Z = D2*(RD2**H) [L]	u = (D3/D2)U	SHAPE FACTOR (D1/D2)	DISPLACEMENT THICKNESS [L]	MOMENTUM THICKNESS [L]	99.9% B.L. THICKNESS [L]	NOM. THICK. REYNOLDS NUMBER	LOCAL SKIN FRICTION COEFFICIENT	DIMENSIONAL LOCAL WALL HEAT FLUX
0.	0.	1.61900	----	----	----	0.	----	----	----
.250000E-01	.789184E-02	1.61500	2.28164	.158340E-03	.693976E-04	.754080E-03	113.719	.597166E-02	.274227E-03
.625000E-01	.179925E-01	1.61635	2.31666	.218200E-03	.941873E-04	.101957E-02	191.030	.347768E-02	.160915E-03
.125000	.371903E-01	1.60364	2.41831	.312494E-03	.129220E-03	.135632E-02	287.806	.209198E-02	.970329E-04
.250000	.818150E-01	1.59100	2.52373	.472488E-03	.187218E-03	.190901E-02	437.004	.123208E-02	.572084E-04
.375000	.135369	1.57650	2.65163	.636156E-03	.239914E-03	.237018E-02	564.242	.819589E-03	.387614E-04
.500000	.188309	1.57394	2.67634	.756181E-03	.282543E-03	.277678E-02	666.479	.672927E-03	.312525E-04
.750000	.237737	1.57057	2.73919	.962461E-03	.355258E-03	.346761E-02	838.004	.513080E-03	.238288E-04
1.000000	.414065	1.56623	2.75277	.115349E-02	.419752E-03	.406164E-02	986.452	.411221E-03	.193967E-04
1.250000	.541429	1.56233	2.81553	.135631E-02	.481617E-03	.460737E-02	1124.19	.330600E-03	.153505E-04
1.300000	.569055	1.55862	2.83474	.143088E-02	.494182E-03	.471245E-02	1151.51	.313978E-03	.145781E-04
1.350000	.597142	1.55701	2.85317	.144568E-02	.506691E-03	.481744E-02	1178.51	.298648E-03	.138658E-04
LAMINAR-TURBULENT TRANSITION									
1.400000	.391478E-02	1.66330	1.62235	.725103E-03	.570223E-03	.356620E-02	1323.96	.294812E-02	.106569E-03
1.450000	.466225E-02	1.70306	1.52097	.992638E-03	.654733E-03	.460499E-02	1517.30	.336039E-02	.121466E-03
1.500000	.548979E-02	1.71815	1.44833	.110893E-02	.745085E-03	.552054E-02	1723.38	.343200E-02	.124044E-03

Figure 4(a). Example printout from file OUTPUT for case given in Figure 3.

AXIAL LOCATION [L]	Z = (RD2*RN) [L]	n = (DJ/D2) U	SHAPE FACTOR (D1/D2)	DISPLACEMENT THICKNESS [L]	MOMENTUM THICKNESS [L]	95.9% B.L. THICKNESS [L]	NON. THICK. REYNOLDS NUMBER	LOCAL SKIN FRICTION COEFFICIENT	DIMENSIONLESS LOCAL WALL HEAT FLUX
1.55000	.635495E-02	1.72500	1.47480	.123380E-02	.836581E-03	.634777E-02	1931.13	.340559E-02	.123086E-03
1.60000	.724513E-02	1.72900	1.46677	.136134E-02	.926121E-03	.714612E-02	2137.99	.335862E-02	.121382E-03
1.65000	.815211E-02	1.73182	1.46112	.148895E-02	.131934E-02	.792863E-02	2342.57	.333798E-02	.119505E-03
1.70000	.907497E-02	1.73422	1.45636	.161578E-02	.110947E-02	.870985E-02	2545.13	.326057E-02	.117825E-03
1.75000	.133169E-01	1.73617	1.45245	.174277E-02	.119988E-02	.948930E-02	2746.53	.321491E-02	.116168E-03
2.00000	.149181E-01	1.74399	1.43691	.236569E-02	.164638E-02	.134186E-01	3728.88	.303622E-02	.109678E-03
2.25000	.201485E-01	1.74941	1.42605	.238253E-02	.209145E-02	.174153E-01	4686.82	.290398E-02	.104869E-03
2.50000	.257287E-01	1.75547	1.41777	.303410E-02	.254208E-02	.215157E-01	5634.45	.279844E-02	.101025E-03
2.75000	.316942E-01	1.75648	1.41139	.423946E-02	.300374E-02	.257359E-01	6581.82	.270873E-02	.977528E-04
3.00000	.383115E-01	1.75902	1.40588	.488778E-02	.347667E-02	.301007E-01	7529.90	.263273E-02	.949755E-04
3.25000	.446399E-01	1.76115	1.40119	.554064E-02	.395424E-02	.345381E-01	8469.12	.256726E-02	.925812E-04
3.50000	.517429E-01	1.76270	1.39748	.622400E-02	.445372E-02	.391507E-01	9426.64	.250617E-02	.903434E-04
3.75000	.595390E-01	1.76352	1.39495	.695907E-02	.498875E-02	.439995E-01	10421.8	.244585E-02	.881307E-04
4.00000	.681001E-01	1.76356	1.39369	.775309E-02	.556299E-02	.490623E-01	11457.8	.238529E-02	.859070E-04
4.25000	.787718E-01	1.76072	1.37699	.875214E-02	.626498E-02	.545732E-01	12659.9	.230419E-02	.829305E-04
4.50000	.911959E-01	1.75692	1.40187	.990260E-02	.706394E-02	.635412E-01	13972.0	.222023E-02	.798463E-04
4.75000	.106296	1.75079	1.41074	.113046E-01	.801328E-02	.669423E-01	15459.9	.212274E-02	.762668E-04
5.00000	.123542	1.74000	1.42748	.131253E-01	.919473E-02	.736439E-01	17219.1	.199798E-02	.716975E-04

Figure 4(a). Concluded.

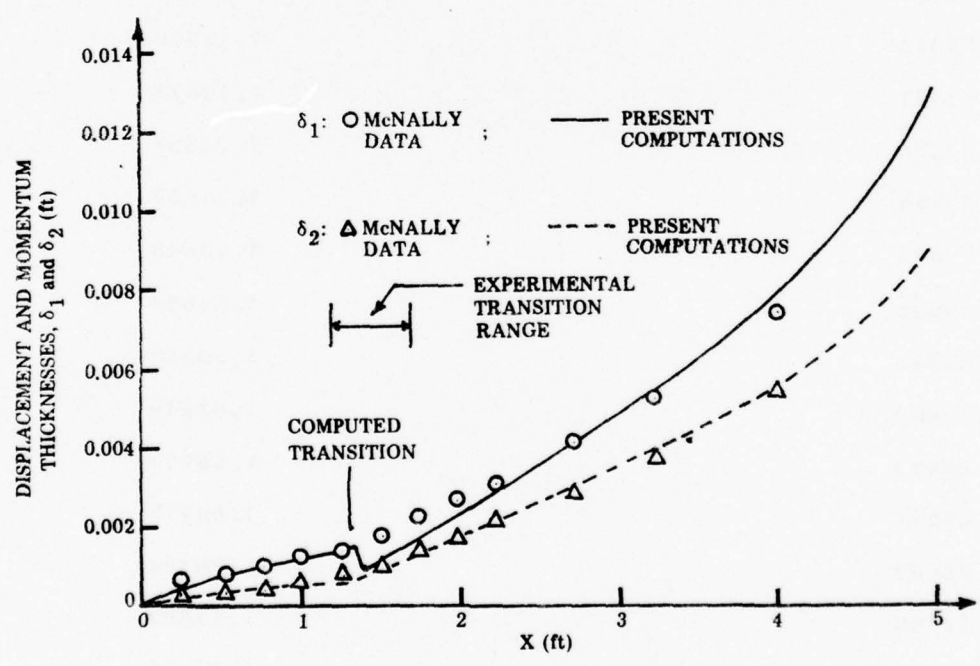
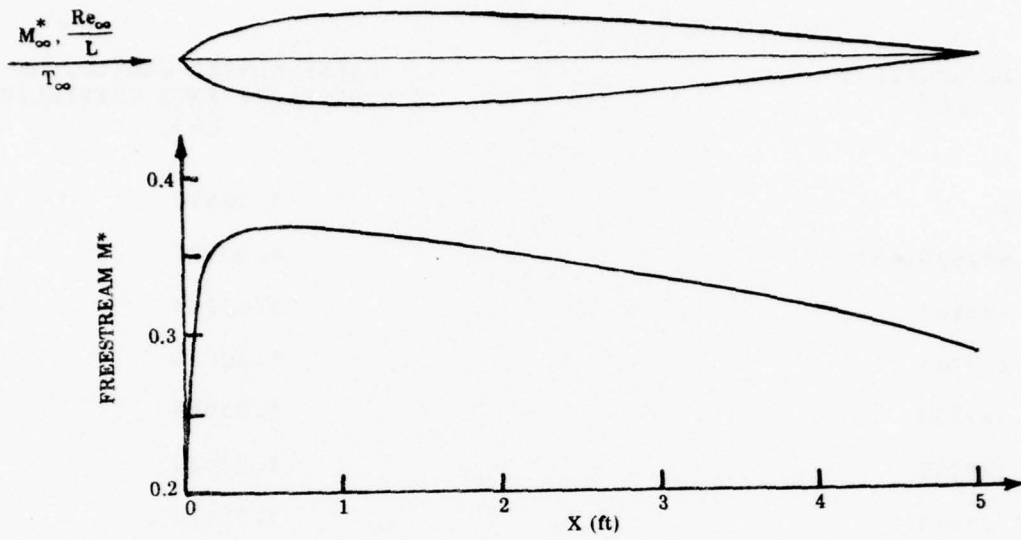


Figure 4(b). Comparison of computed results and data for case given in Figure 3.

CORRECTED BOUNDARY CO-ORDINATES

MACH 2 PLANE 2-D NOZZLE WITH HYPERBOLIC ENTRANCE SECTION (L=CM)

AXIAL LOCATION [L]	AXISYMMETRIC RADIUS, OR 2-D DISTANCE FROM CENTERLINE [L]
0.	1.00000
.812620E-01	1.00099
.178443	1.00239
.284765	1.00525
.397739	1.00948
.516029	1.01522
1.01991	1.05423
1.37683	1.09524
1.71013	1.14248
2.03971	1.19671
2.27076	1.23868
3.00444	1.36607
3.79698	1.48018
4.29855	1.54013
4.82512	1.59286
5.30462	1.63210
5.80483	1.66447
6.28597	1.68770
6.78603	1.70398
7.12789	1.71067
7.47648	1.71394

Figure 5. Example printout from file TAPE4.

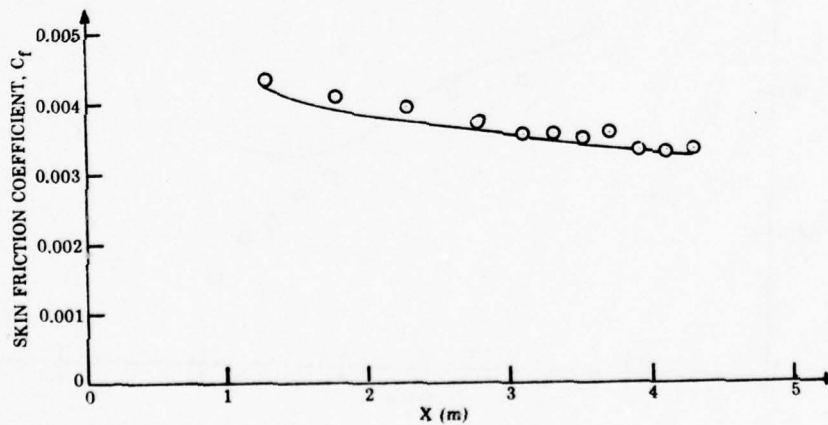
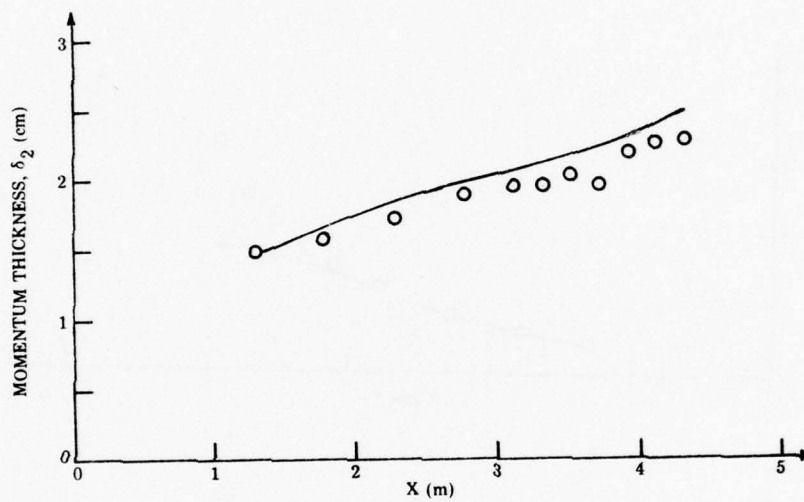
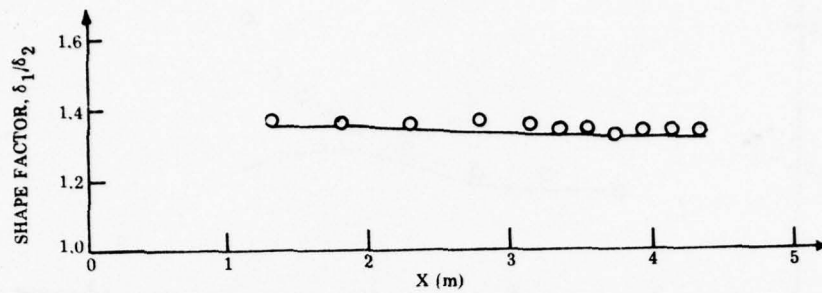


Figure 6. Comparison of computed results and data for Ludwig-Tillmann accelerating flow (1300).

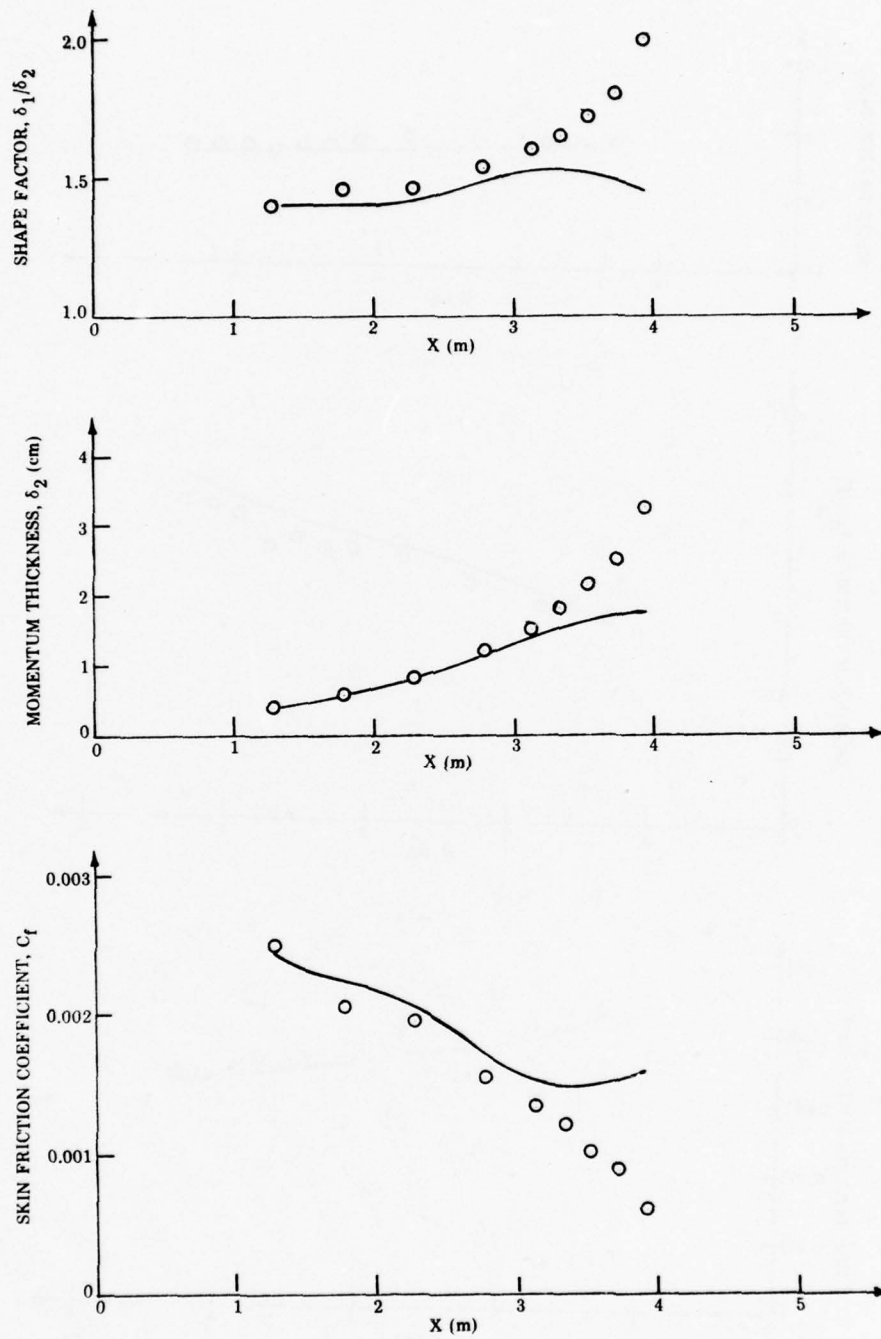


Figure 7. Comparison of computed results and data for Ludwig-Tillmann strong adverse pressure gradient flow (1200).

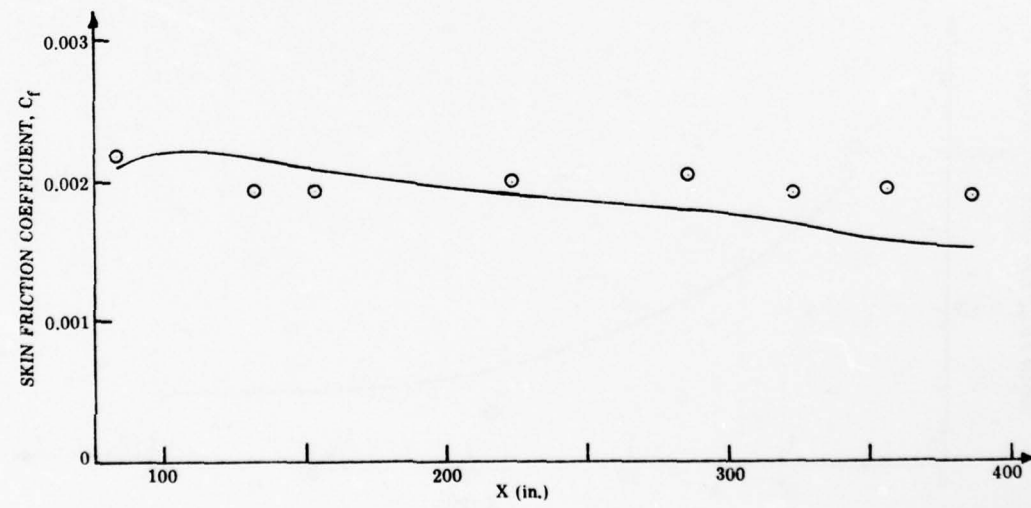
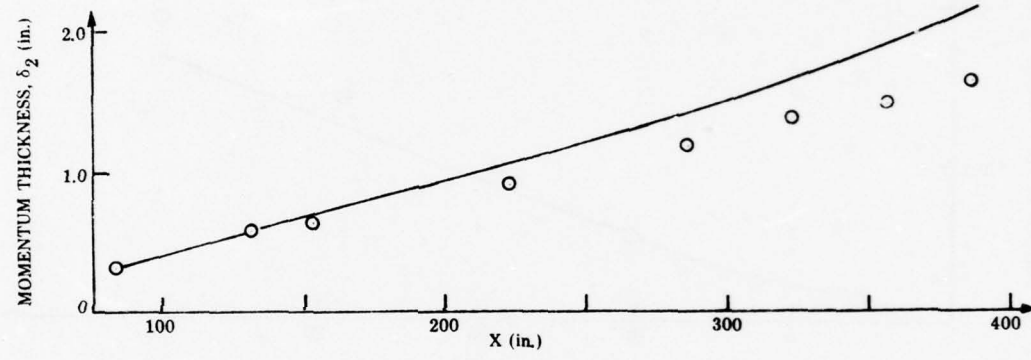
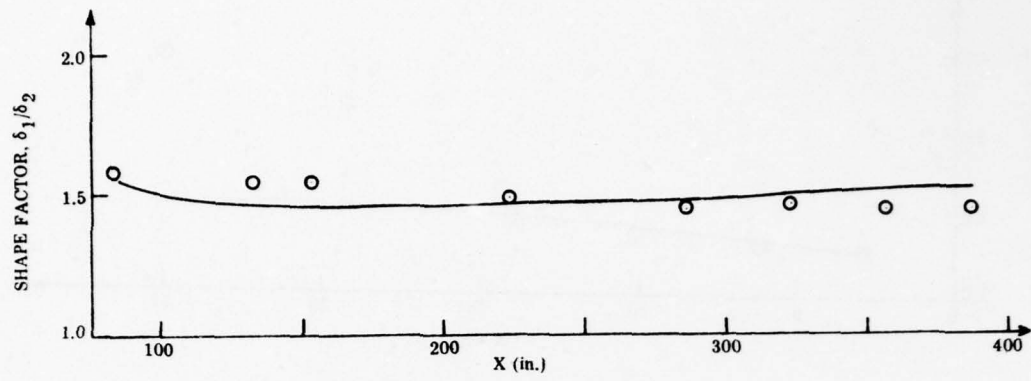


Figure 8. Comparison of computed results and data for Clauser, flow number 1 (2200).

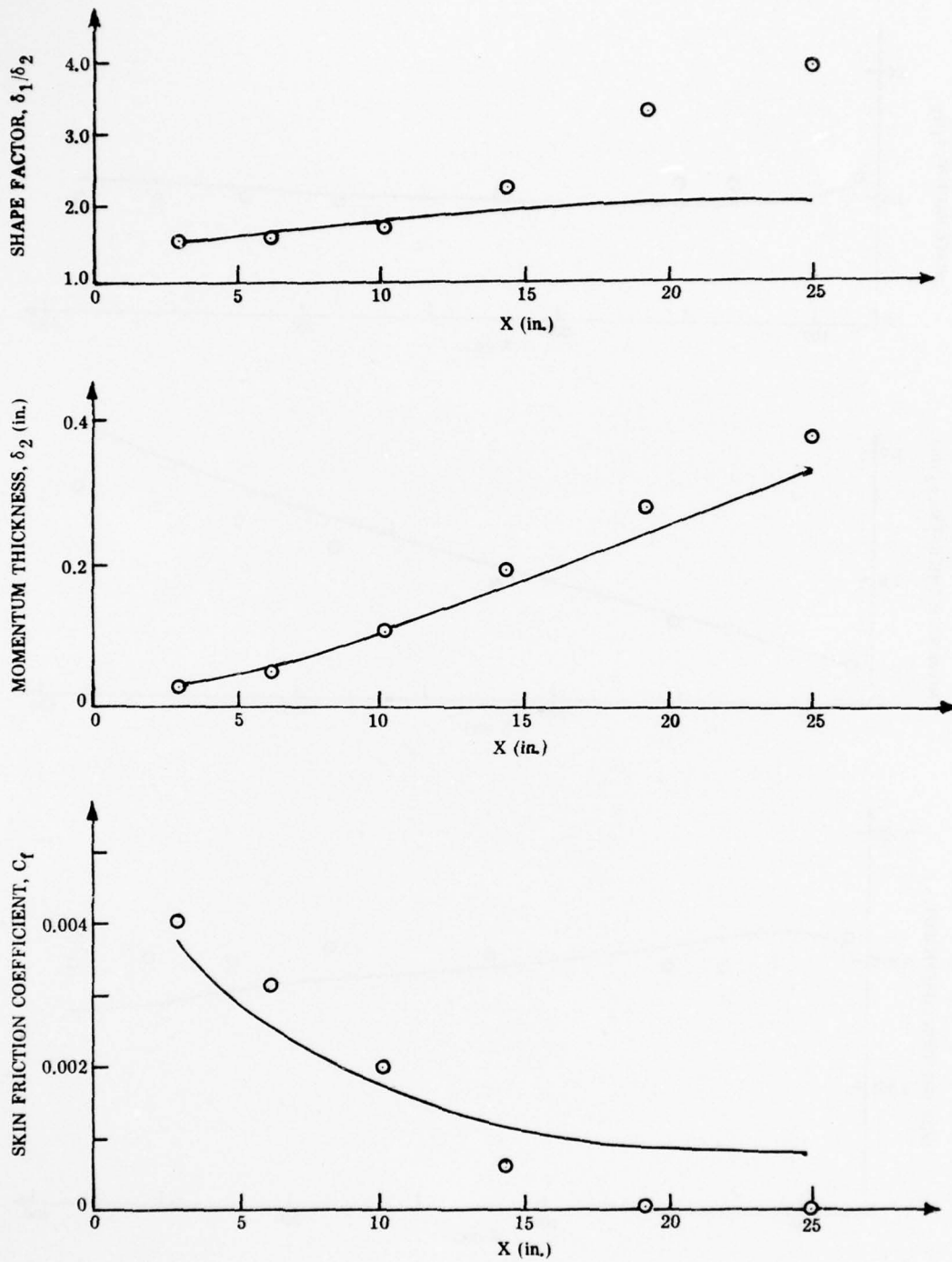


Figure 9. Comparison of computed results and data for Moses, case 3 (3800).

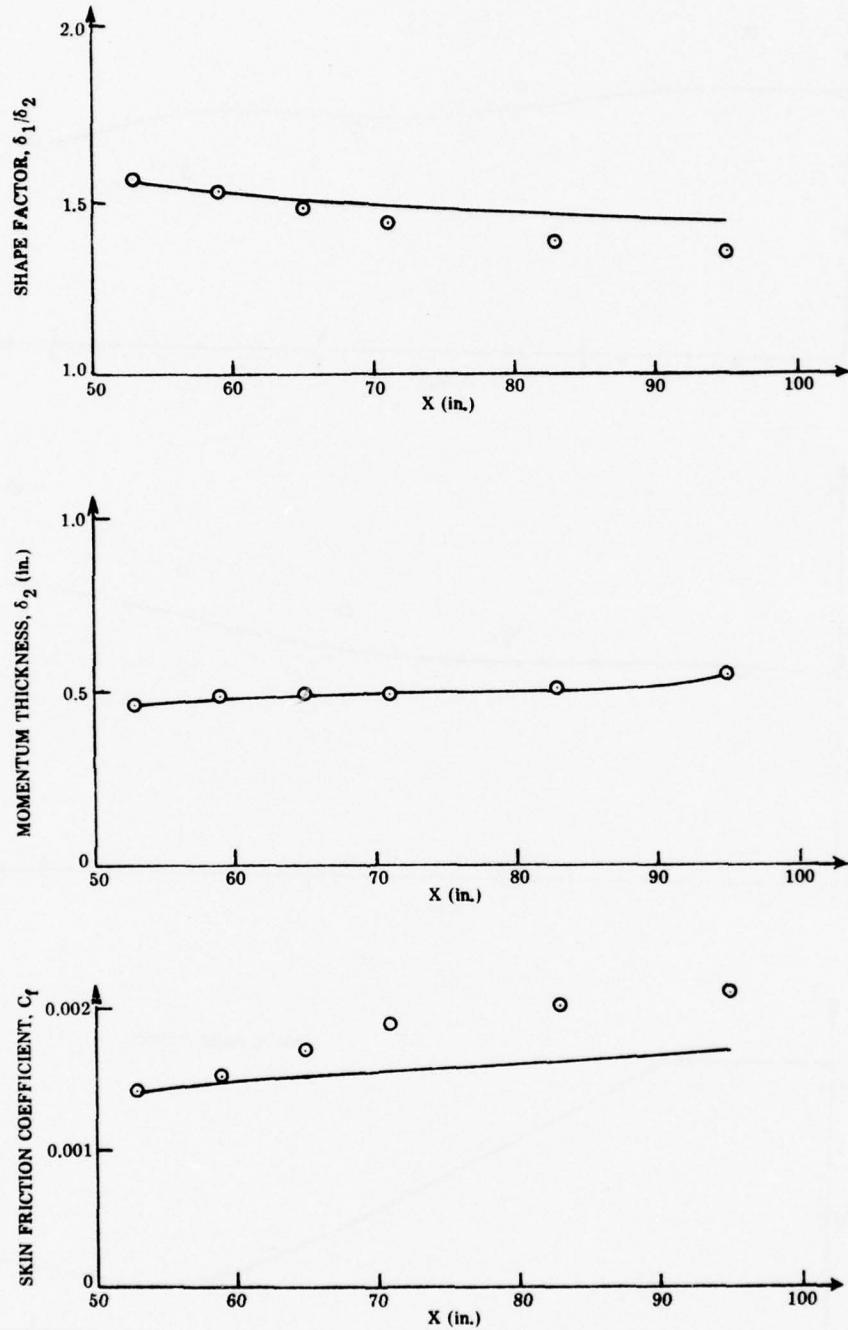


Figure 10. Comparison of computed results and data for Bradshaw and Ferriss relaxing flow (2400).

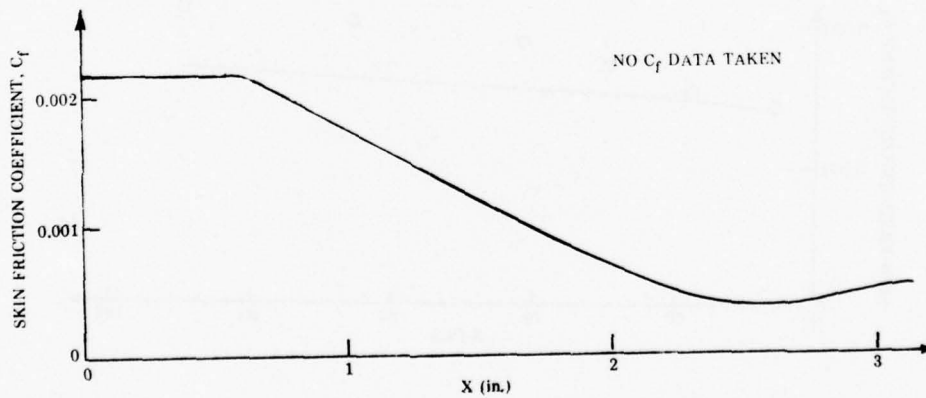
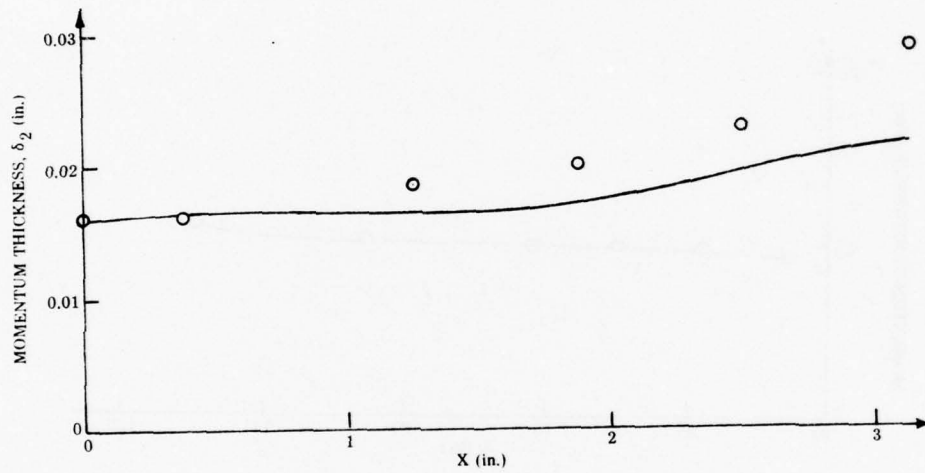
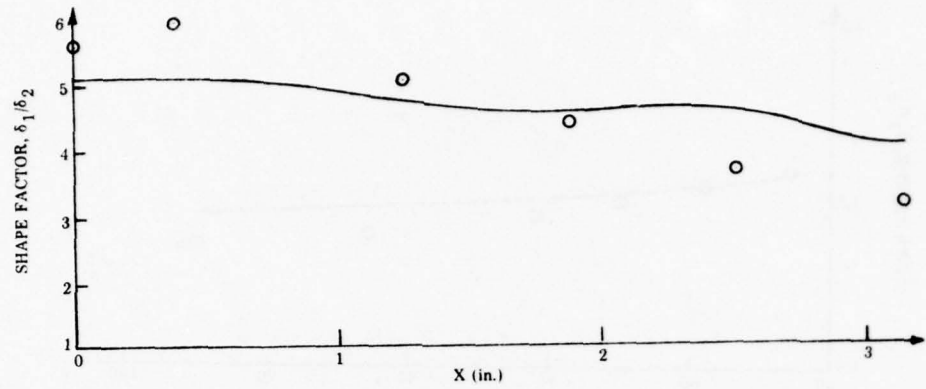


Figure 11. Comparison of computed results and data for McLafferty-Barber supersonic flow.

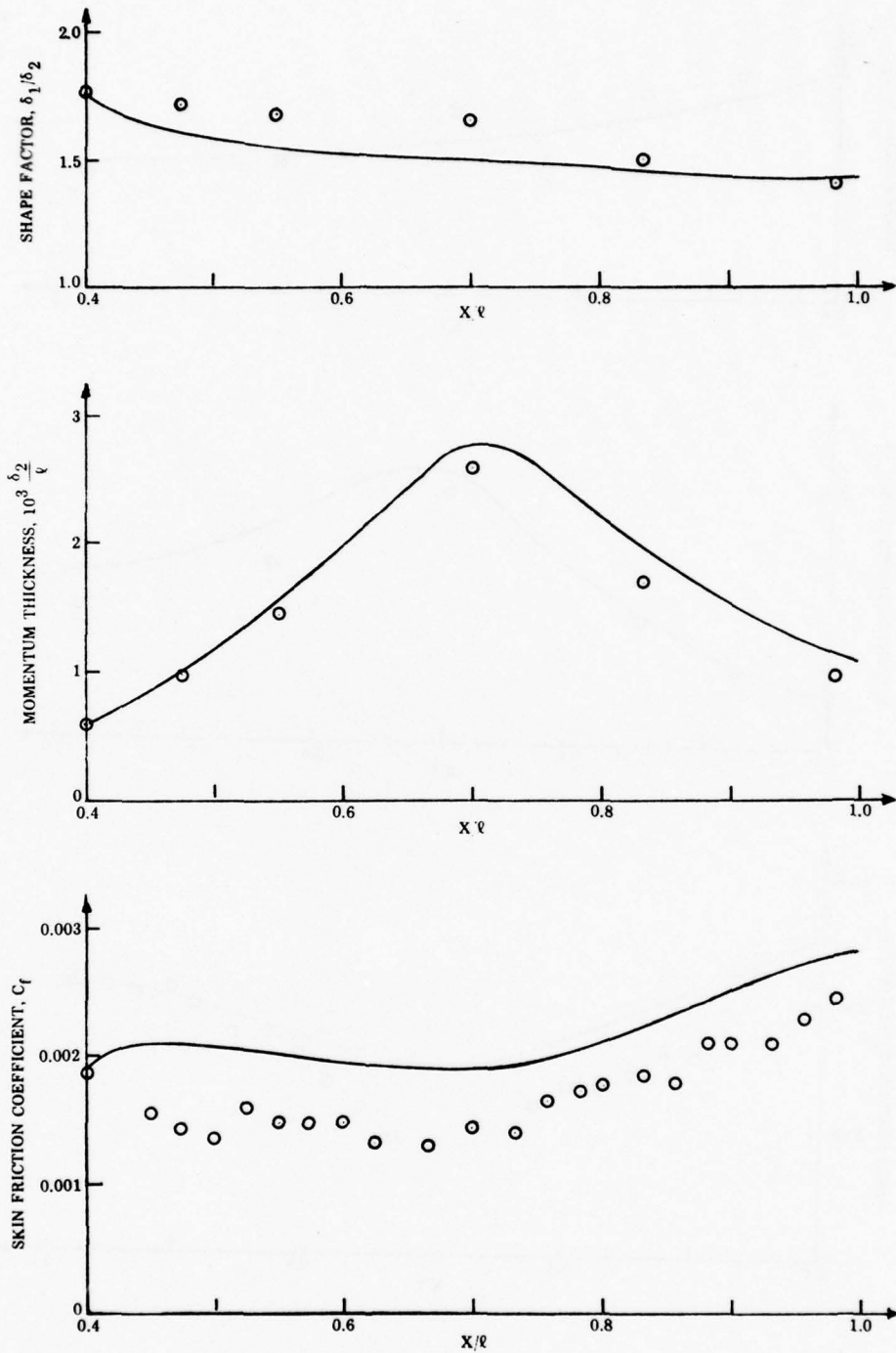


Figure 12. Comparison of computed results and data for Winter, Smith, and Rotta subsonic waisted body flow, $M_\infty = 0.6$.

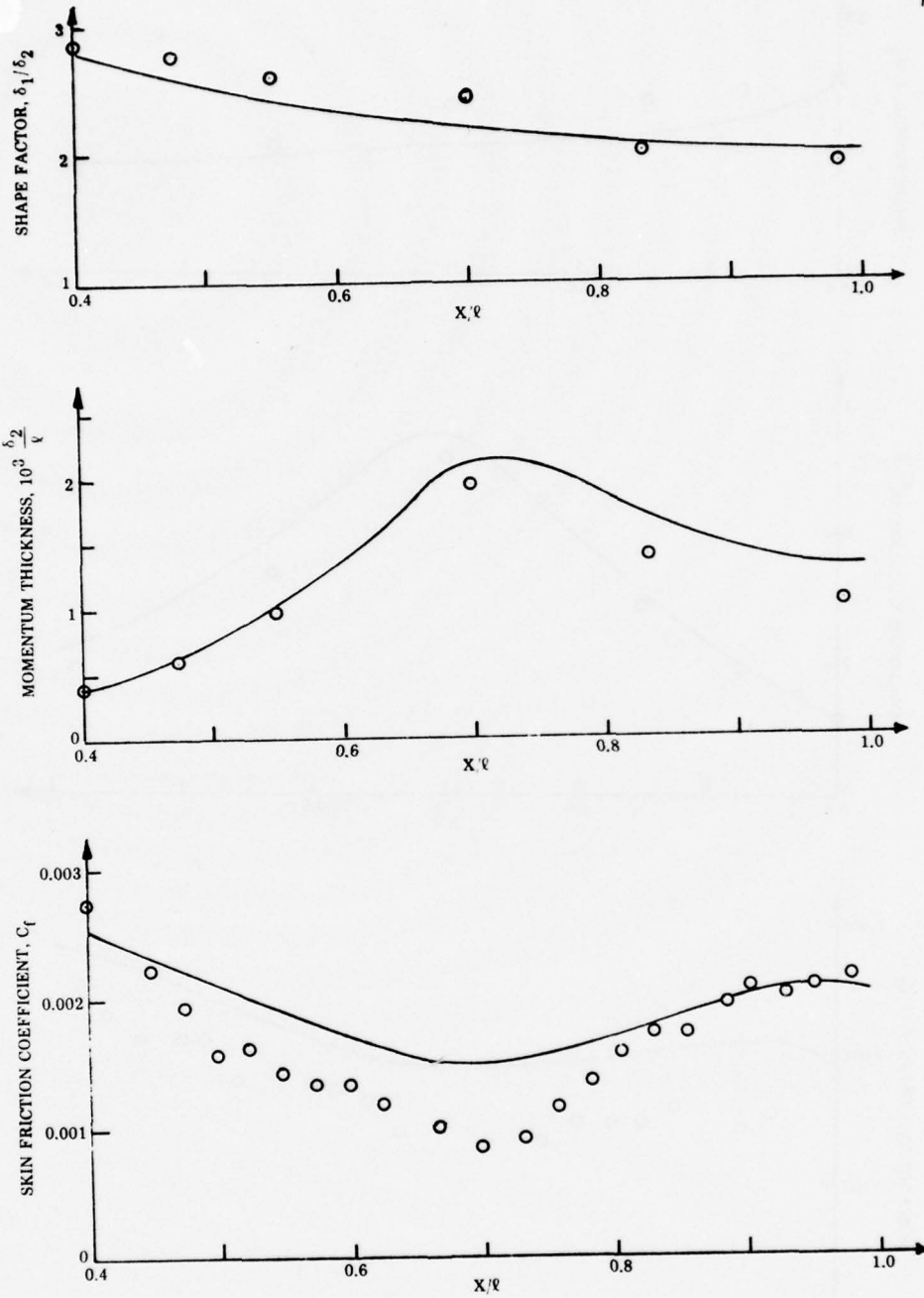


Figure 13. Comparison of computed results and data for Winter, Smith, and Rotta supersonic waisted body flow, $M_\infty = 1.4$.

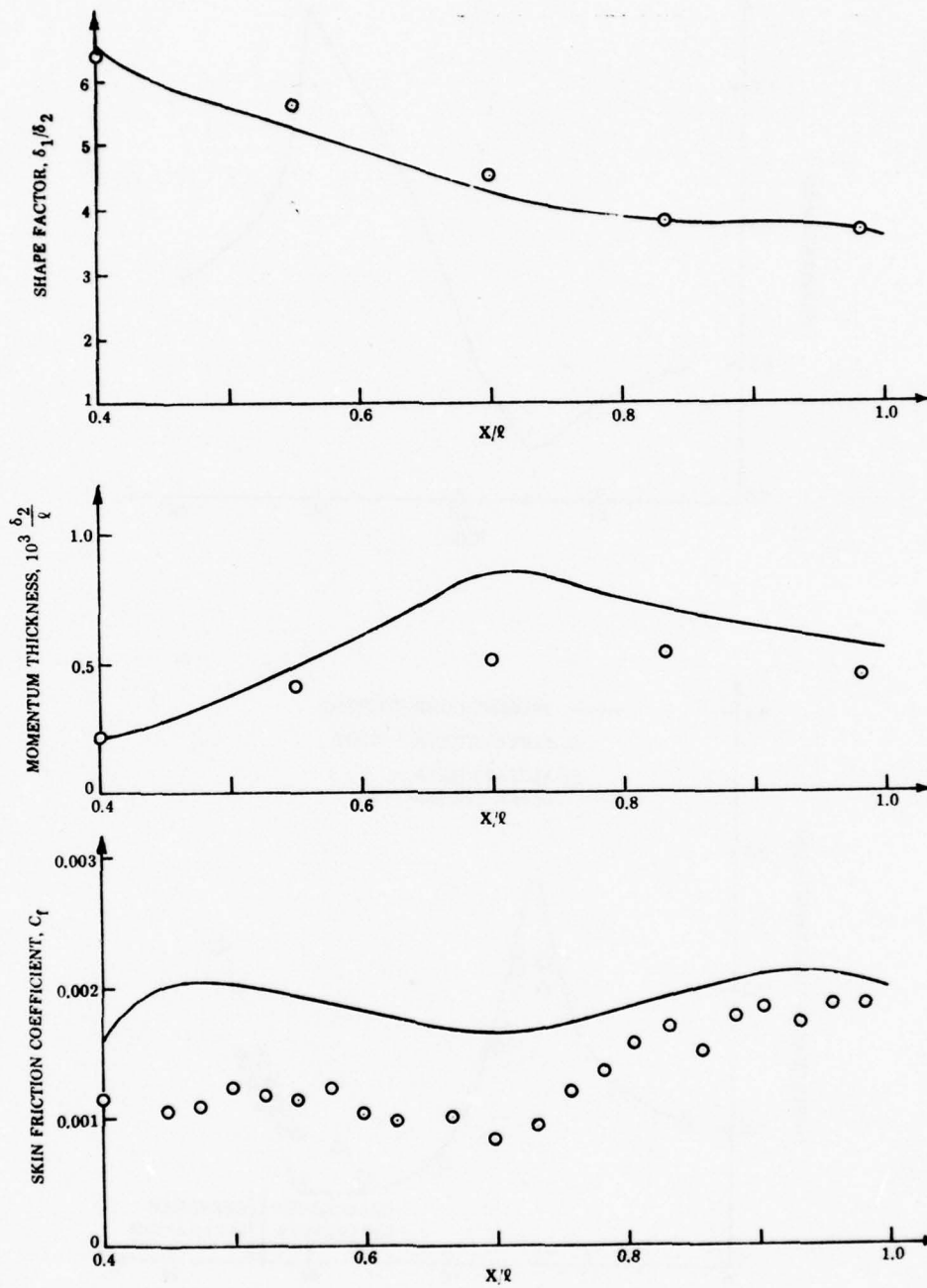


Figure 14. Comparison of computed results and data for Winter, Smith, and Rotta supersonic waisted body flow, $M_\infty = 2.8$.

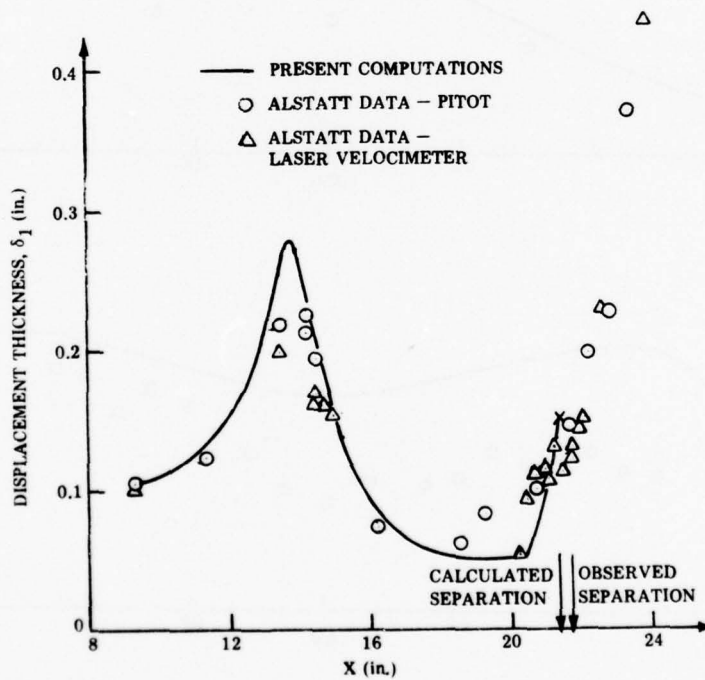
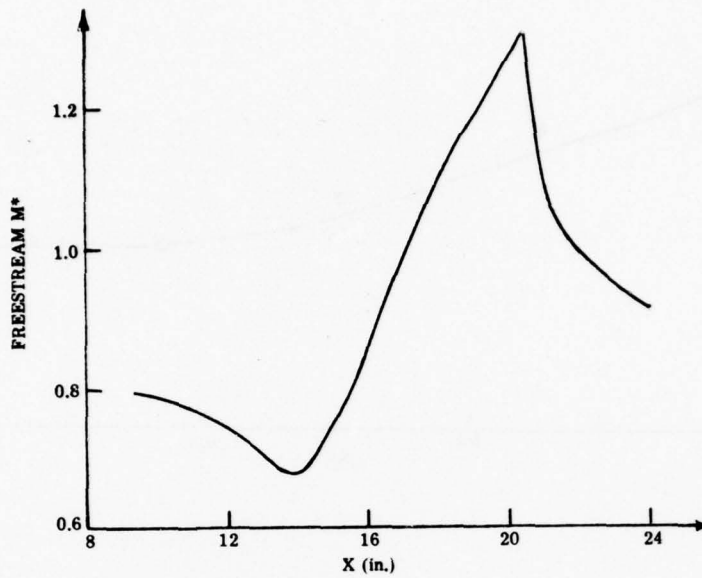


Figure 15. Comparison of computed results and data for Alstatt-AEDC transonic flow.

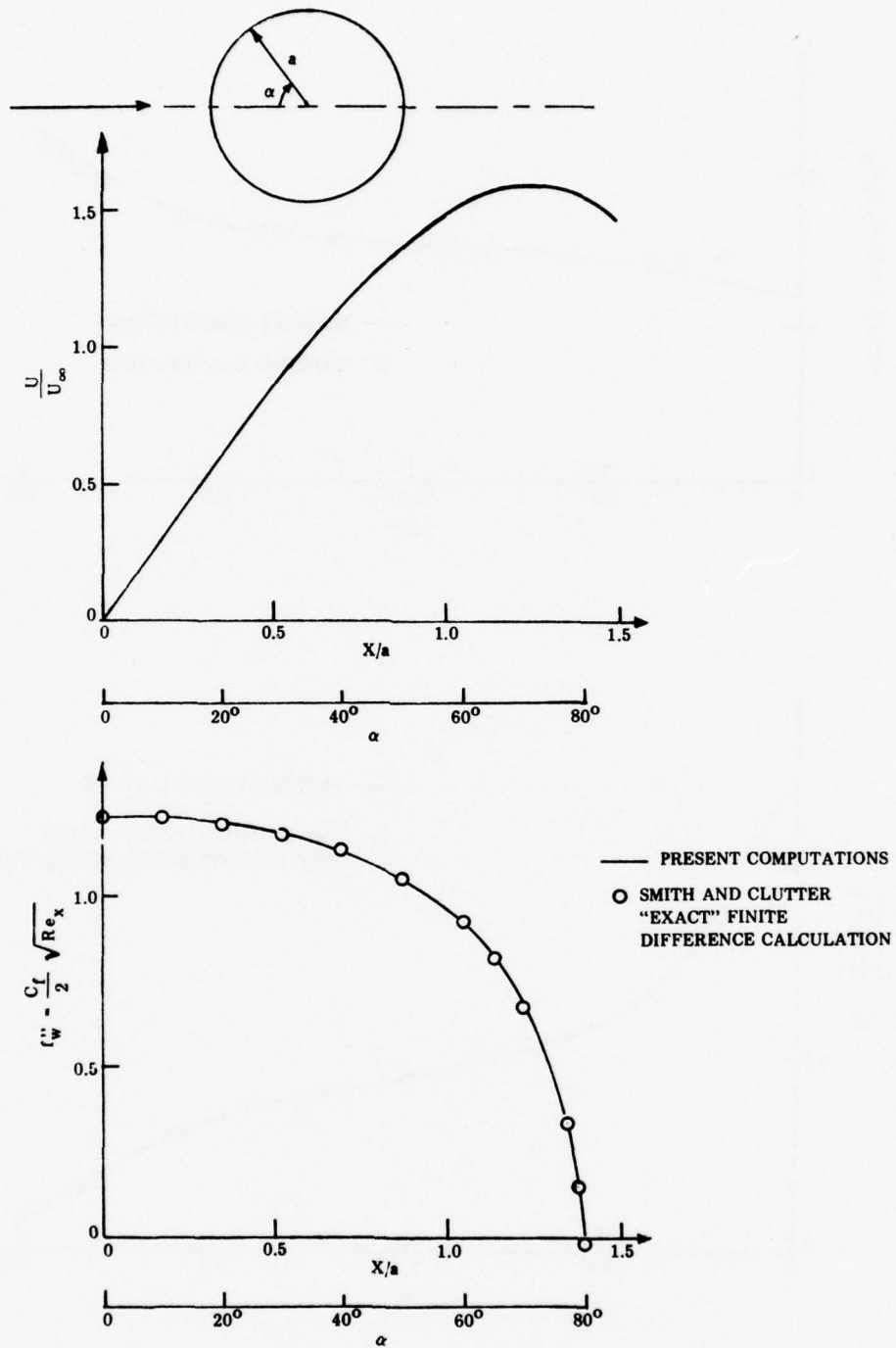


Figure 16. Comparison of present computations and finite difference calculations of Smith and Clutter for Hiemenz cylinder flow.

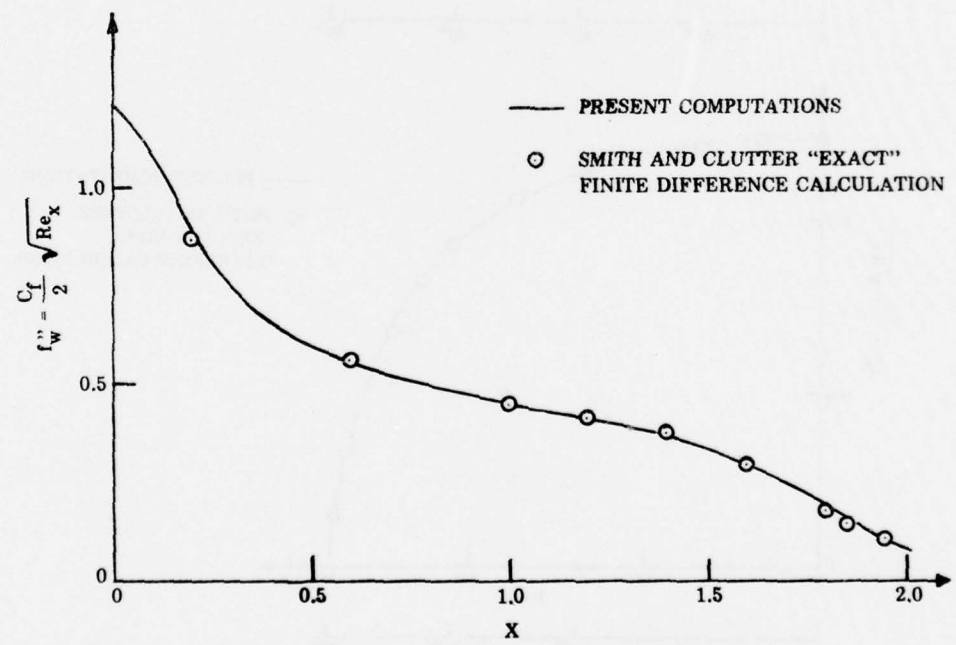
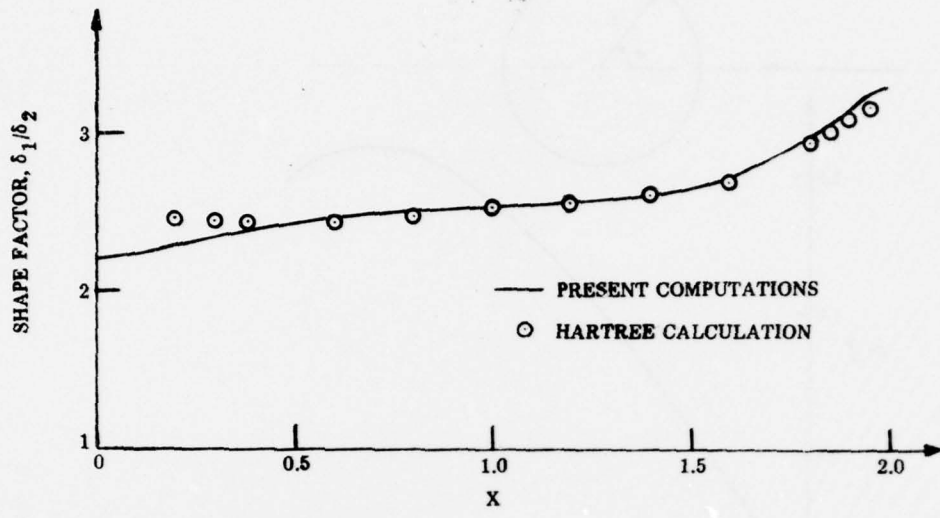


Figure 17. Comparison of present computations with Hartree calculations and Smith and Clutter finite difference calculations for Schubauer elliptic cylinder flow.

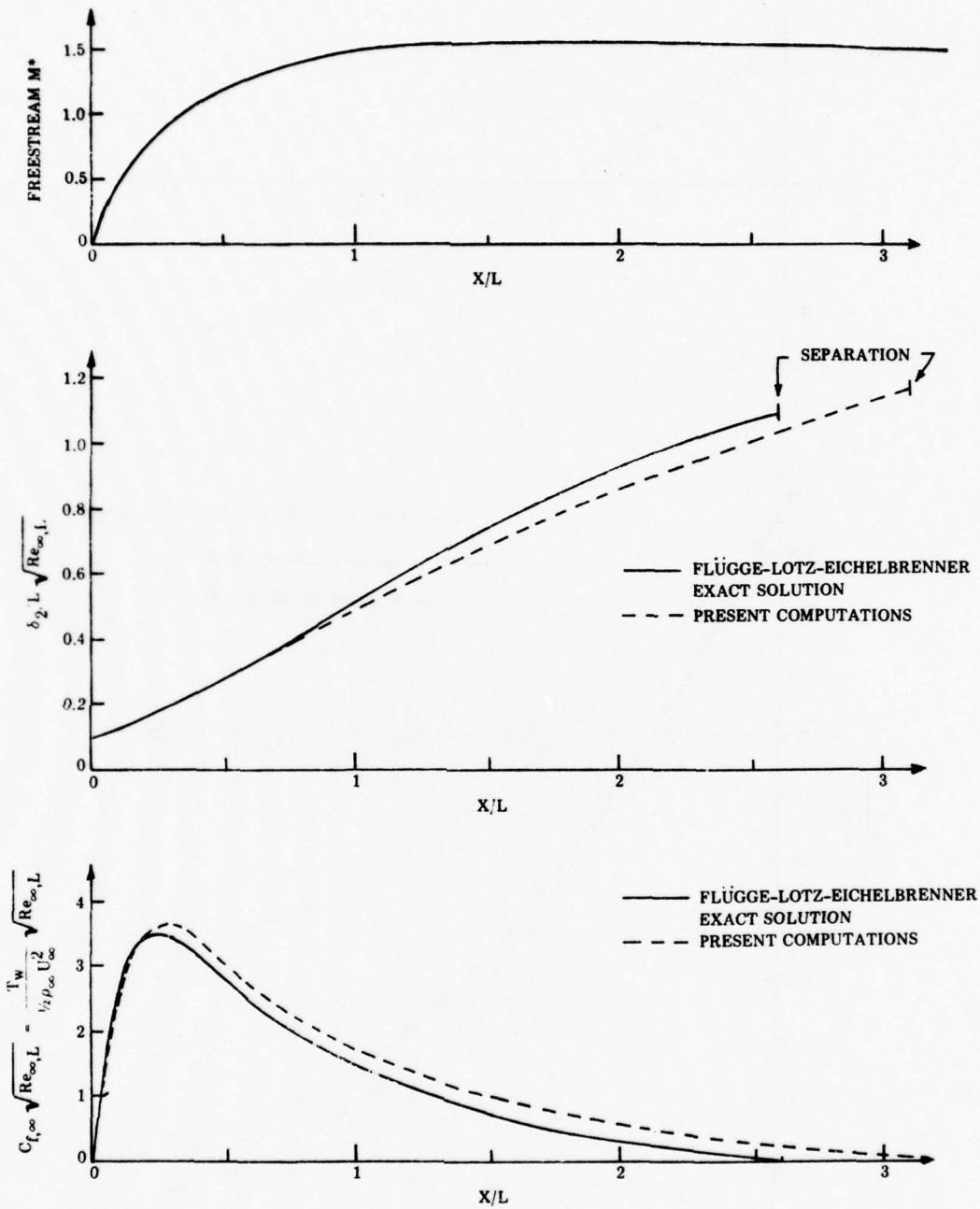


Figure 18. Comparison of present computations and Flügge-Lotz-Eichelbrenner finite difference calculations for compressible laminar flow.

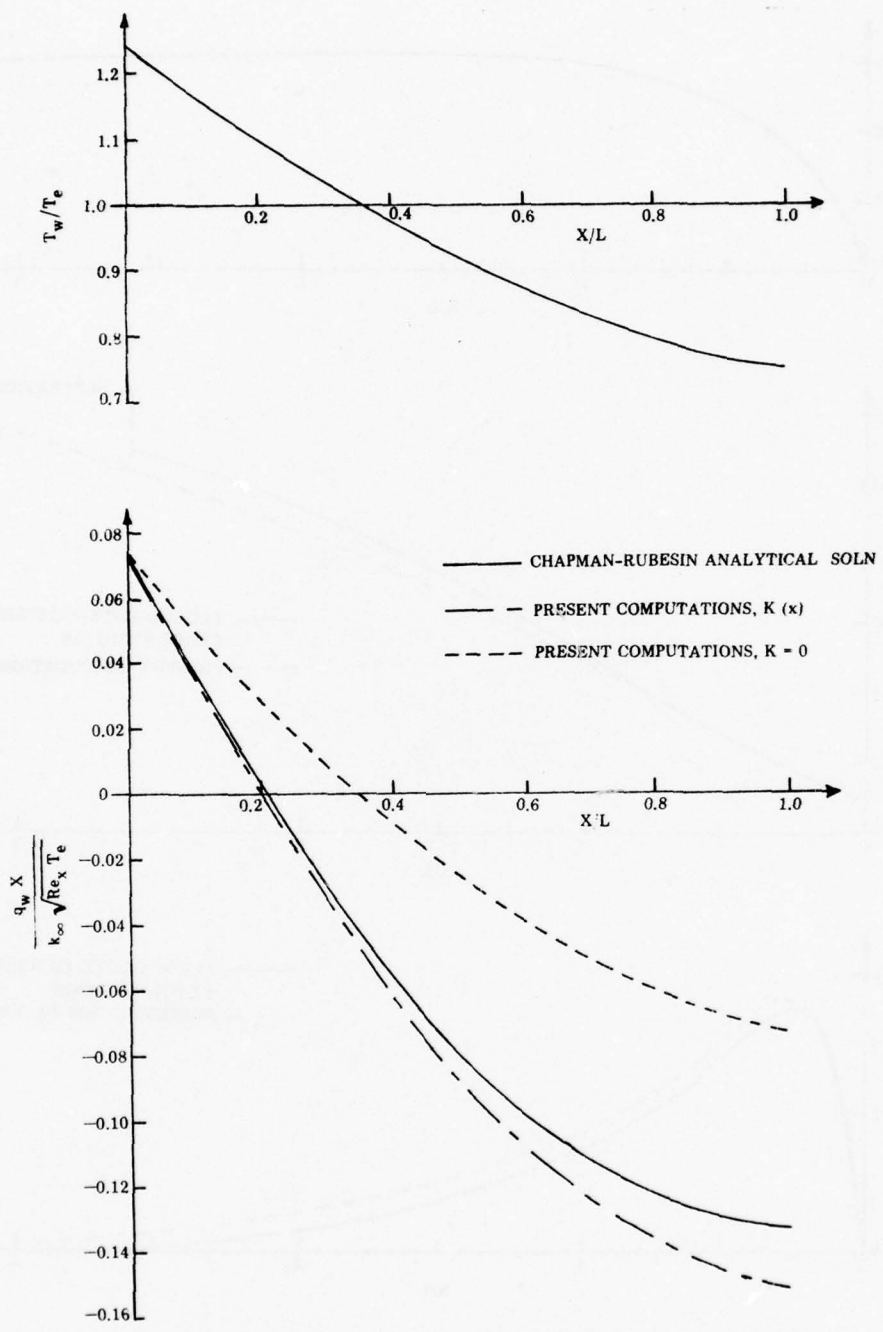


Figure 19. Comparison of present computations and analytical solution of Chapman and Rubesin.

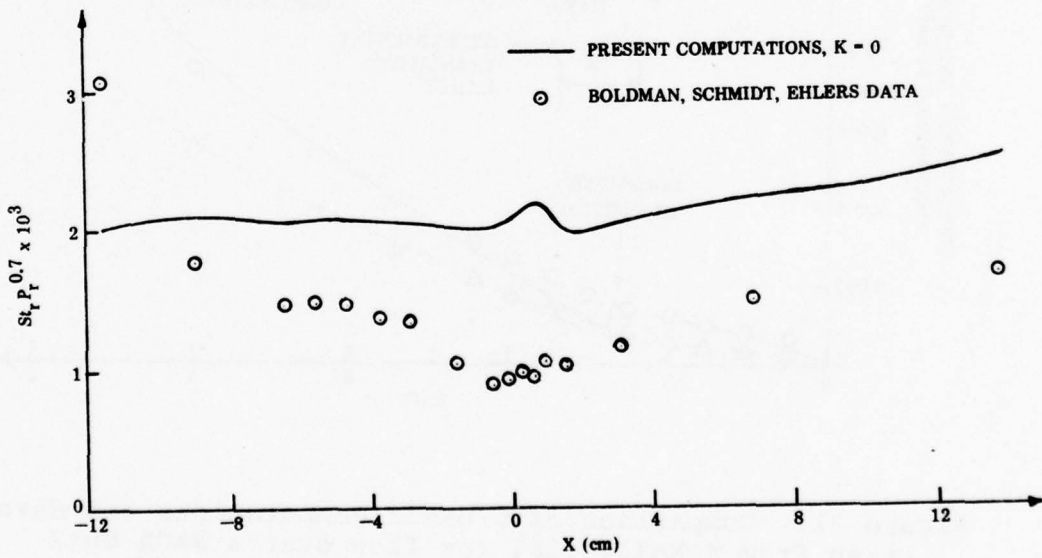
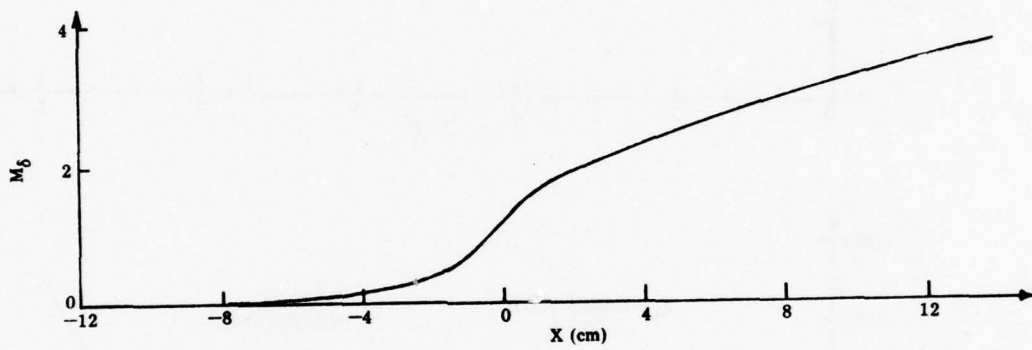
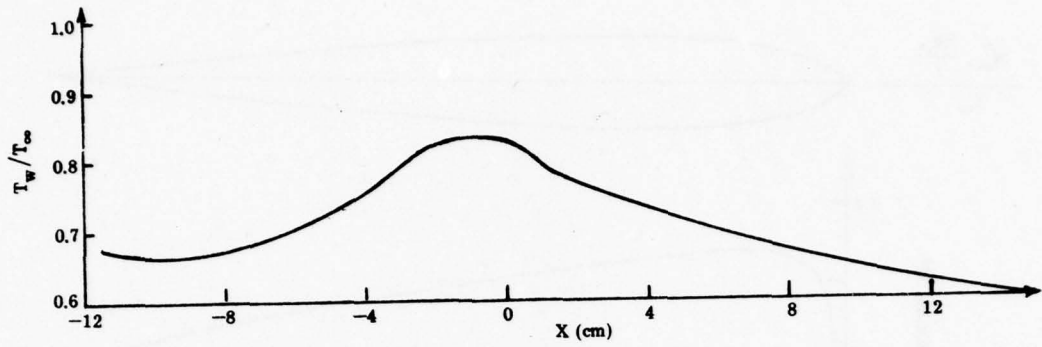


Figure 20. Comparison of present computations and data of Boldman, Schmidt, and Ehlers.

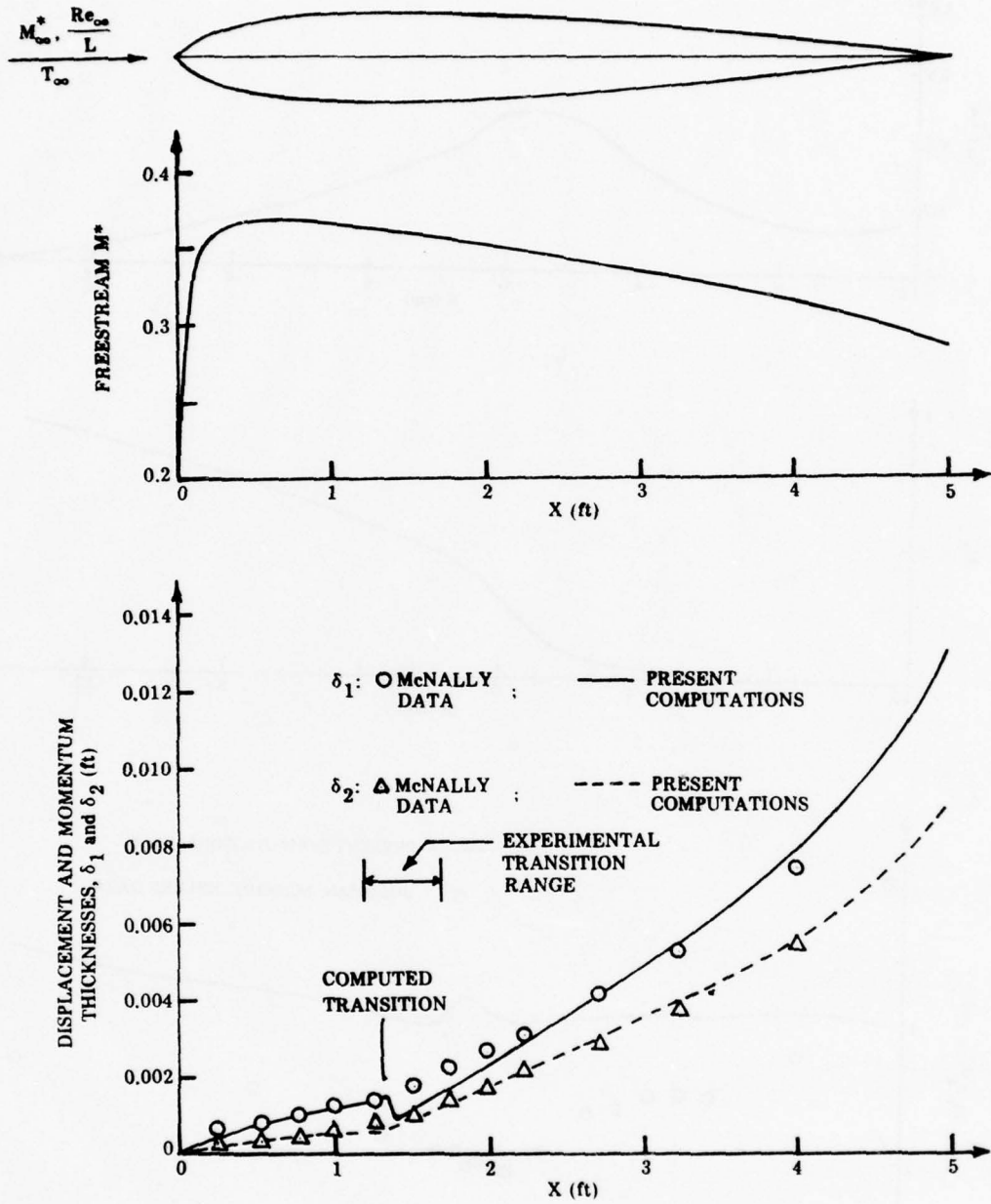


Figure 21. Comparison of present computations and data taken from McNally [16] for flow over a NACA 0012 airfoil. (This is a repeat of Figure 4(b)).

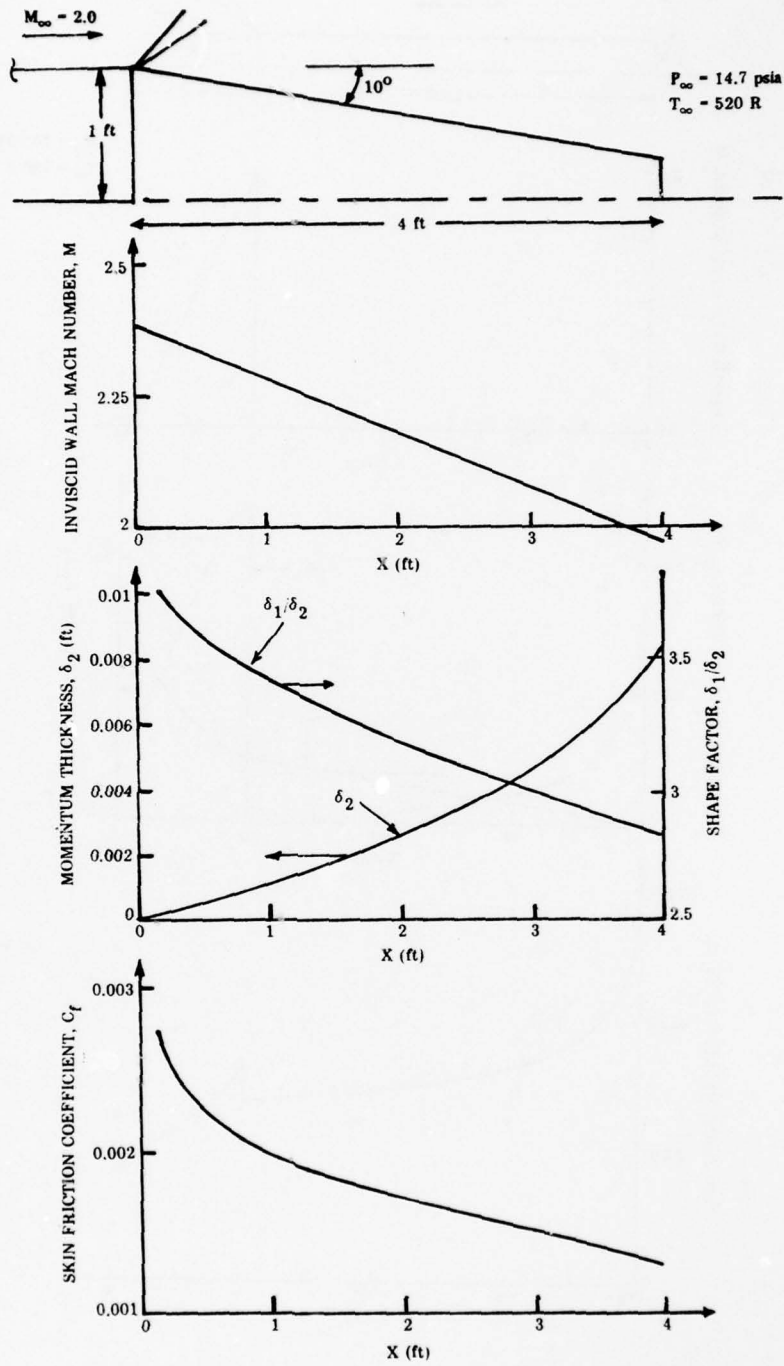


Figure 22. Predicted boundary layer characteristics for flow over a conical afterbody with turbulent boundary layer assumed to begin at the expansion.

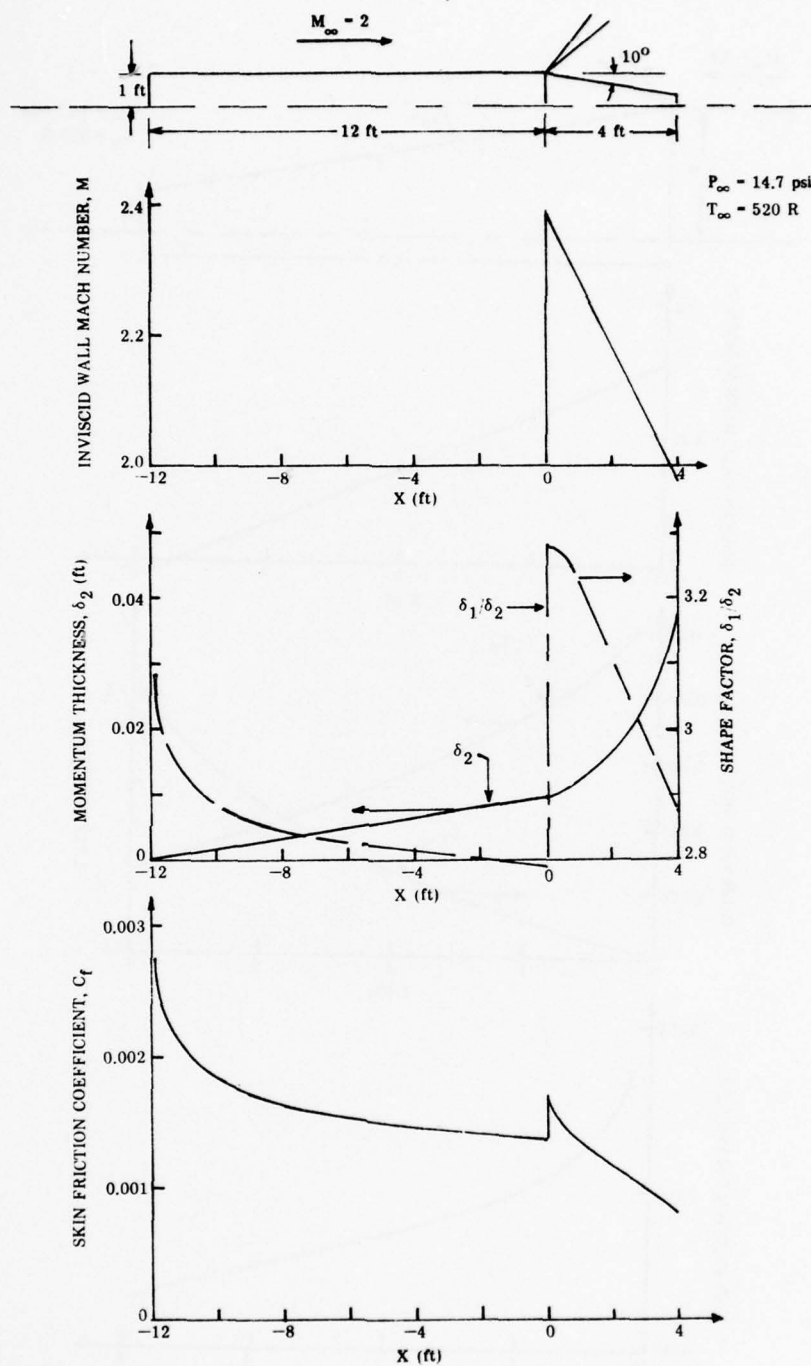


Figure 23. Predicted boundary layer characteristics for flow over a cylindrical missile/conical afterbody combination with turbulent boundary layer assumed to begin on missile body.

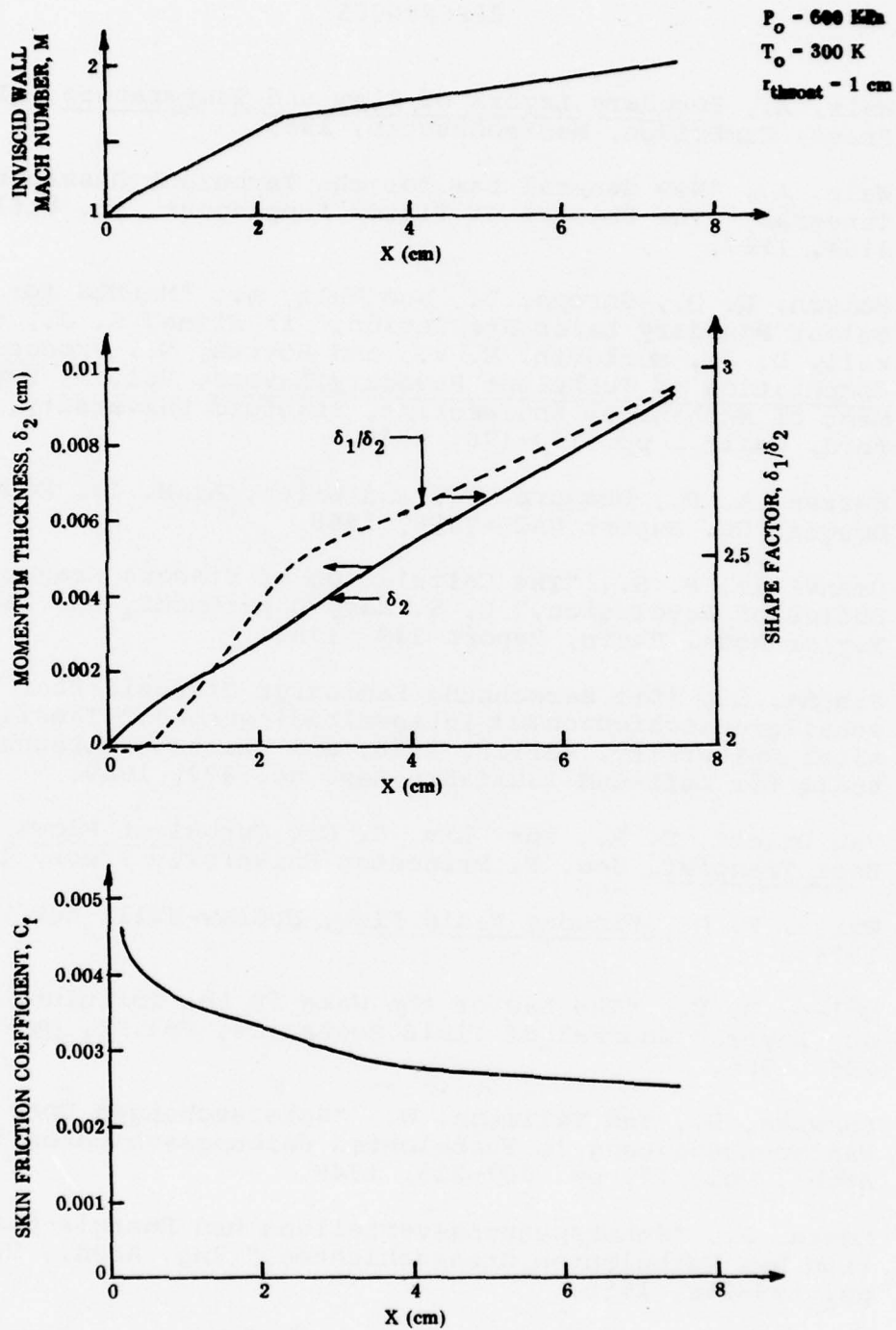


Figure 24. Predicted boundary layer characteristics for flow in a Mach 2 plane two-dimensional nozzle with hyperbolic entrance and expansion section.

REFERENCES

1. Walz, A., Boundary Layers of Flow and Temperature, MIT Press, Cambridge, Massachusetts, 1969.
2. Walz, A., "New General Law for the Turbulent Dissipation Integral," The Physics of Fluids Supplement, pp. S161-S164, 1967.
3. Felsch, K. O., Geropp, D., and Walz, A., "Method for Turbulent Boundary Layer Prediction," in Kline, S. J., Cockrell, D. J., Morkovin, M. V., and Sovran, G., Proceedings Computation of Turbulent Boundary Layers, Vol. I, Department of Mechanical Engineering, Stanford University, Stanford, Calif., pp. 170-176, 1968.
4. Wazzan, A. R., Okamura, T., and Smith, A. M. O., McDonnell-Douglas Co. Report DAC-67086, 1968.
5. Granville, P. S., "The Calculation of Viscous Drag of Bodies of Revolution," U. S. Navy Department, The David Taylor Model Basin, Report 849, 1953.
6. Jischa, M., "Die Berechnung Laminarer Dissoziierter Hyperschallgrenzschichten mit Integralbedingungen," Thesis, Technical University, Berlin, 1968; and Deutsche Versuchsanstalt für Luft-und Raumfahrt Rep. No. 872, 1969.
7. Van Driest, E. R., in: Lin, C. C., Turbulent Flows and Heat Transfer, Sec. F, Princeton University Press, 1959.
8. White, F. M., Viscous Fluid Flow, McGraw-Hill, New York, 1974.
9. Coles, D. E., "The Law of the Wake in the Turbulent Boundary Layer," Journal of Fluid Mechanics, Vol. 1, pp. 191-226, 1956.
10. Ludwig, H., and Tillmann, W., "Untersuchungen über die Wandschubspannung in Turbulenten Reibungsschichten," Ing. Arch., Vol. 17, pp. 207-218, 1949.
11. Rotta, J., "Schubspannungsverteilung und Energie-Dissipation bei Turbulenten Grenzschichten," Ing. Arch., Vol. 20, pp. 195-206, 1952.
12. Truckenbrodt, E., "Ein Quadratur-Verfahren zur Berechnung der Laminaren und Turbulenten Reibungsschicht bei Ebener und Rotationssymmetrischer Strömung," Ing. Arch., Vol. 20, pp. 211-228, 1952.

13. Felsch, K. O., "Beitrag zur Berechnung Turbulenter Grenzschichten in Zweidimensionaler Inkompressibler Strömung," Thesis, Technical University Karlsruhe, 1965.
14. Korst, H. H., Will, D. C., and Bristow, D. R., "Considerations of Viscous Flow Phenomena Affecting Transonic High Lift Airfoil Performance," McDonnell-Douglas Co. Report G 430, 1969.
15. Chapman, D. R., and Rubesin, M. W., "Temperature and Velocity Profiles in the Compressible Laminar Boundary Layer with Arbitrary Distribution of Surface Temperature," *Journal of the Aero. Sci.*, Vol. 16, pp. 547-565, 1949.
16. McNally, W. D., "FORTRAN Program for Calculating Compressible Laminar and Turbulent Boundary Layers in Arbitrary Pressure Gradients," NASA TN D-5681, 1970.
17. Becker, J. V., "Boundary-Layer Transition on the N.A.C.A. 0012 and 23012 Airfoils in the 8-Foot High-Speed Wind Tunnel," NACA WR-L-682, 1940.
18. Coles, D. E., and Hirst, E. A., Proceedings Computation of Turbulent Boundary Layers, Vol. II, Department of Mechanical Engineering, Stanford University, Stanford, Calif., 1968.
19. McLafferty, G. H., and Barber, R. E., "The Effect of Adverse Pressure Gradients on the Characteristics of Turbulent Boundary Layers in Supersonic Streams," *Journal of the Aero. Sci.*, Vol. 29, pp. 1-10, 18, 1962.
20. Winter, K. G., Smith, K. G., and Rotta, J. C., "Turbulent Boundary-Layer Studies on a Waisted Body of Revolution in Subsonic and Supersonic Flow," NATO AGARDograph No. 97, part 2, pp. 933-961, 1965.
21. Lewis, J. E., Kubota, T., and Webb, W. H., "Transformation Theory for the Adiabatic Compressible Turbulent Boundary Layer with Pressure Gradient," *AIAA Journal*, Vol. 8, pp. 1644-1650, 1970.
22. Alstatt, M. C., "An Experimental and Analytical Investigation of a Transonic Shock-Wave/Boundary-Layer Interaction," AEDC-TR-77-47, 1977.
23. Nash, J. F., and Hicks, J. G., "An Integral Method Including the Effect of Upstream History on the Turbulent Shear Stress," in Kline, S. J., Cockrell, D. J., Morkovin, M. V., and Sovran, G., Proceedings Computation of Turbulent Boundary Layers, Vol. I, Department of Mechanical

- Engineering, Stanford University, Stanford, Calif., pp. 37-45.
24. Hiemenz, K., "Die Grenzschicht an einem in den Gleichförmigen Flüssigkeitsstrom eingetauchten Geraden Kreiszyylinder," Thesis, Göttingen, 1911; Dingl. Polytechn. Journal, Vol. 326, p. 321, 1911.
 25. Schubauer, G. B., "Airflow in a Separating Laminar Boundary Layer," NACA Rep. No. 527, 1935.
 26. Smith, A. M. O., and Clutter, D. W., "Solution of the Incompressible Laminar Boundary-Layer Equations," AIAA Journal, Vol. 1, pp. 2062-2071, 1963.
 27. Hartree, D. R., Aeronautical Research Council, London, Reports and Memoranda No. 2427, 1953.
 28. Flügge-Lotz, I., and Eichelbrenner, E. A., "La Couche Limite Laminaire dans L'Ecoulement Compressible le long d'une Surface Courbé," ONERA, Rapport No. 1/694 A, 1948.
 29. Flügge-Lotz, I., and Johnson, A. F., "Laminar Compressible Boundary Layer Along a Curved Insulated Surface," Journal of the Aero. Sci., Vol. 22, pp. 445-454, 1955.
 30. Boldman, D. R., Schmidt, J. F., and Ehlers, R. C. "Prediction of Local and Integrated Heat Transfer in Nozzles Using an Integral Turbulent Boundary Layer Method," NASA TN D-6595, 1972.
 31. Addy, A. L., "Analysis of the Axisymmetric Base-Pressure and Base-Temperature Problem with Supersonic Interacting Freestream-Nozzle Flows Based on the Flow Model of Korst, et. al., Part III: A Computer Program and Representative Results for Cylindrical, Boattailed, or Flared Afterbodies," Report No. RD-TR-69-14, U. S. Army Missile Command, Redstone Arsenal, Alabama, 1970.

APPENDIX A

COMPRESSIBLE BOUNDARY LAYER (COMPBL)
PROGRAM LISTING

APPENDIX A. COMPRESSIBLE BOUNDARY LAYER PROGRAM...COMPBL
PROGRAM COMPBL .

PAGE A- 1

```

PROGRAM COMPBL (INPUT,OUTPUT,TAPE4,TAPE5=INPUT,TAPE6=OUTPUT)      COM 10
C                                                                    COM 20
C                                                                    COM 30
C          WRITTEN BY:                                             COM 30
C          J.C. DUTTON                                             COM 40
C          DEPARTMENT OF MECHANICAL AND INDUSTRIAL ENGINEERING   COM 50
C          UNIVERSITY OF ILLINOIS AT URBANA-CHAMPAIGN              COM 60
C          URBANA, ILLINOIS 61801                                  COM 70
C          OCTOBER, 1977                                           COM 80
C                                                                    COM 90
C...PROGRAM COMPBL IS A TWO-DIMENSIONAL BOUNDARY LAYER ANALYSIS PROGRAM COM 100
C...FOR IDEAL GASES BASED ON COMPUTATIONAL METHOD II OF WALZ ("BOUNDARY COM 110
C...LAYERS OF FLOW AND TEMPERATURE", MIT PRESS, 1969) AND THE DISSIPA- COM 120
C...TION LAWS OF PELSCH AND ROTTA-TRUCKENBRODT. THE METHOD MAY BE COM 130
C...APPLIED TO INCOMPRESSIBLE AND COMPRESSIBLE, LAMINAR AND TURBULENT, COM 140
C...PLANE 2-D AND AXISYMMETRIC BOUNDARY LAYERS, WITH AND WITHOUT HEAT COM 150
C...TRANSFER. THE COMPUTATIONS MAY BE STARTED AT AN ARBITRARY STREAM- COM 160
C...WISE LOCATION WITH THE BOUNDARY LAYER EITHER LAMINAR OR TURBULENT, COM 170
C...AND TRANSITION AND SEPARATION ARE PREDICTED. THE INTEGRAL MOMENTUM COM 180
C...AND MECHANICAL ENERGY EQUATIONS ARE SOLVED ITERATIVELY IN A STEP-BY- COM 190
C...STEP FASHION WITH THE FREESTREAM VELOCITY APPROXIMATED WITH A COM 200
C...PIECEWISE LINEAR FUNCTION. FOR CASES WITH HEAT TRANSFER AN OPTION COM 210
C...IS AVAILABLE (HTCORR=.TRUE.) WHEREBY THE CALCULATION OF THE WALL COM 220
C...HEAT FLUX IS IMPROVED BY SOLVING THE THERMAL ENERGY INTEGRAL COM 230
C...EQUATION FOR A CORRECTION PARAMETER, CHT, TO ACCOUNT FOR THE EFFECTS COM 240
C...OF STREAMWISE WALL TEMPERATURE AND PRESSURE GRADIENTS. COM 250
C...THE DIMENSIONAL VARIABLES IN THE ANALYSIS ARE ZSTART,REINFL,XTRAN, COM 260
C...XI,YI,RI,ZI,D1,D2,D999, AND RCORR WHICH ALL HAVE DIMENSIONS OF COM 270
C...LENGTH, [L] OR [L]**(-1). ZSTART,REINFL,XTRAN,XI,YI, AND RI MUST COM 280
C...BE INPUT WITH CONSISTENT UNITS, AND THEN ON OUTPUT, ZI,D1,D2,D999, COM 290
C...AND RCORR WILL HAVE THE SAME UNITS. COM 300
C                                                                    COM 310
C...THE INPUT VARIABLES FROM FILE INPUT ARE: COM 320
C                                                                    COM 330
C... FLOW----LITERAL VARIABLE DESCRIBING FLOW REGIME--EQUAL TO COM 340
C... "LAMINAR" OR "TURBULENT" COM 350
C... GEOM----LITERAL VARIABLE DESCRIBING GEOMETRY--EQUAL TO COM 360
C... "PLANE 2-D" OR "AXISYM" COM 370
C... MTYPE---LITERAL VARIABLE DESCRIBING VELOCITY INPUT DATA TYPE COM 380
C... --EQUAL TO "MACH" OR "MSTAR" COM 390
C... TTYPE---LITERAL VARIABLE DESCRIBING WALL TEMPERATURE INPUT DATA COM 400
C... TYPE--EQUAL TO "THETA" CR "TWTINE" COM 410
C... ZSTART--STARTING VALUE OF Z, [L] (DEFAULT=0.0) COM 420
C... HSTART--STARTING VALUE OF H; SEE WALZ PP 267-268 AND FIGS I.1 COM 430
C... AND 6.5 AND ACCOMPANYING REPORT, TABLES I AND II COM 440
C... AND FIG. 2 (DEFAULT=1.572) COM 450
C... BSTART--BSTART*PI IS THE INCLUDED ANGLE AT THE LEADING EDGE COM 460
C... FOR BOTH PLANE 2-D AND AXISYMMETRIC EXTERNAL FLOWS COM 470
C... (DEFAULT=0.0) COM 480
C... MINF----MACH NUMBER (OR MSTAR) OF APPROACH FLOW COM 490

```

THIS PAGE IS BEST QUALITY PRACTICABLE
FROM COPY FURNISHED TO DDC

APPENDIX A.
PROGRAM COMPL .

COMPRESSIBLE BOUNDARY LAYER PROGRAM...COMPBL

PAGE A- 2

C...	REINFL--REYNOLDS NUMBER DIVIDED BY CHARACTERISTIC LENGTH OF	COM 500
C...	APPROACH FLOW, I.E. $\text{RHOINF} \cdot \text{UINF} / \mu \text{INF}$, [L]**(-1)	COM 510
C...	XTRAN---X LOCATION FOR SPECIFIED TRANSITION, [L]	COM 520
C...	(DEFAULT=0.0)	COM 530
C...	FSTINT--PRESTREAM TURBULENCE INTENSITY--USED IN TRANSITION	COM 540
C...	SUBROUTINE, IN PERCENT (DEFAULT=0.0)	COM 550
C...	G-----RATIO OF SPECIFIC HEATS (DEFAULT=1.405)	COM 560
C...	W-----EXPONENT ON VISCOSITY POWER LAW (DEFAULT=0.7)	COM 570
C...	RL-----LAMINAR RECOVERY FACTOR (DEFAULT=0.85)	COM 580
C...	RT-----TURBULENT RECOVERY FACTOR (DEFAULT=0.88)	COM 590
C...	SL-----LAMINAR REYNOLDS ANALOGY FACTOR (DEFAULT=0.80)	COM 600
C...	ST-----TURBULENT REYNOLDS ANALOGY FACTOR (DEFAULT=0.82)	COM 610
C...	EPS----CONVERGENCE CRITERION VARIABLE (DEFAULT=1.0E-4)	COM 620
C...	NOTRAN--LOGICAL VARIABLE WHICH IF .TRUE. SUPPRESSES	COM 630
C...	CALLING OF THE TRANSITION SUBROUTINE FOR LAMINAR	COM 640
C...	BOUNDARY LAYERS (DEFAULT=.FALSE.)	COM 650
C...	HTCORR--LOGICAL VARIABLE WHICH IF .TRUE. CAUSES THE THERMAL	COM 660
C...	ENERGY INTEGRAL EQUATION TO BE SOLVED FOR THE HEAT	COM 670
C...	FLUX CORRECTION PARAMETER, CHT (DEFAULT=.FALSE.)	COM 680
C...	ERROR--LOGICAL VARIABLE WHICH IF .TRUE. CAUSES INTERMEDIATE	COM 690
C...	H VALUES AND VARIABLES ASSOCIATED WITH THE TURBULENT	COM 700
C...	DISSIPATION INTEGRAL AND HEAT TRANSFER CORRECTION	COM 710
C...	PARAMETER TO BE PRINTED FOR DEBUGGING PURPOSES	COM 720
C...	(DEFAULT=.FALSE.)	COM 730
C...	XI-----AXIAL LOCATION, [L]	COM 740
C...	YI-----NORMAL LOCATION, [L]	COM 750
C...	MDI-----PRESTREAM MACH NUMBER (OR MSTAR)	COM 760
C...	RI-----CROSS-SECTIONAL RADIUS OF AXISYMMETRIC BODIES, OR	COM 770
C...	LOCATION NORMAL TO CENTERLINE FOR 2-D BODIES, [L]	COM 780
C...	THETI---WALL TEMPERATURE RATIO, (TADWALL-TWALL)/(TADWALL-TSTREAM)	COM 790
C...	(OR TWALL/TINF)	COM 800
C		COM 810
C...	THESE VARIABLES SHOULD BE INPUT IN THE FOLLOWING WAY. THE FIRST	COM 820
C...	CARD (RECORD) IS FOR A TITLE TO HELP IDENTIFY THE OUTPUT. ANY	COM 830
C...	MESSAGE UP TO 80 COLUMNS CAN BE USED, BUT FOR AESTHETIC REASONS	COM 840
C...	THE MESSAGE SHOULD BE CENTERED IN THE 80 COLUMNS. IT IS ALSO	COM 850
C...	SUGGESTED THAT THE UNITS FOR DIMENSION [L] BE ENTERED AS PART OF	COM 860
C...	THE TITLE. ON THE NEXT CARD THE FOUR LITERAL VARIABLES FLOW,GEOM,	COM 870
C...	TYPE,TYPE ARE ENTERED IN 4A10 FCMAT. THE VALUE OF EACH OF	COM 880
C...	THESE LITERALS SHOULD BE LEFT JUSTIFIED IN EACH 10 COLUMN BLOCK.	COM 890
C...	NAMELIST "BL" WHICH ENCOMPASSES VARIABLES ZSTART-ERROR IS ENTERED	COM 900
C...	ON THE NEXT CARD(S). THE FIRST COLUMN ON THE NAMELIST CARD(S)	COM 910
C...	SHOULD BE BLANK. ALL VARIABLES IN NAMELIST "BL" EXCEPT MINF AND	COM 920
C...	REINFL ARE DEFAULTED, SO ONLY THESE TWO AND THOSE WHICH ARE TO BE	COM 930
C...	OVERRIDDEN NEED BE ENTERED. THE REMAINING CARDS CONTAIN THE LOCAL	COM 940
C...	DATA: X,Y,M,B,THETA FOR EACH POINT AT WHICH THE BOUNDARY LAYER	COM 950
C...	PARAMETERS ARE TO BE FOUND. THESE VARIABLES ARE ENTERED IN 5F10	COM 960
C...	FORMAT, AND AS MANY POINTS AS DESIRED CAN BE USED.	COM 970
C		COM 980

THIS PAGE IS BEST QUALITY PRACTICABLE
FROM COPY FURNISHED TO DDG

APPENDIX A.
PROGRAM COMPBL .

COMPRESSIBLE BOUNDARY LAYER PROGRAM...COMPBL

PAGE A- 3

```

C...THE OUTPUT VARIABLES TO FILE OUTPUT ARE:
C
C... XI-----AXIAL LOCATION, [L]
C... ZI-----ZI=D2*(RD2**N) (N=1.0 FOR LAMINAR BOUNDARY LAYERS;
C...          0.268 FOR TURBULENT BOUNDARY LAYERS), [L]
C... HI-----HI=(D3/D2)U (D3=ENERGY LOSS THICKNESS)
C... D1D2----SHAPE FACTOR, D1/D2
C... D1-----DISPLACEMENT THICKNESS, [L]
C... D2-----MOMENTUM THICKNESS, [L]
C... D999----99.9% BOUNDARY LAYER THICKNESS,[L]
C... RD2----MOMENTUM THICKNESS REYNOLDS NUMBER (RHOD*UD*D2/MUWALL)
C... CP-----LOCAL SKIN FRICTION COEFFICIENT (2*TAUWALL/(RHOD*UD**2))
C... QDIM----DIMENSIONLESS LOCAL WALL HEAT FLUX (QWALL/(RHOD*UD**3))=
C...          -R*STANTON*THET1/2)
C
C...THE OUTPUT VARIABLES TO FILE TAPE4 ARE:
C
C... XI-----AXIAL LOCATION, [L]
C... RCORR---CORRECTED RADIUS OR NORMAL LOCATION--EQUAL TO RI+D1, [L]
C
      IMPLICIT REAL (J,M,N)
      LOGICAL ERROR,NOTRAN,HTCORR
      COMMON/CTRANS/RD2,N,R,RT,S,ST,FLOW,G,MTYPE,TTYPE,MINF,KTRANS,
      $KINST,RD2U,PPARI,PPARIM1,DELX,FSTINT
      DIMENSION HMAIN(21),HINNER(21),QWRITE(8)
C
C...DECLARE INPUT NAMELIST AND SET DEFAULT VALUES
C
      NAMELIST/BL/ ZSTART,HSTART,BSTART,MINF,REINFL,XTRAN,FSTINT,G,W,
      $RL,RT,SL,ST,EPS,ERROR,NOTRAN,HTCORR
      DATA ZSTART,HSTART,BSTART,CSTART,XTRAN,FSTINT,G,W,RL,RT,SL,ST,EPS,
      $ERROR,NOTRAN,HTCORR/0.0,1.572,0.0,0.0,0.0,0.0,1.405,0.7,0.85,
      $0.88,0.80,0.82,1.0E-4,.FALSE.,.FALSE.,.FALSE./
C
C...GENERAL STATEMENT FUNCTIONS
C
      FMS(G,M)=SQRT((G+1.)/2.*M**2/(1.+(G-1.)/2.*M**2))
      FTWTF(R,G,MD,MINF,THETA)=(1.+R*(G-1.)/2.*MD**2*(1.-THETA))*
      $(1.+(G-1.)/2.*MINF**2)/(1.+(G-1.)/2.*MD**2)
      FB(THETA,R,G,MD)=THETA**R*(G-1.)/2.*MD**2
      FC1(REINFL,MDS,MINFS,MD,MINF,R,G,THETA,W)=REINFL*MDS/MINFS*((1.+
      $(G-1.)/2.*MINF**2)/(1.+(G-1.)/2.*MD**2))**((1.+(G-1.)/
      $/2.*MD**2)/((1.+R*(G-1.)/2.*MD**2*(1.-THETA))*(1.+(G-1.)/2.*MINF
      $**2))**W
      FD2(N,Z,C1)=(Z/C1**N)**(1./(1.+N))
      FRD2(N,Z,C1)=(Z*C1)**(1./(1.+N))
      FRD2U(RD2,D2D2U,R,G,MD,THETA)=RD2/(D2D2U*(1.+R*(G-1.)/2.*MD**2*
      $(1.-THETA)))
      FCF(A,RD2,N,D2D2U)=2.*A/RD2**N*D2D2U

```

```

PQDIM (CF, S, B, CHT, G, MD) = -CF / (2.*S) * (B+CHT) / (MD**2 * (G-1.)) COM1480
PDELX (XI, YI, XIM1, YIM1) = SQRT ((XI-XIM1)**2 + (YI-YIM1)**2) COM1490
PPPAR (C1, DMSDXMS, D2U, R, G, MD, THETA) = C1 * DMSDXMS * D2U**2 / (1.+R*(G-1.) / COM1500
$2.*MD**2*(1.-THETA)) COM1510
C COM1520
C... UNIVERSAL FUNCTIONS FOR THE METHOD COM1530
C COM1540
PAZ (UIM1UI, F1B, NUWBRN) = UIM1UI**F1B*NUWBRN COM1550
PBZ (UIM1UI, F1B, NUWBRN) = (1.-UIM1UI** (1.+F1B)) / ((1.+F1B) * (1.-UIM1UI COM1560
$) * NUWBRN) COM1570
PAH (UIM1UI, F3B) = UIM1UI**F3B COM1580
PBH (UIM1UI, F3B) = (1.-UIM1UI** (1.+F3B)) / ((1.+F3B) * (1.-UIM1UI)) COM1590
PF1 (N, D1D2, MD) = 2.*N + (1.+N) * D1D2 - MD**2 COM1600
PF2 (N, D2D2U, A) = (1.+N) * D2D2U * A COM1610
PF3 (D1D2, D4D3) = 1. - D1D2 + 2.*D4D3 COM1620
PF4 (RD2, N, CD, A, D2D2U, HS) = RD2**N * CD - A * D2D2U * HS COM1630
PF5 (DMSDXMS, HS, D1D2, G, MD, HSP, DD2DXD2) = (DMSDXMS * (1.+D1D2+ COM1640
$(G-1.) * MD**2 + HS * (1.-G*MD**2)) + HSP * HS * DD2DXD2) / (HS-1.) COM1650
PF6 (HS, BP, B, DMSDXMS, D1D2, G, MD) = (BP - B * DMSDXMS * (1.+D1D2 + (G-1.) * COM1660
$MD**2)) / (HS-1.) COM1670
FD1D2 (H12, D2D2U, R, G, MD, HS, THETA, CHT) = H12 / D2D2U + R * (G-1.) / 2.*MD**2 * COM1680
$(HS-THETA) + CHT * (HS-1.) COM1690
FD4D3 (R, G, MD, HS, THETA, CHT) = R * (G-1.) / 2.*MD**2 * (HS-THETA) / HS COM1700
$ + CHT * (HS-1.) / HS COM1710
FD2D2U (R, G, MD, HS, THETA) = 1. / (1.+R*(G-1.) / 2.*MD**2 * (HS-THETA) * COM1720
$(2.-HS)) COM1730
FHS (H, PSI) = H * PSI COM1740
FH (HS, PSI) = HS / PSI COM1750
FPSI (PSI12, MD, PSIJP) = 1. + (PSI12-1.) * MD / (MD + (PSI12-1.) / PSIJP) COM1760
PPSI12 (D1UD, H, THETA, G1) = (2.-D1UD) * THETA / H + (1.-D1UD) * (1.- COM1770
$THETA) / (H * G1) COM1780
PPSIOP (H, THETA) = 0.0144 * (2.-H) * (2.-THETA) ** 0.8 COM1790
C COM1800
C... STATEMENT FUNCTIONS FOR LAMINAR BOUNDARY LAYERS COM1810
C COM1820
PAL (H) = 1.7261 * (H-1.515) ** J. 7158 COM1830
PCDL (H, H, G, MD, THETA, W, RD2, D2D2U) = 2.*D2D2U / RD2 * (0.1564 + 2.1921 * COM1840
$(H-1.515) ** 1.70) * ((1.+R*(G-1.) / 2.*MD**2 * ((1.160 * H - 1.072) - THETA * COM1850
$(2.*H - 2.581))) / (1.+R*(G-1.) / 2.*MD**2 * (1.-THETA))) ** W COM1860
PH12L (H) = 4.0306 - 4.2845 * (H-1.515) ** J. 3886 COM1870
PD1UDL (H) = 0.420 - (H-1.515) ** (0.424 * H) COM1880
PG1L (H) = 0.324 + 0.336 * (H-1.515) ** 0.555 COM1890
C COM1900
C... STATEMENT FUNCTIONS FOR TURBULENT BOUNDARY LAYERS COM1910
C COM1920
FAT (H) = 0.03894 * (H-1.515) ** 0.7 COM1930
FCDTP (CF, RD2, N, JP, J, JSP, HS, D1D2, PI) = CF / 2. * ((JP - N / 2. * J) / (RD2 ** COM1940
$(N / 2.) * JSP) * (1. + (D1D2 + 1.) * PI / D1D2) + HS * (1. + (D1D2 - 1.) / D1D2 * PI)) COM1950
FCDTRT (D2D2U, RD2) = 0.0112 * D2D2U * RD2 ** (-0.168) COM1960

```

THIS PAGE IS BEST QUALITY PRACTICABLE
FROM COPY FURNISHED TO DDC

APPENDIX A.
PROGRAM COMPBL .

COMPRESSIBLE BOUNDARY LAYER PROGRAM...COMPBL

PAGE A- 5

```

FJ (D1D2,CF) = (D1D2-1.) / (D1D2*SQRT (CF/2.))
PA 1 (D1D2) = 0.029*(0.93-1.95*ALOG10(D1D2)) **1.705
FJSP (A1,D1D2,HS) = (D1D2-(D1D2-1.)*(1.-0.0209366/A1*(0.93-1.95*
$ALOG10(D1D2)) **0.705)) / (SQRT (A1)*D1D2**2) * (0.55216-0.3875*HS+
$0.04855*SQRT (0.775*HS-1.10667)) / ((HS-1.431) **2*SQRT (0.775*HS-
$1.10667))
FPI (D1D2,D2,CF,DMSDXMS) = -2.*D1D2*D2*DMSDXMS/CF
PH12T (H) = 1.+1.48*(2.-H)+104.*(2.-H) **6.7
FD1UDT (H) = (2.-H) / (2.*(H-1.))
FG1T (H) = 0.306+(H-1.5)-0.885*(H-1.5) **1.53
COM1970
COM1980
COM1990
COM2000
COM2010
COM2020
COM2030
COM2040
COM2050
COM2060
COM2070
C
C...READ, CHECK, AND WRITE INPUT VARIABLES AND SET INITIAL
C...PARAMETERS
COM2080
COM2090
C
IP=KTRANS=KINST=LCOUNT=LIM=0
COM2100
RRAT1PN=1.0 $ DELX=DELXIM1=0.0
COM2110
READ (5,900) QWRITE,FLOW,GEOM,MTYPE,TTYPE
COM2120
READ (5,BL)
COM2130
K=0 $ WRITE (6,901) $ WRITE (4,901)
COM2140
IF (FLOW .EQ. "LAMINAR" .OR. FLOW .EQ. "TURBULENT") GO TO 10
COM2150
K=K+1 $ WRITE (6,902)
COM2160
10 IF (GEOM .EQ. "PLANE 2-D" .OR. GEOM .EQ. "AXISYM") GO TO 20
COM2170
K=K+1 $ WRITE (6,903)
COM2180
20 IF (MTYPE .EQ. "MACH" .OR. MTYPE .EQ. "MSTAR") GO TO 30
COM2190
K=K+1 $ WRITE (6,904)
COM2200
30 IF (TTYPE .EQ. "THETA" .OR. TTYPE .EQ. "TWTINF") GO TO 40
COM2210
K=K+1 $ WRITE (6,905)
COM2220
40 IF (HSTART .GT. 1.515 .AND. HSTART .LE. 2.0) GO TO 50
COM2230
K=K+1 $ WRITE (6,906)
COM2240
50 IF (BSTART .GE. -0.1988 .AND. BSTART .LE. 2.0) GO TO 60
COM2250
K=K+1 $ WRITE (6,907)
COM2260
60 IF (ZSTART .GE. 0.0 .AND. MINF .GT. 0.0 .AND. REINFL .GT. 0.0
COM2270
$.AND. FSTINT .GE. 0.0 .AND. W .GE. 0.0 .AND. RL .GT. 0.0 .AND. RT
COM2280
$.GT. 0.0 .AND. SL .GT. 0.0 .AND. ST .GT. 0.0 .AND. EPS .GT. 0.0)
COM2290
$GO TO 70
COM2300
K=K+1 $ WRITE (6,908)
COM2310
70 IF (G .GE. 1.0 .AND. G .LE. 1.67) GO TO 80
COM2320
K=K+1 $ WRITE (6,909)
COM2330
80 IF (.NOT. (MTYPE .EQ. "MSTAR" .AND. MINF .GT. SQRT((G+1.)/(G-1.))))
COM2340
$GO TO 90
COM2350
K=K+1 $ WRITE (6,910)
COM2360
90 IF (K .EQ. 0) GO TO 100
COM2370
WRITE (6,911) $ GO TO 600
COM2380
100 CALL MSORT (MINF,MINES)
COM2390
WRITE (6,912) QWRITE,FLOW,GEOM,MTYPE,TTYPE,ZSTART,HSTART,BSTART,
COM2400
$MINF,REINFL,XTRAN,FSTINT,G,W,RL,RT,SL,ST,EPS,NOTRAN,HTCORR,ERROR
COM2410
WRITE (4,913) QWRITE
COM2420
IF (FLOW .EQ. "TURBULENT" .AND. ZSTART .EQ. 0.0) KTRANS=1
COM2430
IF (FLOW .EQ. "TURBULENT" .AND. KTRANS .NE. 1) GO TO 110
COM2440
COM2450

```

THIS PAGE IS BEST QUALITY PRACTICABLE
FROM COPY FURNISHED TO DDC

APPENDIX A.
PROGRAM COMPBL .

COMPRESSIBLE BOUNDARY LAYER PROGRAM...COMPBL

PAGE A- 6

```

N=1.0 $ R=RL $ S=SL COM2460
FLOW="LAMINAR" $ GO TO 120 COM2470
110 N=J.268 $ R=RT $ S=ST COM2480
C COM2490
C...STARTING SEQUENCE FOR BOUNDARY LAYER CALCULATIONS COM2500
C COM2510
120 WRITE(6,914) COM2523
WRITE(4,915) COM2530
IF(ZSTART.NE.0.0) GO TO 150 COM2540
IF(GEOM.EQ."AXISYM") BSTART=BSTART/(3.-BSTART) COM2550
MSTART=BSTART/(2.-BSTART) COM2560
READ(5,916) XI,YI,MDI,RI,THETI COM2570
CALL MSCRT(MDI,MDIS) COM2580
RCORR=RI $ IP=IP+1 COM2590
IF(MDI.EQ.0.0) GO TO 130 COM2600
D1=D2=D999=RD2=.0 $ D1D2=CF=QDIM="----" COM2610
WRITE(6,917) XI,ZSTART,HSTART,D1D2,D1,D2,D999,RD2,CF,QDIM COM2620
GO TO 140 COM2630
130 RD2=0.0 $ D1=D2=D999=D1D2=CF=QDIM="----" COM2640
WRITE(6,918) XI,ZSTART,HSTART,D1D2,D1,D2,D999,RD2,CF,QDIM COM2650
140 WRITE(4,919) XI,RCORR COM2660
XIM1=XI $ YIM1=YI $ MDIM1=MDI COM2670
MDIM1S=MDIS $ PPARIM1=0.0 COM2680
150 READ(5,916) XI,YI,MDI,RI,THETI COM2690
CALL MSORT(MDI,MDIS) COM2700
CALL ISORT(THETI,TWTII,BI,MDI) $ KPOINT=1 COM2710
IF(ZSTART.NE.0.0) GO TO 160 $ DELX=FDELX(XI,YI,XIM1,YIM1) COM2720
DMSDXMS=(MDIS-MDIM1S)/(DELX*FMS(G,(MDI+MDIM1)/2.)) COM2730
CALL IERROR(DELX,MDI,MDIS,G,RI,GLOM,TWTII),RETURNS(60) COM2740
160 HI=HSTART $ ZI=ZSTART $ CHT=CSTART COM2750
IF(FLOW.EQ."TURBULENT") GO TO 170 COM2760
A=FAL(HI) $ H12=PH12L(HI) COM2770
DIUD=FDIUDL(HI) $ G1=PG1L(HI) $ GO TO 180 COM2780
170 A=FAT(HI) $ H12=PH12T(HI) COM2790
DIUD=FDIUDT(HI) $ G1=PG1T(HI) COM2800
180 IF(ABS(THETI).LE.2.0) GO TO 190 COM2810
PSI=1.0 $ GO TO 200 COM2820
190 PSIOP=FPSIOP(HI,THETI) COM2830
PSI12=FPSI12(DIUD,HI,THETI,G1) COM2840
PSI=FPSI(PSI12,MDI,PSIOP) COM2850
200 HIS=PHS(HI,PSI) COM2860
D2D2U=FD2D2U(R,G,MDI,HIS,THETI) COM2870
D1D2=FD1D2(H12,D2D2U,R,G,MDI,HIS,THETI,CHT) COM2880
IF(ZSTART.EQ.0.0) ZI=PF2(N,D2D2U,A)*DELX/(1.+MSTART*PF1(N,D1D2, COM2890
$MDI)) COM2900
IF(ZSTART.EQ.0.0.AND.GEOM.EQ."AXISYM") ZI=ZI/3. COM2910
C1=FC1(REINFL,MDIS,MINFS,MDI,MINF,R,G,THETI,W) COM2920
GO TO 560 COM2930
COM2940

```

APPENDIX A.
PROGRAM COMPBL .

COMPRESSIBLE BOUNDARY LAYER PROGRAM...COMPBL

PAGE A- 7

```

C...READ AND CHECK INPUT DATA FOR NEXT POINT
C
210 READ(5,916) XI,YI,MDI,RI,THETI
    IF(EOF(5)) 600,220
220 CALL MSORT(MDI,MDIS)
    CALL ISORT(THETI,TWTII,BI,MDI)
    DELX=PDELX(XI,YI,XIM1,YIM1)
    CALL IERROR(DELX,MDI,MDIS,G,RI,GEOM,TWTII),RETURNS(600)
    KPCINT=KPOINT1+1 $ KTRIP=0 $ GO TO 250
C
C...LINEAR INTERPOLATION FOR SUBDIVIDED POINTS
C
230 DLV=FLOAT(LIM)
    DX1=(XI-XIM1)/DIV $ DY1=(YI-YIM1)/DIV
    DM1=(MDI-MDIM1)/DIV
    DT1=(THETI-THETIM1)/DIV $ DR1=(RI-RIM1)/DIV
240 XI=XIM1+DX1 $ YI=YIM1+DY1 $ MDI=MDIM1+DM1
    THETI=THETIM1+DT1 $ RI=RIM1+DR1 $ MDIS=FMS(G,MDI)
    BI=FB(THETI,R,G,MDI) $ TWTII=FTWTINF(R,G,MDI,MINF,THETI)
    IF(FLOW.EQ. FLOWIM1 .OR. ICOUNT.EQ. 1) GO TO 260
C
C...ALLOW FOR INTERVAL SUBDIVISION IF NECESSARY
C
250 ICOUNT=LCOUNT=LIM=0
260 ICCUNT=ICOUNT+1
    HMIN1=MDIM1S/MDIS
    IF(ICOUNT.EQ. 1) LIM1=IPIX(ABS(1./HMIN1-1.)/0.315)+1
C
C...CALCULATE SOME QUANTITIES WHICH ARE CONSTANT THROUGHOUT THE
C...ITERATIONS
C
    DELX=PDELX(XI,YI,XIM1,YIM1) $ MDB=(MDI+MDIM1)/2.
    MDSE=FMS(G,MDB) $ THETB=(THETI+THETIM1)/2.
    TWTIB=FTWTINF(R,G,MDB,MINF,THETB) $ BB=FB(THETB,R,G,MDB)
    DMSDXMS=(MDIS-MDIM1S)/(DELX*MDSB)
    BP=(BI-BIM1)/DELX
    MUWRN=(TWTIIM1/TWTII)**(W*N)
    MUWBRN=(TWTIB/TWTII)**(W*N)
    IF(GEOM.EQ. "AXISYM") RRAT1PN=(RI/RIM1)**(1.+N)
    C1B=FC1(REINFL,MDSB,MINFS,MDB,MINF,R,G,THETB,W)
    C1=FC1(REINFL,MDIS,MINFS,MDI,MINF,R,G,THETI,W)
C
C...MAIN ITERATION LOOP FOR BOUNDARY LAYER CALCULATIONS
C
    I=KCDS=KTRIP=0 $ DHDX=DHDXIM1 $ CHT=CHTIM1
    IF(DELXIM1.EQ. 0.0) GO TO 270
    IF(ABS(DELX/DELXIM1).GT. 2.0) DHDX=0.0
270 H1OLD=HMAIN(1)=HIM1+DHDX*DELX
    IF(ERROR) WRITE(6,920) HMAIN(1)

```

THIS PAGE IS BEST QUALITY PRACTICABLE
FROM COPY FURNISHED TO DDC

APPENDIX A. COMPRESSIBLE BOUNDARY LAYER PROGRAM...COMPBL
PROGRAM COMPBL .

PAGE A- 8

```

280 I=I+1 $ HB=(HIOLD+HIM1)/2. $ CHTB=(CHT+CHTIM1)/2. CON3440
    IF (ERROR) WRITE (6,921) HB CON3450
    IF (HB .LE. 1.515) GO TO 510 CON3460
    IF (HB .LE. 2.0) GO TO 290 $ WRITE (6,922) XI $ GO TO 600 CON3470
290 IF (FLOW .EQ. "TURBULENT") GO TO 300 CON3480
C CON3490
C...EVALUATE AVERAGE QUANTITIES FOR LAMINAR FLOWS CON3500
C CON3510
    AB=FAL (HB) $ H12B=PH12L (HB) CON3520
    D1UDB=FD1U DL (HB) $ G1B=FG1L (HB) $ GO TO 310 CON3530
C CON3540
C...EVALUATE AVERAGE QUANTITIES FOR TURBULENT FLOWS CON3550
C CON3560
300 AB=FAT (HB) $ H12B=PH12T (HB) CON3570
    D1UDB=FD1U DT (HB) $ G1B=FG1T (HB) CON3580
C CON3590
C...EVALUATE UNIVERSAL FUNCTIONS IN ORDER TO OBTAIN A NEW CON3600
C...VALUE FOR Z AT STATION I CON3610
C CON3620
310 IF (ABS (THETB) .LE. 2.0) GO TO 320 CON3630
    PSIB=1.0 $ GO TO 330 CON3640
320 PS10PB=FPS10P (HB, THETB) CON3650
    PS112B=FPS112 (D1UDB, HB, THETB, G1B) CON3660
    PSIB=FPSI (PS112B, MDB, PS10PB) CON3670
330 HSB=FHS (HB, PSIB) CON3680
    D2D2UB=FD2D2U (R, G, MDB, HSB, THETB) CON3690
    D4D3B=FD4D3 (R, G, MDB, HSB, THETB, CHTB) CON3700
    D1D2B=FD1D2 (H12B, D2D2UB, R, G, MDB, HSB, THETB, CHTB) CON3710
    F1B=FP1 (N, D1D2B, MDB) $ F2B=FP2 (N, D2D2UB, AB) CON3720
    F3B=FP3 (D1D2B, D4D3B) CON3730
    BZ=MUWBRN CON3740
    IF (UIM1UI .NE. 1.0) BZ=FBZ (UIM1UI, F1B, MUWBRN) CON3750
    ZI=(FAZ (UIM1UI, F1B, MUWRN) *ZIM1+BZ*P2B*DELX*(1.+RRAT1PN)/2.) CON3760
    $/RRAT1PN CON3770
    ZB=(ZI+ZIM1)/2. $ D2=PD2 (N, ZI, C1) CON3780
C CON3790
C...EVALUATE FUNCTIONS TO OBTAIN A NEW VALUE FOR HSTAR AT CON3800
C...STATION I CON3810
C CON3820
    RD2B=FRD2 (N, ZB, C1B) $ D2B=FC2 (N, ZB, C1B) CON3830
    IF (FLOW .EQ. "TURBULENT") GO TO 340 CON3840
    CDB=FCDL (HB, R, G, MDB, THETB, W, RD2B, D2D2UB) CON3850
    GO TO 360 CON3860
340 IF (KCDS .EQ. 1) GO TO 350 CON3870
    D2UB=D2B/D2D2UB CON3880
    A1B=FA1 (H12B) $ RD2UB=RD2B/D2D2UB CON3890
    CFIB=2.*A1B/RD2UB**N $ CFB=FCF (AB, RD2B, N, D2D2UB) CON3900
    JB=FJ (H12B, CFIB) $ JSPB=FJSP (A1B, H12B, HB) CON3910
    PIB=PI (H12B, D2UB, CFIB, DNSDXMS) CON3920

```

```

JPB=FJP(JB,PIB,KCDS)                                COM3930
IF(KCDS .EQ. 1) GO TO 350                             COM3940
CDB=PCDTF(CFB, RD2UB, N, JPB, JB, JSPB, HB, H12B, PIB) $ GO TO 360 COM3950
350 CDB=PCDTRT(D2D2UB, RD2B)                          COM3960
360 F4B=FP4(RD2B, N, CDB, AB, D2D2UB, HSB)            COM3970
IF(ERROR .AND. FLOW .EQ. "TURBULENT") WRITE(6,923) A1B,CFIB,JB, COM3980
$JSPB,PIB,JPB,CDB,F4B                                COM3990
BH=1.0                                                COM4000
IF(UIM1UI .NE. 1.0) BH=FBH(UIM1UI,F3B)                COM4010
HIS=FAH(UIM1UI,F3B)*HIM1S+BH*F4B/ZB*DELX             COM4020
C                                                     COM4030
C...ALLOW FOR INTERVAL SUBDIVISION IF NECESSARY     COM4040
C                                                     COM4050
IF(ICOUNT .GT. 1 .OR. I .GT. 1) GO TO 370            COM4060
LIM2=IPX(ABS(HIS-HIM1S)/0.0025)+1                    COM4070
LIM=MAX0(LIM1,LIM2) $ LIMUP=50                       COM4080
LIM=MIN0(LIM,LIMUP)                                  COM4090
IF(FLOW .EQ. "LAMINAR" .AND. KPOINT .LE. 10) LIM=20 COM4100
IF(KPOINT .LE. 2 .OR. FLOW .NE. FLOWIM1) LIM=50     COM4110
IF(LIM .GT. 1) GO TO 230                             COM4120
C                                                     COM4130
C...EVALUATE FUNCTIONS TO FIND A NEW VALUE OF CHT FOR HTCORR=.TRUE. COM4140
C                                                     COM4150
370 IF(.NOT.(HTCORR)) GO TO 390                       COM4160
HSP=(HIS-HIM1S)/DELX $ DD2DXD2=(D2-D2IM1)/(D2B*DELX) COM4170
F5B=FP5(DMSDXMS,HSB,D1D2B,G,MDB,HSP,DD2DXD2)        COM4180
F6B=FP6(HSB,BP,BB,DMSDXMS,D1D2B,G,MDB)              COM4190
IF(F5B .NE. J.J) GO TO 380                           COM4200
CHT=CHTIM1+F6B*DELX $ GO TO 390                     COM4210
380 CHT=F6B/F5B+(CHTIM1-F6B/F5B)*EXP(-F5B*DELX)     COM4220
C                                                     COM4230
C...A NEW VALUE FOR HSTAR AT STATION I IS NOW KNOWN. ITERATE COM4240
C...TO FIND THE CORRESPONDING H VALUE                COM4250
C                                                     COM4260
390 II=J $ HI=HINNER(1)=PH(HIS,PSIB)                 COM4270
IF(ERROR) WRITE(6,924) HINNER(1)                     COM4280
400 II=II+1                                           COM4290
IF(HI .LE. 1.515) GO TO 510                          COM4300
IF(HI .LE. 2.0) GO TO 410 $ WRITE(6,922) XI $ GO TO 600 COM4310
410 IF(FLOW .EQ. "TURBULENT") GO TO 420              COM4320
D1UD=FD1UDL(HI) $ G1=FG1L(HI) $ GO TO 430           COM4330
420 D1UD=FD1UDT(HI) $ G1=FG1T(HI)                   COM4340
430 IF(ABS(THETI) .LE. 2.0) GO TO 440                COM4350
PSI=1.0 $ GO TO 450                                  COM4360
440 PSIOP=PSSIOP(HI,THETI) $ PSI12=PSSI12(D1UD,HI,THETI,G1) COM4370
PSI=PSSI(PSI12,MDI,PSIOP)                            COM4380
450 HINew=HINNER(II+1)=PH(HIS,PSI)                  COM4390
IF(ERROR) WRITE(6,925) II+1,HINNER(II+1)            COM4400
IF(ABS((H1-HINew)/HINew) .LE. EPS/10.) GO TO 470    COM4410
    
```

THIS PAGE IS BEST QUALITY PRACTICABLE
FROM COPY FURNISHED TO DDC

APPENDIX A.
PROGRAM COMPBL .

COMPRESSIBLE BOUNDARY LAYER PROGRAM...COMPBL

PAGE A-10

```

IF (II .GE. 20) GO TO 460
HI=HINew $ GO TO 400
460 WRITE(6,926) XI, (IP1,HINNER(IP1),IP1=1,21) $ GO TO 600
470 HI=HMAIN(I+1)=(HI+HINew)/2.
IF (ERROR) WRITE(6,927) I+1,HMAIN(I+1),BI,CHT
C
C...THE VALUE OF H AT STATION I FOR THIS ITERATION IN THE MAIN
C...LOOP IS NOW KNOWN. CONTINUE ITERATING IN MAIN LOOP IF
C...NECESSARY
C
IF (ABS((HI-HMAIN(I))/HI) .LE. EPS) GO TO 500
IF (I .GE. 20) GO TO 490
IF (.NOT.(ICOUNT .EQ. 1 .AND. I .GE. 5 .AND. KTRIP .EQ. 0))
$GO TO 480
KTRIP=1 $ LIM=20 $ GO TO 230
480 HIOLD=HI $ GO TO 280
490 WRITE(6,928) XI, (IP2,HMAIN(IP2),IP2=1,21) $ GO TO 600
C
C...CONVERGENCE FOR H AT STATION I IN THE MAIN ITERATION LOOP HAS
C...OCCURRED. CHECK FOR SEPARATION
C
500 HI=(HI+HMAIN(I))/2.
IF (HI .GT. 1.515) GO TO 520
510 IF (FLOW .EQ. "LAMINAR") WRITE(6,929) XI
IF (FLOW .EQ. "TURBULENT") WRITE(6,930) XI
GO TO 600
C
C...CALCULATE AND PRINT OUTPUT VARIABLES OF INTEREST
C
520 IF (HI .LE. 2.0) GO TO 530 $ WRITE(6,922) XI $ GO TO 600
530 IF (FLOW .EQ. "TURBULENT") GO TO 540
A=PAI(HI) $ H12=PH12L(HI) $ D1UD=PD1UDL(HI)
GO TO 550
540 A=PAT(HI) $ H12=PH12T(HI) $ D1UD=PD1UDT(HI)
550 D2D2U=PD2D2U(R,G,MDI,HIS,THETI)
D1D2=FD1D2(H12,D2D2U,R,G,MDI,HIS,THETI,CHT)
560 D2=FD2(N,ZI,C1) $ RD2=FRD2(N,ZI,C1)
RD2U=FRD2U(RD2,D2D2U,R,G,MDI,THET1) $ D2U=D2/D2D2U
D1=D2*D1D2 $ CF=PCF(A,RD2,N,D2D2U) $ RCORR=RI+D1
QDIM=FQDIM(CF,S,BI,CHT,G,MDI) $ D999=(H12*D2)/(D1UD*D2D2U)
LCCUNT=LCCOUNT+1
IF (LCCOUNT .LT. LIM .AND. (.NOT.ERROR)) GO TO 580
IF (ERROR .OR. (IP .NE. 17 .AND. FLOAT(IP-17) .NE. 25.*FLOAT((
$IP-17)/25))) GO TO 570
WRITE(6,901) $ WRITE(6,914)
WRITE(4,901) $ WRITE(4,915)
570 IP=IP+1
WRITE(6,931) XI,ZI,HI,D1D2,D1,D2,D999,RD2,CF,QDIM
WRITE(4,919) XI,RCORR

```

THIS PAGE IS BEST QUALITY PRACTICABLE
FROM COPY FURNISHED TO DDC

APPENDIX A. COMPRESSIBLE BOUNDARY LAYER PROGRAM...COMPBL
PROGRAM COMPBL .

PAGE A-11

C		COM4910
C...	CHECK FOR TRANSITION	COM4920
C		COM4930
580	FLOWIM1=FLOW	COM4940
	IF (FLOW .EQ. "TURBULENT" .OR. NOTRAN .OR. (XTRAN .NE. 0.0 .AND. XI	COM4950
	\$.LT. XTRAN)) GO TO 59J	COM4960
	PPARI=FPPAR(C1,DMSDXMS,D2U,R,G,MDI,THETI)	COM4970
	IF (ZSTART .NE. 0.0 .AND. KPOINT .EQ. 2) PPARIM1=FPPAR(C1IM1,	COM4980
	\$DMSDXMS,D2UIM1,R,G,MDIM1,THETIM1)	COM4990
	IF (XTRAN .NE. 0.0 .AND. XI .GE. XTRAN) KTRANS=1	COM5000
	CALL TRANS(ZI,HI)	COM5010
C		COM5020
C...	SHIFT I QUANTITIES TO I-1 QUANTITIES AND READ THE NEXT POINT	COM5030
C...	FOR THE BOUNDARY LAYER COMPUTATIONS	COM5040
C		COM5050
590	DHDXIM1=0.0	COM5060
	IF (KPOINT .GT. 1) DHDXIM1=(HI-HI1)/DELX	COM5070
	XI1=XI \$ MDIM1=MDI \$ MDIM1S=MDIS \$ DELXIM1=DELX	COM5080
	THETIM1=THETI \$ TWIIM1=TWII \$ RIM1=RI \$ YIM1=YI	COM5090
	HIM1=HI \$ HIM1S=HIS \$ ZIM1=ZI \$ PPARIM1=PPARI	COM5100
	BI1=BI \$ D2IM1=D2 \$ CHTIM1=CHT \$ D2UIM1=D2U	COM5110
	C1IM1=C1	COM5120
	IF (LCOUNT .LT. LIM) GO TO 240	COM5130
	GO TO 210	COM5140
600	STOP	COM5150
C		COM5160
C...	FORMAT STATEMENTS	COM5170
C		COM5180
900	FORMAT(8A10,/,4A10)	COM5190
901	FORMAT(1H1)	COM5200
902	FORMAT(/,40X,*INPUT ERROR: FLOW MUST EQUAL "LAMINAR" OR *,	COM5210
	\$*"TURBULENT"*)	COM5220
903	FORMAT(/,40X,*INPUT ERROR: GEOM MUST EQUAL "PLANE 2-D" OR *,	COM5230
	\$*"AXISYM"*)	COM5240
904	FORMAT(/,40X,*INPUT ERROR: MTYPE MUST EQUAL "MACH" OR *,	COM5250
	\$*"MSTAR"*)	COM5260
905	FORMAT(/,40X,*INPUT ERROR: TTYPE MUST EQUAL "THETA" OR *,	COM5270
	\$*"TWTINF"*)	COM5280
906	FORMAT(/,40X,"INPUT ERROR: HSTART MUST BE .GT. 1.515 AND .LE.",	COM5290
	\$" 2.0")	COM5300
907	FORMAT(/,40X,"INPUT ERROR: BSTART MUST BE .GE. -0.1988 AND ",	COM5310
	\$".LE. 2.0")	COM5320
908	FORMAT(/,30X,"INPUT ERROR: ZSTART,FSTINT,W MUST BE .GE. 0.0 ",	COM5330
	\$"AND MINF,REINFL,RL,RT,SL,ST,EPS MUST BE .GT. 0.0")	COM5340
909	FORMAT(/,40X,"INPUT ERROR: G MUST BE .GE. 1.0 AND .LE. 1.67")	COM5350
910	FORMAT(/,40X,"INPUT ERROR: MINF* MUST BE .LE. SQRT((G+1.)/",	COM5360
	\$"(G-1.)")	COM5370
911	FORMAT(/,58X,"EXECUTION DELETED")	COM5380
912	FORMAT(32X,"COMPRESSIBLE BOUNDARY LAYER RESULTS--COMPUTATIONAL",	COM5390

**THIS PAGE IS BEST QUALITY PRACTICABLE
FROM COPY FURNISHED TO DDC**

APPENDIX A.
PROGRAM CCOMPBL .

COMPRESSIBLE BOUNDARY LAYER PROGRAM...COMPBL

PAGE A-12

```

$" METHOD II OF WALZ",///,26X,8A10,/,58X,"INPUT PARAMETERS:",///, COM5400
$36X,"FLOW =",1X,A10,6X,"GEOM =",1X,A10,5X,"MTYPE =",1X,A10,/, COM5410
$35X,"TTYPE =",1X,A10,4X,"ZSTART =",G10.4,5X,"HSTART =",G10.4,/, COM5420
$34X,"BSTART =",G10.4,7X,"MINP =",G10.4,5X,"REINPL =",G10.4,/, COM5430
$35X,"XTRAN =",G10.4,5X,"PSTINT =",G10.4,10X,"G =",G10.4,/, COM5440
$39X,"W =",G10.4,9X,"RL =",G10.4,9X,"RT =",G10.4,/, COM5450
$38X,"SL =",G10.4,9X,"ST =",G10.4,8X,"EPS =",G10.4,/, COM5460
$34X,"NOTRAN =",1X,L1,13X,"HTCORB =",1X,L1,14X,"ERROR =",1X,L1, COM5470
$///,62X,"RESULTS:",/), COM5480
913 FORMAT(///,50X,"CORRECTED BOUNDARY CO-ORDINATES",////,25X,8A10,///), COM5490
914 FORMAT(4X,"AXIAL",10X,"Z=",11X,"H=",9X,"SHAPE",5X,"DISPLACEMENT", COM5500
$3X,"MOMENTUM",4X,"99.9% B.L.",2X,"MOM. THICK.",3X,"LOCAL SKIN", COM5510
$2X,"DIMENSIONLESS",/,3X,"LOCATION",3X,"D2*(RD2**N)",4X, COM5520
$(D3/D2)U",6X,"FACTOR",5X,"THICKNESS",4X,"THICKNESS",4X, COM5530
$"THICKNESS",5X,"REYNOLDS",5X,"FRICTION",4X,"LOCAL WALL",/,5X, COM5540
$"[L]",10X,"[L]",21X,"(D1/D2)",8X,"[L]",10X,"[L]",9X, COM5550
$"NUMBER",4X,"COEFFICIENT",4X,"HEAT FLUX",/), COM5560
915 FORMAT(34X,"AXIAL LOCATION",29X,"AXISYMMETRIC RADIUS, OR",/, COM5570
$40X,"[L]",31X,"2-D DISTANCE FROM CENTERLINE",/,87X,"[L]",/), COM5580
916 FORMAT(5F10.5) COM5590
917 FORMAT(3(1X,G12.6),5X,A4,4X,4(1X,G12.6),2(5X,A4,4X),/) COM5600
918 FORMAT(3(1X,G12.6),4(5X,A4,4X),1X,G12.6,2(5X,A4,4X),/) COM5610
919 FORMAT(2(35X,G12.6),/) COM5620
920 FORMAT(17X,"HMAIN(1)=",G12.6) COM5630
921 FORMAT(22X,"HBAR=",G12.6) COM5640
922 FORMAT(1X,G12.6,/,24X,"PROBABLE CONVERGENCE PROBLEMS: H ", COM5650
$"EXCEEDS 2.0--BOUNDARY LAYER COMPUTATIONS TERMINATED") COM5660
923 FORMAT(2X,"A=",G12.6,1X,"CFI=",G12.6,1X,"J=",G12.6,1X, COM5670
$"J*=",G12.6,1X,"PI=",G12.6,1X,"J'",G12.6,1X,"CD=",G12.6, COM5680
$1X,"F4=",G12.6) COM5690
924 FORMAT(16X,"HINNER(1)=",G12.6) COM5700
925 FORMAT(16X,"HINNER(",I2,")=",G12.6) COM5710
926 FORMAT(1X,G12.6,/,38X,"CONVERGENCE PROBLEMS FOR H GIVEN HSTAR:", COM5720
$" EXECUTION HALTED",/,(54X,"HINNER(",I2,")=",G12.6)) COM5730
927 FORMAT(17X,"HMAIN(",I2,")=",G12.6,20X,"B=",G12.6,20X,"CHT=",G12.6) COM5740
928 FORMAT(1X,G12.6,/,32X,"CONVERGENCE PROBLEMS FOR H IN MAIN ", COM5750
$"ITERATION LOOP: EXECUTION HALTED",/,(55X,"HMAIN(",I2,")=", COM5760
$G12.6)) COM5770
929 FORMAT(1X,G12.6,/,37X,"LAMINAR SEPARATION--BOUNDARY LAYER ", COM5780
$"COMPUTATIONS TERMINATED") COM5790
930 FORMAT(1X,G12.6,/,38X,"TURBULENT SEPARATION--BOUNDARY LAYER ", COM5800
$"COMPUTATIONS TERMINATED") COM5810
931 FORMAT(10(1X,G12.6),/) COM5820
END COM5830

```

FUNCTION FJP (J,P,KCDS)	FJP 10
C	FJP 20
C...FUNCTION SUBPROGRAM FJP EVALUATES J' FOR PELSCH'S TURBULENT	FJP 30
C...DISSIPATION LAW IF J AND P ARE IN THE PROPER RANGES. OTHER-	FJP 40
C...WISE KCDS IS SET TO 1 AND THE ROTTA-TRUCKENBRODT DISSIPATION	FJP 50
C...LAW IS USED IN THE MAIN PROGRAM	FJP 60
C	FJP 70
IMPLICIT REAL (J)	FJP 80
DIMENSION JP (17)	FJP 90
DATA JP /-300.,-200.,-100.,-50.,-40.,-20.,0.,20.,40.,60.,80.,	FJP 100
510.),-300.),-200.),-100.),,100.)	FJP 110
JP100 (X)=-9.5188658783729+1.1903454132063*X	FJP 120
S+J.5559J158362227E-3*X**2-J.18343543J5468E-3*X**3	FJP 130
S+0.14160913331716E-5*X**4	FJP 140
JP80 (X)=-4.3413731761876+1.3068426011584*X	FJP 150
S-0.11250087159924E-1*X**2+0.47275510546308E-4*X**3	FJP 160
JP60 (X)=-1.008847848443+1.3562907313705*X	FJP 170
S-0.14502522813689E-1*X**2+0.7650906557654E-4*X**3	FJP 180
JP40 (X)=1.545234511719+1.6548135905638*X	FJP 190
S-0.34083016059681E-1*X**2+0.44973331872342E-3*X**3	FJP 200
S-).22376917587056E-5*X**4	FJP 210
JP20 (X)=3.6075105311794+1.8535283201070*X	FJP 220
S-).47116195526722E-1*X**2+0.70032701758516E-3*X**3	FJP 230
S-0.38494386907596E-5*X**4	FJP 240
JP0 (X)=7.0182436396026+1.8406611937541*X	FJP 250
S-0.51611222869189E-1*X**2+0.81749430838999E-3*X**3	FJP 260
S-).4684300978392E-5*X**4	FJP 270
JP*20 (X)=8.9236172182768+2.0455319625133*X	FJP 280
S-).65536057718205E-1*X**2+0.10907175315598E-2*X**3	FJP 290
S-0.64025886805882E-5*X**4	FJP 300
JP*40 (X)=10.758893608409+2.0628627346909*X	FJP 310
S-0.69080702100035E-1*X**2+0.11750641115571E-2*X**3	FJP 320
S-).69932512818012E-5*X**4	FJP 330
JP*50 (X)=11.734292528921+2.0573683487056*X	FJP 340
S-).6570982279238E-1*X**2+0.11905329219484E-2*X**3	FJP 350
S-).70390435617543E-5*X**4	FJP 360
JP*100 (X)=13.292137560329+2.1798985516861*X	FJP 370
S-).75124133400646E-1*X**2+0.12632741874606E-2*X**3	FJP 380
S-).74244995094160E-5*X**4	FJP 390
JP*200 (X)=14.408492394429+2.4639430984792*X	FJP 400
S-).88133858783339E-1*X**2+0.1505433958791E-2*X**3	FJP 410
S-).89672073534135E-5*X**4	FJP 420
JP*300 (X)=15.488153369608+2.5984911767399*X	FJP 430
S-0.87020309611832E-1*X**2+0.14480538616363E-2*X**3	FJP 440
S-).84915524085188E-5*X**4	FJP 450
JP101 (X)=47.61+J.4*X	FJP 460
JP11 (X)=7.9+J.4*X	FJP 470
JP*101 (X)=52.82+0.4*X	FJP 480
JP*201 (X)=57.46+J.4*X	FJP 490

THIS PAGE IS BEST QUALITY PRACTICABLE
FROM COPY FURNISHED TO DDC

APPENDIX A.
FUNCTION FJF .

COMPRESSIBLE BOUNDARY LAYER PROGRAM...COMPBL

PAGE A-14

```

JPM301(X)=63.79+0.4*X
JLIMU=JPM300(P) $ JLIML=JP100(P)
IF(P.GT.70.) JLIMU=JPM301(P)
IF(P.GT.70.) JLIML=JP101(P)
IF(.NOT.(P.LT.0.0.OR.J.GT.JLIMU.OR.J.LT.JLIML)) GO TO 10
KCDS=1 $ RETURN
1) IF(P.GT.70.) GO TO 12)
IF(J.LE.JPM200(P)) GO TO 20
I=1 $ FRAC=(J-JPM300(P))/(JPM200(P)-JPM300(P)) $ GO TO 16)
20 IF(J.LE.JPM100(P)) GO TO 30
I=2 $ FRAC=(J-JPM200(P))/(JPM100(P)-JPM200(P)) $ GO TO 16)
30 IF(J.LE.JPM50(P)) GO TO 40
I=3 $ FRAC=(J-JPM100(P))/(JPM50(P)-JPM100(P)) $ GO TO 16)
40 IF(J.LE.JPM40(P)) GO TO 50
I=4 $ FRAC=(J-JPM50(P))/(JPM40(P)-JPM50(P)) $ GO TO 16)
50 IF(J.LE.JPM20(P)) GO TO 60
I=5 $ FRAC=(J-JPM40(P))/(JPM20(P)-JPM40(P)) $ GO TO 16)
60 IF(J.LE.JP0(P)) GO TO 70
I=6 $ FRAC=(J-JPM20(P))/(JP0(P)-JPM20(P)) $ GO TO 16)
70 IF(J.LE.JP20(P)) GO TO 80
I=7 $ FRAC=(J-JP0(P))/(JP20(P)-JP0(P)) $ GO TO 16)
80 IF(J.LE.JP40(P)) GO TO 90
I=8 $ FRAC=(J-JP20(P))/(JP40(P)-JP20(P)) $ GO TO 16)
90 IF(J.LE.JP60(P)) GO TO 100
I=9 $ FRAC=(J-JP40(P))/(JP60(P)-JP40(P)) $ GO TO 16)
100 IF(J.LE.JP80(P)) GO TO 110
I=10 $ FRAC=(J-JP60(P))/(JP80(P)-JP60(P)) $ GO TO 16)
110 IF(J.LE.JP100(P)) GO TO 12)
I=11 $ FRAC=(J-JP80(P))/(JP100(P)-JP80(P)) $ GO TO 16)
12) IF(J.LE.JPM201(P)) GO TO 13)
I=12 $ FRAC=(J-JPM301(P))/(JPM201(P)-JPM301(P))
GO TO 16)
130 IF(J.LE.JPM101(P)) GO TO 140
I=13 $ FRAC=(J-JPM201(P))/(JPM101(P)-JPM201(P))
GO TO 16)
140 IF(J.LE.JP01(P)) GO TO 150
I=14 $ FRAC=(J-JPM101(P))/(JP01(P)-JPM101(P)) $ GO TO 16)
150 IF(J.LE.JP01(P)) GO TO 16)
I=15 $ FRAC=(J-JP01(P))/(JP01(P)-JP01(P)) $ GO TO 16)
16) FJF=JP(I)+FRAC*(JP(I+1)-JP(I))
RETURN
END

```

**THIS PAGE IS BEST QUALITY PRACTICABLE
FROM COPY FURNISHED TO DDC**

APPENDIX A.
SUBROUTINE TRANS .

COMPRESSIBLE BOUNDARY LAYER PROGRAM...COMPBL

PAGE A-15

SUBROUTINE TRANS (Z,H)	TRA 10
C	TRA 20
C...SUBROUTINE TRANS CHECKS FOR TRANSITION FROM A LAMINAR TO A TURBU-	TRA 30
C...LENT BOUNDARY LAYER USING THE REYNOLDS NUMBER BASED ON THE INCOM-	TRA 40
C...PRESSIBLE, ADIABATIC MOMENTUM THICKNESS. THE POINT OF INSTABILITY	TRA 50
C...IS FOUND USING A CURVE FIT TO THE INCOMPRESSIBLE COMPUTATIONS OF	TRA 60
C...WAZZAN, ET. AL. THE TRANSITION POINT IS THEN FOUND USING A COR-	TRA 70
C...RELATION TO GRANVILLE'S DATA FOR THE DISTANCE BETWEEN THE	TRA 80
C...INSTABILITY AND TRANSITION POINTS, AND A CORRECTION FOR FREESTREAM	TRA 90
C...TURBULENCE EFFECTS.	TRA 100
C	TRA 110
IMPLICIT REAL (J,M,N)	TRA 120
REAL INTEGRAL	TRA 130
COMMON/CTRANS/RD2,N,R,RI,S,ST,FLOW,G,MTYPE,TTYPE,MINF,KTRANS,	TRA 140
SKINST,RD2U,PPARI,PPARIM1,DELX,PSTINT	TRA 150
IF (KTRANS .EQ. 1) GO TO 20	TRA 160
IF (KINST .EQ. 1) GO TO 10	TRA 170
C	TRA 180
C...CHECK FOR INSTABILITY USING WAZZAN'S RESULTS	TRA 190
C	TRA 200
RD2INST=10.**(-5077986.1033982+15932101.403096*H	TRA 210
\$-19984208.722177*H**2+12526914.458584*H**3	TRA 220
\$-3924156.6804909*H**4+491415.25735785*H**5)	TRA 230
IF (H .GT. 1.625) RD2INST=5093.+177209.*(H-1.625)	TRA 240
IF (RD2U .LT. RD2INST) RETURN	TRA 250
WRITE(6,900)	TRA 260
IF (PSTINT .GT. 2.163) GO TO 20	TRA 270
KINST=1 \$ DELSUM=0.0 \$ INTEGRAL=0.0	TRA 280
TCORF=(900.-760.*PSTINT+159.*PSTINT**2)/900. \$ RETURN	TRA 290
C	TRA 300
C...FIND THE TRANSITION POINT USING A CORRELATION TO GRANVILLE'S	TRA 310
C...DATA	TRA 320
C	TRA 330
1) INTEGRAL=INTEGRAL+(PPARI+PPARIM1)/2.*DELX	TRA 340
DELSUM=DELSUM+DELX	TRA 350
PPARM=INTEGRAL/DELSUM	TRA 360
RD2TRAN=RD2INST*(450.+400.*EXP(60.*PPARM))*TCORF	TRA 370
IF (RD2U .LT. RD2TRAN) RETURN	TRA 380
2) WRITE(6,901)	TRA 390
N=0.268 \$ h=RT \$ S=ST \$ FLOW="TURBULENT"	TRA 400
Z=Z*(RD2**(-0.732))	TRA 410
RETURN	TRA 420
C	TRA 430
C...FORMAT STATEMENTS	TRA 440
C	TRA 450
900 FORMAT (/,53X,"LAMINAR INSTABILITY POINT",//)	TRA 460
901 FORMAT (/,52X,"LAMINAR-TURBULENT TRANSITION",//)	TRA 470
END	TRA 480

```
      SUBROUTINE MSORT(M,MS)                                MSO 10
C                                                                 MSO 20
C...SUBROUTINE MSORT DETERMINES WHETHER M IS A MACH NUMBER OR  MSO 30
C...MSTAR AND CONVERTS M TO A MACH NUMBER AND MS TO AN MSTAR  MSO 40
C                                                                 MSO 50
      IMPLICIT REAL (J,M,N)                                MSO 60
      COMMON/CTRANS/RD2,N,R,RT,S,ST,FLOW,G,MTYPE,TTYPE,MINF,KTRANS, MSO 70
      SKINST,HD2U,PPARI,PPARIM1,DELX,PSTINT.                MSO 80
C                                                                 MSO 90
C...STATEMENT FUNCTIONS                                     MSO 100
C                                                                 MSO 110
      FM(G,MS)=SQRT(2./(G+1.)*MS**2/(1.-(G-1.)/(G+1.)*MS**2)) MSO 120
      FMS(G,M)=SQRT((G+1.)/2.*M**2/(1.+(G-1.)/2.*M**2))      MSO 130
C                                                                 MSO 140
C...DO SORTING AND CONVERTING                             MSO 150
C                                                                 MSO 160
      IF (MTYPE .EQ. "MSTAR") GO TO 10                     MSO 170
      MS=FMS(G,M) * RETURN                                  MSO 180
10  MS=M * M=FM(G,M)                                       MSO 190
      RETURN                                                MSO 200
      END                                                    MSO 210
```

THIS PAGE IS BEST QUALITY PRACTICABLE
FROM COPY FURNISHED TO DDG

APPENDIX A. COMPRESSIBLE BOUNDARY LAYER PROGRAM...COMPBL
SUBROUTINE TSORT .

PAGE A-17

```

SUBROUTINE TSORT (L,Theta,TWTINF,B,MD)
C
C...SUBROUTINE TSORT DETERMINES WHETHER THE INPUT TEMPERATURE DATA
C...IS IN TERMS OF THETA OR TWALL/TINF AND CALCULATES AND STORES
C...THETA VALUES IN THETA, TWALL/TINF VALUES IN TWTINF, AND B VALUES
C...IN B
C
      IMPLICIT REAL (J,M,N)
      COMMON/CTRANS/RD2,N,R,RT,S,ST,FLOW,G,MTYPE,TTYPE,MINF,KTRANS,
      $KINST,RDZU,PPARI,PPARIM1,DELY,FSTINT
C
C...STATEMENT FUNCTIONS
C
      FTHETA (R,G,MD,MINF,TWTINF) = ((1.+R*(G-1.)/2.*MD**2) - (1.+(G-1.)/2.
      $*MD**2)/(1.+(G-1.)/2.*MINF**2)*TWTINF)/(R*(G-1.)/2.*MD**2)
      FTWTINF (R,G,MD,MINF,THETA) = (1.+(G-1.)/2.*MINF**2)/(1.+(G-1.)/2.
      $*MD**2)*(1.+R*(G-1.)/2.*MD**2*(1.-THETA))
      FB (THETA,R,G,MD) = THETA*R*(G-1.)/2.*MD**2
C
C...DO SORTING AND CONVERTING
C
      IF (TTYPE .EQ. "TWTINF") GO TO 10
      TWTINF=FTWTINF (R,G,MD,MINF,THETA) $ GO TO 2J
10  TWTINF=THETA $ THETA=FTHETA (R,G,MD,MINF,THETA)
2J  B=FB (THETA,R,G,MD)
      RETURN
      END

```

THIS PAGE IS BEST QUALITY PRACTICABLE
FROM COPY FURNISHED TO DDC

APPENDIX A. COMPRESSIBLE BOUNDARY LAYER PROGRAM...COMPBL
SUBROUTINE IERROR .

PAGE A-18

	SUBROUTINE IERROR (DELX,MDI,MDIS,G,RI,GEOM,TWTINF), RETURNS (I)	IER 10
C		IER 20
C...	SUBROUTINE IERROR CHECKS FOR INPUT ERRORS ON THE VALUES OF XI,YI,	IER 30
C...	MDI,MDIS,RI, AND TWTINF	IER 40
C		IER 50
	IMPLICIT REAL (J,M,N)	IER 60
	K=0	IER 70
	IF (DELX .GT. 0.0) GO TO 10 \$ K=K+1 \$ WRITE (6,900)	IER 80
1)	IF (MDI .GT. 0.0) GO TO 20 \$ K=K+1 \$ WRITE (6,901)	IER 90
20	IF (MDIS .LE. SQRT ((G+1.)/(G-1.)) .AND. MDIS .GT. 0.0) GO TO 30	IER 100
	K=K+1 \$ WRITE (6,902)	IER 110
30	IF (.NOT. (GEOM .EQ. "AXISYM" .AND. RI .LE. 0.0)) GO TO 40	IER 120
	K=K+1 \$ WRITE (6,903)	IER 130
40	IF (.NOT. (GEOM .EQ. "PLANE 2-D" .AND. RI .LT. 0.0)) GO TO 50	IER 140
	K=K+1 \$ WRITE (6,904)	IER 150
50	IF (TWTINF .GE. 0.0) GO TO 60	IER 160
	K=K+1 \$ WRITE (6,905)	IER 170
60	IF (K .EQ. 0) RETURN	IER 180
	RETURN I	IER 190
C		IER 200
C...	FORMAT STATEMENTS	IER 210
C		IER 220
900	FORMAT (//,30X,"IDENTICAL INPUT LINES: DELX=0.0--BOUNDARY ",	IER 230
	\$"LAYER COMPUTATIONS TERMINATED")	IER 240
901	FORMAT (//,27X,"NEGATIVE OR ZERO MACH NUMBER ENTERED",	IER 250
	\$"--BOUNDARY LAYER COMPUTATIONS TERMINATED")	IER 260
902	FORMAT (//,19X,"NEGATIVE MSTAR OR MSTAR .GT. SQRT ((G+1.)/(G-1.)) "	IER 270
	\$"ENTERED--BOUNDARY LAYER COMPUTATIONS TERMINATED")	IER 280
903	FORMAT (//,15X,"NO (OR NEGATIVE) BODY RADIUS ENTERED FOR AXISYM",	IER 290
	\$"METRIC GEOMETRY--BOUNDARY LAYER COMPUTATIONS TERMINATED")	IER 300
904	FORMAT (//,17X,"NEGATIVE CENTERLINE DISTANCE ENTERED FOR PLANE ",	IER 310
	\$"2-D GEOMETRY--BOUNDARY LAYER COMPUTATIONS TERMINATED")	IER 320
905	FORMAT (//,33X,"NEGATIVE VALUE OF TWTINF ENTERED--BOUNDARY ",	IER 330
	\$"LAYER COMPUTATIONS TERMINATED")	IER 340
	END	IER 350

NOT
Preceding Page BLANK - FILMED

APPENDIX B

ERROR MESSAGES AND DISCUSSION

APPENDIX B

ERROR MESSAGES AND DISCUSSION

Program COMPBL consists of a main program, in which most of the calculations are performed, and five subprograms: function FJP evaluates the quantity J' in Felsch's [13] turbulent dissipation law; subroutine TRANS locates the laminar instability and transition points; subroutine MSORT sorts and converts M and M^* velocity input data; subroutine TSORT sorts and converts θ and T_w/T_∞ temperature input data; and subroutine IERROR checks for input errors.

A listing of the error messages generated by program COMPBL and subroutine IERROR is given below, together with an explanation of each. Most of these messages involve incorrect input values.

1. INPUT ERROR: FLOW MUST EQUAL "LAMINAR" OR "TURBULENT"
Literal variable FLOW, entered in A1Ø format, must have one of the values given.
2. INPUT ERROR: GEOM MUST EQUAL "PLANE 2-D" OR "ASIXYM"
Literal variable GEOM, entered in A1Ø format, must have one of the values given.
3. INPUT ERROR: MTYPE MUST EQUAL "MACH" OR "MSTAR"
Literal variable MTYPE, entered in A1Ø format, must have one of the values given.
4. INPUT ERROR: TTYPE MUST EQUAL "THETA" OR "TWTINF"
Literal variable TTYPE, entered in A1Ø format, must have one of the values given.
5. INPUT ERROR: HSTART MUST BE .GT. 1.515 AND .LE. 2.Ø
Variable HSTART, entered in NAMELIST BL, must satisfy the inequalities: $1.515 < HSTART \leq 2.0$. (These inequalities must be satisfied for H at any location.)
6. INPUT ERROR: BSTART MUST BE .GE. -Ø.1988 AND .LE. 2.Ø
Variable BSTART, entered in NAMELIST BL, must satisfy the following inequalities: $-0.1988 \leq BSTART \leq 2.0$.
7. INPUT ERROR: ZSTART, FSTINT, W MUST BE .GE. Ø.Ø AND MINF, REINFL, RL, RT, SL, ST, EPS MUST BE .GT. Ø.Ø
Variables ZSTART, FSTINT, W, MINF, REINFL, RL, RT, SL, ST, and EPS, all entered in NAMELIST BL, must satisfy the following inequalities: $ZSTART, FSTINT, W \geq \underline{\underline{\delta.\delta}}$, $MINF, REINFL, RL, RT, SL, ST, EPS > \delta.\delta$.

8. INPUT ERROR: G MUST BE .GE. 1.0 AND .LE. 1.67
Variable G, entered in NAMELIST BL, must satisfy the following inequalities: $1.0 \leq G \leq 1.67$.
9. INPUT ERROR: MINF** MUST BE .LE. SQRT ((G+1.)/(G-1.))
If MTYPE = MSTAR, variable MINF, which is entered in NAMELIST BL, must satisfy the following inequality:

$$\text{MINF} \leq \sqrt{\frac{(G+1)}{(G-1)}}$$

10. EXECUTION DELETED
If any of the errors above are detected, this message is also printed.
11. IDENTICAL INPUT LINES: DELX = 0.0--BOUNDARY LAYER COMPUTATIONS TERMINATED
If the X, Y coordinates of successive points are identical, the distance between them, given by Eq. (33) is zero, which would lead to division by zero.
12. NEGATIVE OR ZERO MACH NUMBER ENTERED--BOUNDARY LAYER COMPUTATIONS TERMINATED
The Mach number velocity input data must satisfy the inequality $M > 0$ (first point not checked in order to allow stagnation there).
13. NEGATIVE MSTAR OR MSTAR .GT. SQRT ((G+1.)/(G-1.)) ENTERED--BOUNDARY LAYER COMPUTATIONS TERMINATED
The M** velocity input data must satisfy the inequalities: $0 < M^* \leq \sqrt{(G+1)/(G-1)}$ (first point not checked in order to allow stagnation there).
14. NO (OR NEGATIVE) BODY RADIUS ENTERED FOR AXISYMMETRIC GEOMETRY--BOUNDARY LAYER COMPUTATIONS TERMINATED
For axisymmetric geometries, a radius value, R, must be entered, and for all but the first point it must satisfy: $R > 0$.
15. NEGATIVE CENTERLINE DISTANCE ENTERED FOR PLANE 2-D GEOMETRY--BOUNDARY LAYER COMPUTATIONS TERMINATED
For plane geometries the centerline-to-boundary distance, R, must satisfy the inequality: $R \geq 0$.
16. NEGATIVE VALUE OF TWTINF ENTERED--BOUNDARY LAYER COMPUTATIONS TERMINATED
For TTYPE = TWTINF, the temperature input data must satisfy the inequality: $\text{TWTINF} \geq 0$.
17. PROBABLE CONVERGENCE PROBLEMS: H EXCEEDS 2.0--BOUNDARY LAYER COMPUTATIONS TERMINATED

The largest value that H can obtain is 2.0. If H exceeds this value, it is probable that the iterations for H have become unstable. This may occur in starting laminar boundary layers if an incorrect value of HSTART is specified or if the base points are too widely separated. Re-examination of HSTART, finer base point spacing, and/or use of the ERROR = .TRUE. option are recommended.

18. CONVERGENCE PROBLEMS FOR H GIVEN HSTAR: EXECUTION HALTED
An iterative technique is utilized to solve for H given the corresponding H^* value. If the required number of iterations exceeds 20, the message above is written. This error condition has never been encountered.
19. CONVERGENCE PROBLEMS FOR H IN MAIN ITERATION LOOP: EXECUTION HALTED
This message is printed if the number of iterations required to determine H in the iterative technique explained in Section II-A exceeds 20. This error condition has been encountered, although very infrequently. Increasing the number of base points and/or use of the ERROR = .TRUE. option to determine the source of the problem are recommended.
20. LAMINAR SEPARATION--BOUNDARY LAYER COMPUTATIONS TERMINATED
or
TURBULENT SEPARATION--BOUNDARY LAYER COMPUTATIONS TERMINATED
Although these are not normally error messages, they may indicate instability in the iterations for H if they occur at totally unexpected locations, e.g., regions of favorable pressure gradient. This is true because separation is defined as: $H < 1.515$. As explained above in Error 17, the most likely occurrence of this condition is in starting laminar boundary layer computations. Re-examination of the value of HSTART, finer base point spacing, and/or use of the ERROR = .TRUE. option are recommended.

AD-A056 308

ILLINOIS UNIV AT URBANA-CHAMPAIGN DEPT OF MECHANICAL --ETC F/G 20/4
THEORY, COMPUTER PROGRAM, AND ILLUSTRATIVE EXAMPLES FOR THE TWO--ETC(U)
MAR 78 J C DUTTON, A L ADDY

DAAK40-76-C-0942

DRDMI-T-CR-78-10

NL

UNCLASSIFIED

2 OF 2

AD
A056 308



END

DATE

FILMED

8-78

DDC

FILED

2 OF 2

056 308

Defense
Cameron
Alexandr

DRCPM-HE
DRSMI-LP
DRDMI-T,
-TD
-TE
-TI



MICROCOPY RESOLUTION TEST CHART
NATIONAL BUREAU OF STANDARDS-1963-A

DISTRIBUTION

	<u>No. of Copies</u>
Defense Documentation Center Cameron Station Alexandria, VA 22314	6
DRCPM-HEL, Ms. Levaas	1
DRSMI-LP, Mr. Voigt	1
DRDMI-T, Dr. Kobler	1
-TDK, Dr. Walker	50
-TBD	3
-TI	2